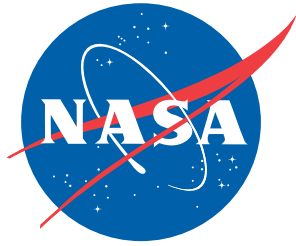


NASA/TM-2009-215752
NESC-RP-08-00494



Assessment of Ocean Wave Model used to Analyze the Constellation Program (CxP) Orion Project Crew Module Water Landing Conditions

*Bryan K. Smith/NESC
Glenn Research Center, Cleveland, Ohio*

*Richard Bouchard and Chung-Chu Teng
NOAA National Data Buoy Center, Stennis Space Center, Mississippi*

*Rodger Dyson
Glenn Research Center, Cleveland, Ohio*

*Robert Jenson
US Army Corps of Engineers, Vicksburg, Mississippi*

*William O'Reilly
Scripps Institute of Oceanography, San Diego, California*

*Erick Rogers and David Wang
Naval Research Laboratory, Stennis Space Center, Mississippi*

*Vitali Volovoi
Georgia Institute of Technology, Atlanta, Georgia*

May 2009

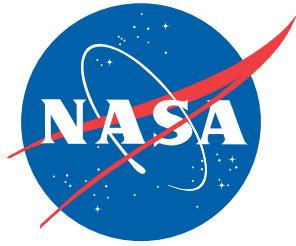
NASA STI Program . . . in Profile

Since its founding, NASA has been dedicated to the advancement of aeronautics and space science. The NASA scientific and technical information (STI) program plays a key part in helping NASA maintain this important role.

The NASA STI program operates under the auspices of the Agency Chief Information Officer. It collects, organizes, provides for archiving, and disseminates NASA's STI. The NASA STI program provides access to the NASA Aeronautics and Space Database and its public interface, the NASA Technical Report Server, thus providing one of the largest collections of aeronautical and space science STI in the world. Results are published in both non-NASA channels and by NASA in the NASA STI Report Series, which includes the following report types:

- **TECHNICAL PUBLICATION.** Reports of completed research or a major significant phase of research that present the results of NASA programs and include extensive data or theoretical analysis. Includes compilations of significant scientific and technical data and information deemed to be of continuing reference value. NASA counterpart of peer-reviewed formal professional papers, but having less stringent limitations on manuscript length and extent of graphic presentations.
 - **TECHNICAL MEMORANDUM.** Scientific and technical findings that are preliminary or of specialized interest, e.g., quick release reports, working papers, and bibliographies that contain minimal annotation. Does not contain extensive analysis.
 - **CONTRACTOR REPORT.** Scientific and technical findings by NASA-sponsored contractors and grantees.
 - **CONFERENCE PUBLICATION.** Collected papers from scientific and technical conferences, symposia, seminars, or other meetings sponsored or co-sponsored by NASA.
 - **SPECIAL PUBLICATION.** Scientific, technical, or historical information from NASA programs, projects, and missions, often concerned with subjects having substantial public interest.
 - **TECHNICAL TRANSLATION.** English-language translations of foreign scientific and technical material pertinent to NASA's mission.
- Specialized services also include creating custom thesauri, building customized databases, and organizing and publishing research results.
- For more information about the NASA STI program, see the following:
- Access the NASA STI program home page at <http://www.sti.nasa.gov>
 - E-mail your question via the Internet to help@sti.nasa.gov
 - Fax your question to the NASA STI Help Desk at 443-757-5803
 - Phone the NASA STI Help Desk at 443-757-5802
 - Write to:
NASA STI Help Desk
NASA Center for AeroSpace Information
7115 Standard Drive
Hanover, MD 21076-1320

NASA/TM-2009-215752
NESC-RP-08-00494



Assessment of Ocean Wave Model used to Analyze the Constellation Program (CxP) Orion Project Crew Module Water Landing Conditions

*Bryan K. Smith/NESC
Glenn Research Center, Cleveland, Ohio*

*Richard Bouchard and Chung-Chu Teng
NOAA National Data Buoy Center, Stennis Space Center, Mississippi*

*Rodger Dyson
Glenn Research Center, Cleveland, Ohio*

*Robert Jenson
US Army Corps of Engineers, Vicksburg, Mississippi*

*William O'Reilly
Scripps Institute of Oceanography, San Diego, California*

*Erick Rogers and David Wang
Naval Research Laboratory, Stennis Space Center, Mississippi*

*Vitali Volovoi
Georgia Institute of Technology, Atlanta, Georgia*

National Aeronautics and
Space Administration


Langley Research Center
Hampton, Virginia 23681-2199

May 2009

The use of trademarks or names of manufacturers in the report is for accurate reporting and does not constitute an official endorsement, either expressed or implied, of such products or manufacturers by the National Aeronautics and Space Administration.


Available from:

NASA Center for AeroSpace Information
7115 Standard Drive
Hanover, MD 21076-1320
443-757-5802

	NASA Engineering and Safety Center Technical Report	Document #: NESC-RP-08- 00494	Version: 1.0
Title: Assessment of Orion Crew Module Ocean Wave Model			Page #: 1 of 158

Assessment of Ocean Wave Model used to Analyze the Constellation Program (CxP) Orion Project Crew Module Water Landing Conditions

March 12, 2009

	NASA Engineering and Safety Center Technical Report	Document #: NESC-RP-08- 00494	Version: 1.0
Title: Assessment of Orion Crew Module Ocean Wave Model			Page #: 2 of 158

Approval and Document Revision History

NOTE: This document was approved at the March 12, 2009, NRB. This document was submitted to the NESC Director on April 22, 2009, for configuration control.

Approved Version:	<i>Original Signature on File</i>	4/23/09
1.0	NESC Director	Date

Version	Description of Revision	Author	Effective Date
1.0	Initial Release	Bryan Smith, NESC Chief Engineer, GRC	3/12/09



	NASA Engineering and Safety Center Technical Report	Document #: NESC-RP-08- 00494	Version: 1.0
Title: Assessment of Orion Crew Module Ocean Wave Model			Page #: 3 of 158

Table of Contents

Volume I: Technical Report

1.0	Authorization and Notification	5
2.0	Signature Page.....	6
3.0	Team List	7
4.0	Executive Summary	8
5.0	Assessment Plan	9
6.0	Problem Background and Approach	9
6.1	Orion Crew Module Landing Model	9
6.2	Application of Basic Wave Theory.....	10
6.3	Apollo Program's Approach to Wave Modeling	12
6.4	Advances in Wave Modeling and Data Collection.....	12
6.4.1	NOAA NDBC Data Availability and Data Format	13
6.4.2	Wave Measurements from CDIP	20
6.5	Constellation Program Design for Natural Environments	22
6.6	Orion Crew Module Wave Model	22
6.7	Approaches to Model Assessment	24
7.0	Data Analysis of the AMA, Inc. Report	24
7.1	Interfaces to Overall Crew Module Landing Model.....	24
7.1.1	Integrated Model and Overall Model Accuracy	25
7.1.2	Model Verification.....	30
7.1.3	Other Salient Model Assumptions	31
7.2	Use of Buoy Data to Drive the Monte Carlo Wave Model.....	32
7.2.1	Wave Data Availability.....	32
7.2.2	Buoy Data Synthesis and Correlations: Slope, Vertical Velocity, and Azimuth	34
7.2.3	Atlantic and Pacific Wave Climates	36
7.3	Oceanographic Considerations	43
7.3.1	Data Interpretation and Measurement Error	43
7.3.2	Environmental Factors	43
7.3.3	Breaking Waves for Crew Module's Off-nominal and Nominal Water Landing.....	45
8.0	Findings, Observations, and Recommendations	47
8.1	Findings	47
8.2	Observations	49
8.3	Recommendations.....	50
9.0	Alternate Viewpoints	54
10.0	Other Deliverables	54

	NASA Engineering and Safety Center Technical Report	Document #: NESC-RP-08- 00494	Version: 1.0
Title: Assessment of Orion Crew Module Ocean Wave Model			Page #: 4 of 158


11.0	Lessons Learned.....	54
12.0	Definition of Terms.....	54
13.0	List of Acronyms.....	58
13.1	Nomenclature.....	59
14.0	References.....	60

List of Figures

Figure 6.1-1.	Ocean Wave Model Portion of the Overall Model and its Constituent Components	10
Figure 6.6-1.	Ocean Wave Model (AMA).....	23
Figure 7.1-1.	Probability Density Function for the Total Distribution (Blue Line Corresponds to a Standard Normal Distribution).....	26
Figure 7.1-2a.	Difference between the modeled distribution (green) and its approximations (blue is normal distribution based on total variance and purple is the normal distribution with correction factor).....	28
Figure 7.1-2b.	(Zoom in of Figure 7.1-1a): Difference between the modeled distribution (green) and its approximations (blue is normal distribution based on total variance and purple is the normal distribution with correction factor).....	29
Figure 7.2-1.	Current Sea Surface Landing Conditions for the CDIP Cape Canaveral, FL Buoy	34
Figure 7.2-2.	Classification of Wave Climate at NDBC Buoy 44004 at various Significant Wave Height Categories	38
Figure 7.2-3.	Classification of Wave Climate at NDBC Buoy 46047 at various Significant Wave Height Categories	39
Figure 7.2-4.	Monthly Averaged Mean Significant Wave Height, variance in the Mean, Maximum and Number of Observations at NDBC Buoy 44004	41
Figure 7.2-5.	Monthly Averaged Mean Significant Wave Height, variance in the Mean, Maximum and Number of Observations at NDBC Buoy 46047	42
Figure 7.3-1.	Steepness Factors with Currents and Following or Opposing Seas (left) and for Opposing and Following Vessel Speed (right) (speeds in knots).....	44
Figure 7.3-2.	Whitecap Coverage as a Function of Wind Speed.....	46

Volume II: Appendices

- A. Overview of the Monte Carlo Analysis Process used to Establish Crew Module Water Landing Conditions, January 8, 2008
- B. Monte Carlo Ocean Wave Modeling, Rev. D, December 2008
- C. Wave Simulations (AMA, Inc. Report, Section 3.1.2)
- D. Spatial-Temporal Variability
- E. NDBC Wave Measurements (Data Format)
- F. CDIP Wave Measurements (Data Format)

	NASA Engineering and Safety Center Technical Report	Document #: NESC-RP-08- 00494	Version: 1.0
Title: Assessment of Orion Crew Module Ocean Wave Model			Page #: 5 of 158


Volume I: Technical Report

1.0 Authorization and Notification

Mr. Christopher Johnson, NASA's Systems Manager for the Orion Project Crew Module (CM) Landing and Recovery at the Johnson Space Center (JSC), and Mr. James Corliss, Project Engineer for the Orion CM Landing System Advanced Development Project at the Langley Research Center (LaRC) requested an independent assessment of the wave model that was developed to analyze the CM water landing conditions.

A NASA Engineering and Safety Center (NESC) initial evaluation was approved November 20, 2008. Mr. Bryan Smith, NESC Chief Engineer at the NASA Glenn Research Center (GRC), was selected to lead this assessment. The Assessment Plan was presented and approved by the NESC Review Board (NRB) on December 18, 2008. The Assessment Report was presented to the NRB on March 12, 2009.


The key stakeholders for this assessment are Mr. Christopher Johnson, Mr. James Corliss, the Orion Project Office, and the NESC.

	NASA Engineering and Safety Center Technical Report	Document #: NESC-RP-08- 00494	Version: 1.0
Title: Assessment of Orion Crew Module Ocean Wave Model			Page #: 6 of 158

2.0 Signature Page


Assessment Team Members

<hr/> Mr. Bryan K. Smith Date	<hr/> Mr. Richard Bouchard Date
<hr/> Dr.Chung-Chu Teng Date	<hr/> Dr. Rodger Dyson Date
<hr/> Dr. Robert Jensen Date	<hr/> Dr. William O'Reilly Date
<hr/> Mr. Erick Rogers Date	<hr/> Dr. Vitali Volovoi Date
<hr/> Dr. David Wang Date	

	NASA Engineering and Safety Center Technical Report	Document #: NESC-RP-08- 00494	Version: 1.0
Title: Assessment of Orion Crew Module Ocean Wave Model			Page #: 7 of 158

3.0 Team List

Name	Discipline	Organization/Location
Core Team		
Bryan Smith	NESC Team Lead	GRC
Richard Bouchard	NDBC Buoy Data	NOAA NDBC
Chung-Chu Teng	NDBC Buoy Data	NOAA NDBC
Rodger Dyson	Numerical Methods/Statistical Modeling	GRC
Robert Jensen	Buoy Data and Modeling	US Army Corps of Engineers
William O'Reilly	Scripps CDIP Buoy Data	Scripps Institute of Oceanography
Erick Rogers	Wave Modeling	Naval Research Laboratory
Vitali Volovoi	Statistical Models/ Simulation Uncertainty	Georgia Institute of Technology
David Wang	Buoy Data and Observation	Naval Research Laboratory
Consultants		
James Corliss	Orion Project	LaRC
Chris Johnson	Landing and Recovery	JSC
Kristin Cummings	Constellation Natural Environments	MSFC, JTI
Support		
Loutricia Johnson	MTSO Program Analyst	LaRC
Pam Sparks	Project Coordinator	LaRC, ATK
Linda Burgess	Planning and Control Analyst	LaRC, ATK
Erin Moran	Technical Writer	LaRC, ATK


	NASA Engineering and Safety Center Technical Report	Document #: NESC-RP-08- 00494	Version: 1.0
Title: Assessment of Orion Crew Module Ocean Wave Model			Page #: 8 of 158

4.0 Executive Summary

The Orion Project Office contracted with Analytical Mechanics Associates (AMA), Incorporated (Inc.) to develop an ocean wave model used to determine water-landing conditions for Orion Crew Module (CM) ocean landings. The model is used in conjunction with the overall CM landing model that considers vehicle orientation and landing velocities. The overall landing model statistically treats both CM and wave properties in a Monte Carlo model that provides a probabilistic model for design loads. Due to the critical nature of the wave model component of the overall model, the Orion Project requested the NASA Engineering and Safety Center (NESC) provide a peer review of the AMA, Inc. model. Oceanographic consultants and other Government Agencies with domain specific knowledge were selected to be part of the NESC team to review the AMA, Inc. model.

The analytical wave model uses historical buoy data to characterize wave properties and predict potential water landing conditions for a given wind speed. The availability and fidelity of ocean measurements (e.g., buoy data) has advanced significantly since the time of the development of a similar model for the Apollo Program, and has contributed to the improvement of the overall model. The nature of the problem can lend itself to extensive study, research, and refinement so a balance of critical oceanographic contributing factors must be determined for practical application in the overall landing model. The properties of interest from the wave model, then used in the overall landing model, are: wave slope; wave vertical velocity; and wave azimuth (or orientation relative to the steady-state wind direction). The critical property used to correlate these conditions both internal to the wave model and to the overall landing model is wind speed.

The NESC team provided written questions, conducted face-to-face reviews, and considered potentially relevant externalities to the model. The AMA, Inc. wave model will be provided to the CM contractor, Lockheed Martin Corporation, for use in the design and verification of vehicle landing conditions. The NESC team identified 11 findings and 12 recommendations. The findings addressed the model, buoy data selection and limitations, the statistical treatment of the data, analytical methods, uncertainties, and underlying assumptions. This report was developed considering its potential use as a supplement to the AMA, Inc. report and future use with the CM landing model.

	NASA Engineering and Safety Center Technical Report	Document #: NESC-RP-08- 00494	Version: 1.0
Title: Assessment of Orion Crew Module Ocean Wave Model			Page #: 9 of 158


5.0 Assessment Plan

The NESC team reviewed the wave model developed AMA, Inc. (provided in Appendix B) which is used to determine wave slope, wave vertical velocity, and wave azimuth for the overall Orion CM landing model. Key elements of this review included: the model, buoy data selection and limitations, the statistical treatment of the data, analytical methods, uncertainties, and underlying assumptions. Prior to the face-to-face review with AMA, Inc., the NESC team provided written questions on their draft report to accelerate the technical dialogue and allow for the potential acceptance and discussion of initial observations. In preparation for the review, the NESC team additionally reviewed: methods used by the Apollo Program, CM ocean landing corridors, the overall CM landing model process, and relevant sections of the Constellation Program (CxP) Design Specification for Natural Environments (DSNE) [ref. 14]. The assessment plan allowed AMA, Inc. the ability to incorporate draft findings, observations, and recommendations in their model prior to formal contract completion at the end of February 2009. The AMA, Inc. wave model will be provided to the CM contractor, Lockheed Martin Corporation, for use in the design and verification of vehicle landing conditions. The NESC report will be used as supplemental information for the AMA, Inc. report.

6.0 Problem Background and Approach

6.1 Orion Crew Module Landing Model

The Monte Carlo Orion CM Landing Model establishes statistically viable landing conditions and avoids designing for worst on worst design cases. The model combines the CM descent velocities and orientation with the impact surface slope and, for water landings, wave vertical velocity. The model provides a method to develop conditional probabilities of landings for various scenarios and compliance to Orion Project and CxP requirements. Due to the unique nature of this model, an independent assessment and related oceanographic assumptions was requested. The focus of this assessment is the ocean wave model portion of the overall model and its constituent components depicted in Figure 6.1-1.

	NASA Engineering and Safety Center Technical Report	Document #: NESC-RP-08- 00494	Version: 1.0
Title: Assessment of Orion Crew Module Ocean Wave Model			Page #: 10 of 158

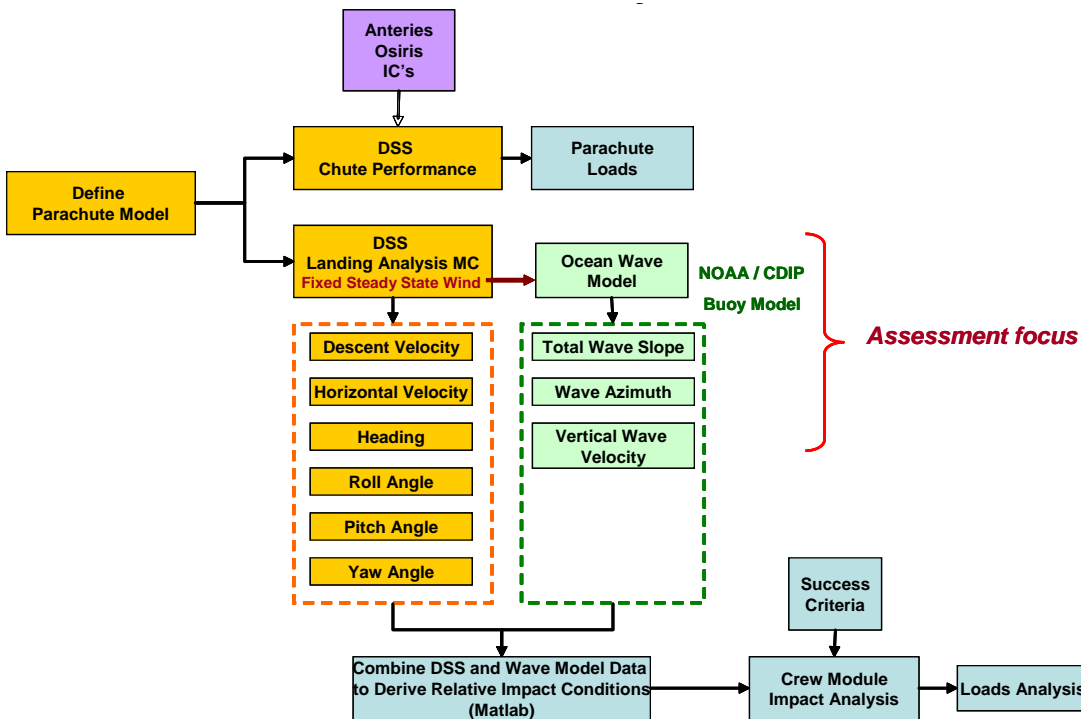


Figure 6.1-1. Ocean Wave Model Portion of the Overall Model and its Constituent Components


6.2 Application of Basic Wave Theory

Sea surface motion is the combined result of forced waves (e.g., wind seas and tides) and free waves (e.g., swell). Forced wave motions are bound to their driving mechanism (e.g., constant gravitational forces of celestial bodies on the oceans, or wind stress on the sea surface) while free waves are sea surface perturbations that were originally forced, but then freely propagate across the sea surface when the direct forcing ends.

Free wave propagation is most often modeled using first-order linear progressive, or small amplitude, wave theory. Wave behavior is independent of height, and there is a one-to-one relationship between the free wave frequency (or inversely, period), wavelength and water depth, which is governed by the linear dispersion relationship:

$$\omega^2 = gk \cdot \tanh(kh) \quad (\text{EQ. 1})$$

where $\omega = 2\pi f$ = angular frequency, f =frequency, $k=2\pi$ /wavelength, and h =water depth.

	NASA Engineering and Safety Center Technical Report	Document #: NESC-RP-08- 00494	Version: 1.0
Title: Assessment of Orion Crew Module Ocean Wave Model			Page #: 11 of 158

Linear wave theory is widely used to model wave energy propagation across ocean basins and across continental shelves to the coastline. For many practical applications the small amplitude, free wave assumption is robust, and linear wave modeling provides sufficiently accurate predictions of time or space-integrated sea surface parameters (e.g., the wave height or period).

However, when significant local wave forcing is present, as when winds are actively generating waves, forced linear theory is insufficient to represent the wave characteristics. Higher order terms must be included in the dispersion relationship. Wave behavior is not independent of height, and nonlinear wave theory must be used to accurately describe the combined forced and free wave sea surface evolution in space and time. Rapid changes in other boundary conditions (e.g., bottom depth or currents) can also result in localized direct wave forcing and nonlinear wave evolution.


A common way to characterize wave conditions at a specific time and location is by the distribution of wave energy as a function of wave frequency only (a frequency spectrum) or both frequency and direction (a directional spectrum). The linear theory interpretation of the directional spectrum is that each spectral energy component can be represented by a sine wave of finite amplitude with a random phase. Sea surfaces that are consistent with a given directional wave spectrum are a linear superposition of these sine waves, and statistical aspects of the sea surface (e.g., height, slope, and particle velocity distributions) have straightforward analytic solutions.

The nonlinear theory interpretation of a directional spectrum is that some of the sine waves have random phases, but others are “phase-locked” with each other creating persistent sea surface features that lead to more statistically extreme behavior than would otherwise be predicted using linear theory.

Nonlinear modeling of directional spectra and simulations of nonlinear sea surfaces is significantly more complex than the linear approach. However, nonlinear effects must be considered in applications where aspects of sea surface behavior at the statistical extremes (high or low) is important.

In practice, there is a better understanding of ocean frequency spectra than directional spectra. Frequency spectra are derived from measurements of the sea surface vertical motion, and the uncertainty is mostly limited by the length of the time it is assumed the spectrum are stationary (a fraction of an hour for short period local seas, several hours for long period swell).

Measuring directional wave spectra is vastly more complicated. In situ observations with buoys are typically restricted to measuring the two lowest-order moments of the directional wave spectrum at each frequency, or equivalently, the mean direction, spread, skewness, and kurtosis

	NASA Engineering and Safety Center Technical Report	Document #: NESC-RP-08- 00494	Version: 1.0
Title: Assessment of Orion Crew Module Ocean Wave Model			Page #: 12 of 158

of the distribution. The larger spatial sea surface coverage of remote sensing offers the promise of high resolution directional spectra, but the resulting trade-offs in measurement accuracy and temporal coverage have hindered advances in this field.

6.3 Apollo Program's Approach to Wave Modeling

For the Apollo Program, slope variance was computed through integration of the Neumann wave spectrum for fully developed seas [ref. 17]. The integration was performed at two wind speeds (10 and 15 m/s) with linear interpolation/extrapolation for analysis at other wind speeds. The breakdown of slope variance into upwind-downwind and crosswind components was assumed to be 0.625 and 0.375, respectively. Total slope (μ) for each Monte Carlo case was computed using the below equation with upwind-downwind (μ_{ud}) and crosswind (μ_c) components cast independently, as referenced in the AMA, Inc. report (provided in Appendix B).

$$\mu = \tan^{-1}(\sqrt{\tan^2 \mu_{ud} + \tan^2 \mu_c})$$

Wave speed was determined as the product of wave age and wind speed with wave age cast according to prescribed probability distributions. The distributions were a function of wind speed.


Wave age was correlated to wave slope by limiting the probability distribution to three regions based on the value of the upwind-downwind component of wave slope. Wave direction (deviation from the direction of the prevailing wind) was assumed to have roughly a \cos^2 directional distribution with a loose correlation to wave age.

Further information on the Apollo analytical landing model and the statistics applied can be found in references 16, 27 and 55.

6.4 Advances in Wave Modeling and Data Collection

Advances in wave theory and ocean engineering, since the Apollo Program model was developed, allow improvements to modeling capabilities. AMA, Inc. reviewed the Apollo Program model and in consultation with external oceanographic experts identified opportunities for improvement.

The availability of ocean measurements (e.g., buoy data) has advanced since the Apollo Program with online data archives and real time data servers contributing to the final model product. Availability and fidelity of measured data includes National Oceanic and Atmospheric Administration's (NOAA's) National Data Buoy Center (NDBC) and Coastal Data Information Program (CDIP).

	NASA Engineering and Safety Center Technical Report	Document #: NESC-RP-08- 00494	Version: 1.0
Title: Assessment of Orion Crew Module Ocean Wave Model			Page #: 13 of 158

6.4.1 NOAA NDBC Data Availability and Data Format

Review of Wind Measurements from NDBC Buoys

NDBC's wind measurements from its moored buoys were collected by impeller anemometers. In the 1970s and early 1980s, Bendix® aerovanes were used. Since the mid-1980s, the R.M. Young Model 05103 has been the standard wind sensor. Wind sensors are calibrated before deployments to ensure that the reported speed lies within 1 m/s of the wind tunnel standard (Gilhousen, 1999, ref. 23). Numerous studies have documented the accuracy and representativeness of winds measured from moored buoys with the possible exception of sheltering effects when wave heights approach and exceed anemometer heights (Gilhousen, 2006 ref. 25 and Taylor *et al.*, 2002, ref. 50).


Anemometer heights vary by hull type. The 3-m discus and 6-m Navy Oceanographic Meteorological Automatic Device (NOMAD) buoys have anemometers mounted at approximately 5 m above the water-line. The 10 and 12-m discus hulls have anemometers mounted at approximately 10 m above the water-line. The buoys of the Tropical Atmosphere Ocean Array (TAO) have anemometers at 4 m above the water-line.

Sampling rates and averaging durations are a product of the buoy's on-board electronic dataloggers or *payloads* in NDBC parlance (see Table 6.4-1). NDBC buoys report these winds generally at one-hour intervals, but a few buoys have 30-minute reporting periods. The valid time of the wind measurements is assigned to the minute at which the sampling is completed. So, for hourly measurements, the valid times are assigned to minute 50 past the hour and for 30-minute intervals, minutes 20 and 50 past the hour. In previous data files these times are rounded to the nearest hour or half hour.

The GSBP (General Service Buoy Payload), and TAO (using the Next Generation ATLAS (Autonomous Temperature Line Acquisition System) payloads use vector averaging for wind speeds that can result in winds several percent lower when winds exceed 10 m/s (Gilhousen, 1987, ref. 24 and Taylor *et al.*, 2002, ref. 50).

Table 6.4-1. Buoy Payload Sampling Rates and Averaging Durations


Payload	Averaging Duration (minutes)	Averaging Method	Sampling Rate (Hz)
ARES	8	Scalar	1.71
DACT and MARS	8	Scalar	1.0
VEEP	8	Scalar	1.28
GSBP	8.5	Vector	1.0
TAO (Next Generation ATLAS)	2	Vector	2.0

	NASA Engineering and Safety Center Technical Report	Document #: NESC-RP-08- 00494	Version: 1.0
Title: Assessment of Orion Crew Module Ocean Wave Model			Page #: 14 of 158

NDBC adjusts wind speeds to conform to the universally accepted reference standard of 10 m. The NDBC 10-m winds are not available to the public either through the NDBC web pages or the archives at the National Ocean Data Center, but can be requested from NDBC since 1999. NDBC also adjusts wind speeds to 20 m, a height closer to that typical of ship anemometers. This is done to provide marine forecasters and data modelers a means to directly compare buoy and ship observations. Using the buoy's wind speed, air temperature, and water temperature, the adjustments are made following the method of Liu *et al.*, 1979 [ref. 35] with relative humidity set to 85 percent. If the air or water temperature is missing, then the algorithm uses a neutral atmosphere. If both temperatures are missing, then adjustments are not made which reduces the number of records available for the study. NDBC stores the 10- and 20-m wind speeds in its database. The method of Liu *et al.*, 1979 [ref. 35] includes the adjustment for atmospheric stability. This is in contrast to the methods that assume neutral stability, such as Bidlot et al. 2002 [ref. 7] (which is referenced in DSNE's reference Caires and Sterl, 2005, and used in computing 10-m winds in the C-ERA 40 data) or Hsu *et al.*, 1994 [ref. 28] that provides a discussion on atmospheric stability and wind profiles. A more comprehensive adjustment procedure is provided by the Coupled Ocean-Atmosphere Response Experiment (COARE algorithm 3.0 (Fairall et al., 2003, ref. 21) which is generally valid up to wind speeds of 20 m/s and includes atmospheric stability and wave effects (the algorithm's MATLAB code is available for download).

NDBC also provides wind speed and direction at 10-minute intervals on select stations (listing found at http://www.ndbc.noaa.gov/historical_data.shtml#cwind). These are known as *Continuous Winds*, which provides a continuous record of winds for a full hour. They are available in the monthly and yearly files for the applicable stations. However, because air and water temperatures are not measured every 10 minutes, NDBC does not make adjustments of Continuous Winds from the anemometer height to the 10-m height (the exception being the 10 and 12-m) discus buoys in which the anemometers are already at the 10-m height.

NDBC also provides gusts, which are an average over a very short time (3 or 5 seconds). Because of the long-period of observations at NDBC stations, the National Weather Service produces Model Output Statistics (MOS) for most stations (<http://www.weather.gov/mdl/synop/buoytbl.htm>), as *Marine MOS Products* (<http://www.weather.gov/mdl/synop/marinedesc.php>). Marine MOS Products include short-range forecasts for wind direction and speed, at the anemometer height and at 10 m, as air temperature and dew point. The Marine MOS Products statistically tune the numerical model output to produce generally better forecasts of the parameters.

	NASA Engineering and Safety Center Technical Report	Document #: NESC-RP-08- 00494	Version: 1.0
Title: Assessment of Orion Crew Module Ocean Wave Model			Page #: 15 of 158

Wave Measurements from NDBC

The NDBC operates a large number of buoys in areas of interest to the United States. Each hour (in a few cases every 30 minutes) meteorological, oceanographic, and wave data are acquired, transmitted to shore via satellite telecommunications, and distributed to users following real-time, automated data quality control (NDBC, 2003, ref. 41). NDBC made its first nondirectional wave measurements from buoys in 1973 and its first directional wave measurements in 1975. The program has expanded so that now all NDBC buoys make wave measurements and most make directional wave measurements. Complete details on NDBC wave measurements can be found in NDBC, 1996, [ref. 40].

After the wave spectrum is determined and transmitted to shore, additional wave parameters are derived. These parameters include the significant wave height (SWH), peak (or dominant) wave period, and average wave period. The peak wave period is the inverse of the peak frequency (i.e., period of the highest wave energy). The significant waveheight (H_s) and the mean zero-downcrossing wave period (T_z) are computed from:

$$H_s \approx H_{m0} = 4\sqrt{m_0} \quad \text{and} \quad T_z \approx T_{m02} = \sqrt{\frac{m_0}{m_2}}$$

in which m_0 and m_2 are the zeroth and second spectral moment, respectively, H_{m0} is zero moment waveheight and T_{m02} is spectral mean period¹ [ref. 56].


Nondirectional Spectral Wave Measurements

Buoy heave motion is needed for nondirectional (or one-dimensional) wave measurements. Once the heave motion is measured, the wave power spectrum $S_w(f)$ can be derived from the spectrum of the buoy heave motion $S_h(f)$:

$$S_w(f) = \frac{S_h(f)}{PTF}$$

in which PTF is the Power Transfer Function between the wave vertical motion and the buoy heave motion. Since the PTF is a function of wave frequency, wave data measured from a buoy are usually processed in the frequency domain as wave spectra. Since both the spectral values

¹ H_s and T_z can be calculated exactly from free surface time series data, whereas zero moment waveheight H_{m0} and mean period T_{m02} are calculated from a spectrum. Outside the surf zone, they are safely assumed equivalent; thus these equations are generally appropriate for buoy data. See also WMO (1998) [ref. 56].

	NASA Engineering and Safety Center Technical Report	Document #: NESC-RP-08- 00494	Version: 1.0
Title: Assessment of Orion Crew Module Ocean Wave Model			Page #: 16 of 158

and the *PTFs* are functions of wave frequency, both the waves and the motion responses are assumed linear. Thus, wave nonlinearity cannot be measured accurately from data buoys.

The buoy heave motion is usually measured as acceleration. From the time series record of acceleration, the acceleration spectrum is determined. Then, the displacement spectrum is derived by dividing the acceleration spectrum by a factor of ω^4 (where ω is equal to 2π times the wave frequency).


Since the wave's vertical motion is described in an Earth-fixed coordinate system, it is desired that the buoy's heave motion also be measured in the same coordinate system. In other words, it is preferred that a motion sensor measure the buoy's vertical displacement from an earth-fixed coordinate without being affected by the buoy's pitch and roll motion (e.g., a gimbaled-accelerometer or an accelerometer on a vertically stabilized platform). Under this circumstance, the wave spectrum can be directly obtained from the measured heave motion. However, if a motion sensor is "fixed" on the buoy hull, the heave motion is measured from a buoy-fixed coordinate.

Due to the buoy's pitch and roll motion, the measured heave motion usually is not truly parallel to the vertical water surface motion below the buoy (described from the earth-fixed coordinate), but is contaminated by the corresponding tilting motion. Earle and Bush (1982) [ref. 19] showed acceleration spectra measured with an accelerometer fixed on a buoy hull have excess low-frequency energy, which is considered as noise. During the conversion from an acceleration spectrum to a displacement spectrum (i.e., derivation described above using ω^4), the low-frequency noise will be amplified. Accordingly, the wave spectrum at the low-frequency range (i.e., the swell range) and the wave parameters derived from the wave spectrum will be contaminated. NDBC uses the following noise correction function (*NC*), which is determined empirically (Earle, *et al.*, 1984) [ref. 20], to remove the low-frequency noise of an acceleration spectrum:

$$NC(f) = \begin{cases} K(f_c - f) & ; f \leq f_c \\ 0 & ; otherwise \end{cases}$$

in which K is an empirical correction constant and f_c is the upper frequency limit for noise correction. Based on actual measurements from NDBC data buoys, the correction constant can be empirically derived from the spectral energy at low frequencies, typically $f=0.01$ and 0.02 Hz. Lang (1987) [ref. 34] proposed the following formula for K :

$$K = G \cdot \frac{S_{0.01} + S_{0.02}}{2}$$

	NASA Engineering and Safety Center Technical Report	Document #: NESC-RP-08- 00494	Version: 1.0
Title: Assessment of Orion Crew Module Ocean Wave Model			Page #: 17 of 158

in which G is a constant for a particular buoy deployment, and $S_{0.01}$ and $S_{0.02}$ are values of the acceleration spectral energy at $f = 0.01$ and 0.02 Hz, respectively. Lang (1987) [ref. 34] showed G varied from 13 to 18 and f_c varied from 0.150 to 0.178 Hz, depending on the types of buoy hull, water depth, and mooring configuration. With the advent of Wave Processing Module (WPM) wave system, which only has one noise band, 0.02 Hz, G and f_c were adjusted accordingly.

Directional Spectral Wave Measurements from NDBC Buoys

For directional waves, in addition to the heave motion, other buoy motions are required to derive the wave direction information. NDBC's directional wave systems are based on the slope-following principle proposed by Longuet-Higgins, et al. (1963) [ref. 36], which uses the buoy slopes to derive the directional wave data. Buoy slopes can be computed from buoy's azimuth, pitch, and roll angles. Similar to the wave's vertical motion and buoy's heave motion, a transfer function exists between the wave slopes and the buoy's slopes (e.g., pitch/roll motion). It is preferred that a slope-following buoy follows the wave's vertical motion and slopes. Discus buoys, such as NDBC's 3- and 10-m buoys, are usually good slope-following buoys. Directional wave measurements are not made from the 6-m NOMAD hulls because of the hull's asymmetry.

The determination of wave direction from data buoys is usually based on the assumption that a directional spectrum, $S(f, \theta)$, can be expressed as a Fourier series expansion:


$$S(f, \theta) = \frac{a_0}{2} + a_1 \cdot \cos\theta + b_1 \cdot \sin\theta + a_2 \cdot \cos 2\theta + b_2 \cdot \sin 2\theta + \dots$$

in which f is the wave frequency, θ is the direction of wave propagation (counterclockwise from east by convention), and a_i and b_i are Fourier coefficients. Note that coordinate systems for Fourier coefficients are not universal across data providers. For a slope-following buoy, the first five Fourier coefficients in the previous equation can be determined from the co- and quad-spectra of the vertical water surface displacement (represented by subscript 1) and two orthogonal components of surface slope (represented by subscripts 2 and 3, respectively) in the following manner:

$$a_0 = \frac{1}{\pi} C_{11}; \quad a_1 = \frac{1}{\pi k} Q_{12}; \quad b_1 = \frac{1}{\pi k} Q_{13}$$

$$a_2 = \frac{1}{\pi k^2} (C_{22} - C_{33}); \quad b_2 = \frac{2}{\pi k^2} C_{23}$$

in which k is the wave number (equal to 2π divided by the wave length), and C and Q represent the co- and quad-spectra, respectively. Then, the directional wave spectrum can be expressed as

	NASA Engineering and Safety Center Technical Report	Document #: NESC-RP-08- 00494	Version: 1.0
Title: Assessment of Orion Crew Module Ocean Wave Model			Page #: 18 of 158

$$S(f, \theta) = C_{11} \cdot \frac{1}{\pi} \left[\frac{1}{2} + r_1 \cos(\theta - \theta_1) + r_2 \cos 2(\theta - \theta_2) \right]$$

in which

$$r_1 = \frac{1}{a_0} \sqrt{a_1^2 + b_1^2}; \quad r_2 = \frac{1}{a_0} \sqrt{a_2^2 + b_2^2}$$

$$\theta_1 = \tan^{-1}(b_1, a_1); \quad \theta_2 = \frac{1}{2} \tan^{-1}(b_2, a_2)$$

In the prior equations, C_{11} is the spectral density of the water surface vertical motion (i.e., the nondirectional wave spectrum), θ_1 and θ_2 are referred to as the mean and principal wave directions, respectively, and r_1 and r_2 are the parameters representing the directional energy spreading in the corresponding direction, and are known as the first and second normalized polar coordinates from Fourier coefficients, respectively. All of the above wave parameters are functions of wave frequency. To be consistent with wind and marine conventions, NDBC reports a wave direction as the direction from which waves come measured clockwise from true North². Thus, the mean and principal wave directions reported by NDBC wave systems, α_1 and α_2 , are computed from equations:

$$\alpha_1 = 270^\circ - \theta_1; \quad \alpha_2 = 270^\circ - \theta_2$$


WMO (1995³) [ref. 56] provides guidance in applying these reportable parameters:

- If $\alpha_1 \approx \alpha_2$ and $r_1 > r_2$, there is a single wave train in the direction given by the common value of α_1 and α_2 , and
- If $|\alpha_1 - \alpha_2| > 8$ degrees and $r_1 < r_2$, a confused sea exists and no simple assumption can be made about the direction of the wave energy.

The transfer functions between the buoy motions (e.g., heave, pitch, and roll) and water surface motions (e.g., surface elevation and two orthogonal wave slopes) play a key role in accurately determining directional waves. As discussed in Steele, et al. (1992) [ref. 48], NDBC handles the transfer functions by calculating Fourier coefficients and wave parameters without directly using

² Thus use of the term *alpha* and symbol α which IAHR (1989) uses to indicate the convention of the direction FROM which the waves originate, while *theta* (θ) indicates direction TOWARDS.

³ NDBC reports spectral data in real-time via the WMO FM-65 WAVEOB alphanumeric code (WMO, 1995).

	NASA Engineering and Safety Center Technical Report	Document #: NESC-RP-08- 00494	Version: 1.0
Title: Assessment of Orion Crew Module Ocean Wave Model			Page #: 19 of 158


all the transfer functions. This is based on the equation $k^2 \cdot C_{11} = C_{22} + C_{33}$ (which is derived based on the linear wave assumption, and the terms can be rearranged to form the *check ratio* or *check factor*. See Barrick et al., (1989) [ref. 5] for a discussion of non-linear effects on buoy wave measurements. Detailed descriptions and discussion of NDBC's directional wave processing algorithms are presented in Steele, *et al.* (1985 and 1992) [ref. 45, 48] and are summarized in NDBC (1996) [ref. 40]. In addition to the buoy hull-mooring effect, the effects from sensors/electronics, data acquisition/processing, and digital signal processing also affect the transformation or derivation (e.g., transfer functions) between wave and buoy motions. Since these effects can be determined from manufactures' specifications or the corresponding theories, they are also included in NDBC's wave processing algorithm in the form of transfer functions (see Steele, *et al.*, 1985 and 1992) [ref. 45, 48].

Because NDBC's directional wave systems are based on the slope-following principle, information about the buoy's pitch and roll is used with heave motion for determining wave directions. Three types of sensor configurations may be used with the wave systems so buoy pitch and roll can be determined. These are the Hippy (e.g., heave, pitch, and roll sensor), the Magnetometer-Only (MO), and the Angular-Rate-Sensor (ARS). Traditionally, NDBC directional wave systems have used a Hippy sensor, which is a gimbaled gyro system to measure pitch and roll angles directly. NDBC also developed the MO technique of estimating pitch and roll angles (Steele and Earle, 1991; Teng, *et al.*, 1991) [ref. 47, 51]. It has been proven that the MO method can estimate the pitch/roll angles and, hence, the wave direction information relatively well, especially in areas without long-period swells. Most recently, the ARS technique, which uses angular rate sensors and linear accelerometers to derive the pitch/roll angles, was developed (Steele, et al., 1998) [ref. 49].

NDBC Wave Measurement Systems

Over the years, NDBC has developed and deployed the following wave measurement systems:

- (1) GSBP Wave Data Analyzer (WDA)
- (2) DACT Wave Analyzer (WA)
- (3) DACT Directional Wave Analyzer (DWA)
- (4) VEEP Wave Analyzer (WA)
- (5) Wave Processing Module (WPM)
- (6) Directional Wave Processing Module (DWPM)
- (7) Non-Directional Wave Processing Module (NDWPM)
- (8) Digital Directional Wave Module (DDWM)

	NASA Engineering and Safety Center Technical Report	Document #: NESC-RP-08- 00494	Version: 1.0
Title: Assessment of Orion Crew Module Ocean Wave Model			Page #: 20 of 158

The changes to hulls and wave processing systems are not readily in publicly available data or metadata files, and NDBC should be contacted if such information is needed. The two most recent systems can be distinguished by the frequency bands:

- WPM, NDWPM, DWPM, DDWM: 47 frequency bands, from 0.02 to 0.485 Hz. 0.02 Hz is a noise band and are not used in deriving the bulk wave parameters (e.g., height, period). The sampling rate for these systems 1.7066 Hz and the sampling period can be either 20 or 40 minutes.
- DWA: 38 frequency bands with nondirectional data 0.03 to 0.40 Hz, and 33 frequency bands with directional data, from 0.03 to 0.35 Hz. The sampling rate for DWA is 2.0 Hz and the sampling period is 20 minutes.


Refer to <http://www.ndbc.noaa.gov/wavespectra.shtml> for more details on the differences between WPM and DWA. Refer to Appendix E of this report for more information on data availability and NDBC formats.

6.4.2 Wave Measurements from CDIP

The CDIP is part of the Integrative Oceanography Division, Scripps Institution of Oceanography, at the University of California, San Diego. CDIP's research mission is to develop innovative ways to monitor and predict coastal waves and beach change on regional scales. Since its inception in 1975, CDIP has acquired a large database of publicly-accessible environmental data for use by coastal engineers and planners, scientists, mariners, and marine enthusiasts.

The CDIP currently maintains a network of approximately 36 Datawell Directional Waverider® buoys (22 in CA, 1 OR, 1 WA, 3 HA, 4 FL, 1 VA, 1 NC, 1 NH, 1 Guam, 1 Virgin Islands). Waverider® buoys are relatively small (0.9 m diameter) spheres that are designed to follow the orbital path, or x-y-z translation, of a sea surface water particle. They measure the same wave parameters as NDBC directional buoys, but: 1) Use a slightly different measurement principle (Lagrangian translation) rather than inferring directions directly from the pitch-roll motion of the buoy; and 2) They measure waves nearly continuously (27 minutes of each half-hour). The wave-following method, and longer time series records, allow for more accurate spectral wave measurements, but make the buoy unsuitable for a meteorological measurement mast or the collection of additional time series of other environmental variables (e.g., wind). With the exception of providing the sea surface temperature, the Waveriders® are “waves-only” buoys designed to make the highest quality wave measurements.

Waveriders® use a Hippy pitch-roll sensor affixed with 3 accelerometers. The pitch-roll measurements are used in this instance to place the accelerometer measurements in a fixed North-South, East-West, up-down reference frame. The accelerations are double-integrated to produce time series of the buoy x-y-z motion. These in turn are processed using similar methods

	NASA Engineering and Safety Center Technical Report	Document #: NESC-RP-08- 00494	Version: 1.0
Title: Assessment of Orion Crew Module Ocean Wave Model			Page #: 21 of 158

to those described in the NDBC data description to estimate the wave energy and first 4 directional Fourier coefficients at each wave frequency.

Waveriders® sample at 1.2804 Hz for 1600 seconds each half hour (~27 minutes), producing x-y-z time series with 2048 samples for subsequent onboard processing into spectral parameters in the remaining few minutes of the half-hour cycle. Historically, line-of-sight FM transmission was used, buoys were only deployed relatively close to the coastline, and data was collected on a shore station. The x-y-z data is transmitted in real time (1 time) along with processed spectral data (7 times) from the previous half-hour time period. The redundant spectral data transmission minimizes the potential for spectral data loss. Because the time series themselves are only transmitted once, spikes and gaps in the archived time series can occur owing to transmission errors. These do not affect the spectral data (which were processed onboard the buoy) and identifying these time series errors is described in the Section 6.5 on x-y-z data formats.

Newer Waveriders® are equipped with Iridium satellite communication systems and these buoys can be deployed anywhere there is sufficient Iridium coverage. In addition, they store the x-y-z data onboard, along with the processed spectral data, between Iridium data queries, resulting in more complete x-y-z data sets.

Wave data is provided in many forms on the CDIP website: <http://cdip.ucsd.edu>.

CDIP spectral data is transferred to NDBC in XML format for broader dissemination through the National Weather Service (NWS) system, and is described further at

<http://cdip.ucsd.edu/?nav=documents&sub=index&xitem=product#xml>


In addition, the two file formats, the spectral, or “sp” files and the x-y-z time series, or “xy”, files, are described in more detail in Appendix F of this report. .

The entire archive of CDIP buoy measurements is available at <http://cdip.ucsd.edu>

The last 45 days of CDIP spectral wave data (no time series) are also available from the NDBC website <http://ndbc.noaa.gov> where the CDIP buoys are labeled as "Scripps" stations.

A complete description of CDIP's data processing and quality control procedures can be found at <http://cdip.ucsd.edu/?nav=documents&sub=index&xitem=proc>

CDIP and NDBC are both active participants in QUARTOD (Quality Assurance of Real-Time Ocean Data) under the IOOS (Integrated Ocean Observing System) program. Additional

	NASA Engineering and Safety Center Technical Report	Document #: NESC-RP-08- 00494	Version: 1.0
Title: Assessment of Orion Crew Module Ocean Wave Model			Page #: 22 of 158

information on this topic can be found at

<http://cdip.ucsd.edu/?nav=documents&sub=index&xitem=product#qartod>

6.5 Constellation Program Design for Natural Environments

The DSNE provides design environments for CxP hardware. Sea state design limits are provided for nominal and off-nominal landing conditions. Although values are provided for maximum SWH, minimum average wave period, maximum steady state wind speed and the upper limit of the energy spectrum associated with the respective conditions, the properties reflect values independent of an actual physical wave. For example, a maximum SWH of 4 m does not coincide with a minimum average period of 6 seconds. This allows for a variety of conditions to be specified for different projects and users, but necessitates further refinement for an applications such as determining ocean landing conditions for a given wind speed.


6.6 Orion Crew Module Wave Model

The Orion CM Wave Model “Monte Carlo Ocean Wave Modeling”, Rev D, Draft, was developed for inclusion in the overall CM Landing Model (refer to Appendices B and C in this report). The Monte Carlo wave modeling analysis responsibility will be transitioned to the CM Landing and Recovery System (LRS) team, including the CM prime contractor by March 2009.

The AMA model uses wind speed as the input variable to produce the output attributes of wave slope, wave vertical velocity and wave azimuth or direction. The model uses historical buoy records to determine the variability associated with the attributes for nominal and off-nominal landing winds. The Monte Carlo model then draws upon the distributions to produce a probable representative flat surface for the input wind speed (Figure 6.6-1).

The model identified three major assumptions currently being used in this analysis approach, although others were identified in the assessment process, and indicated that they required future verification:

1. The ocean wave model provides the probability of “point slopes” for a given wind speed, and then the point slope is represented in the impact analysis as an “infinite” flat surface with that slope.
 - Some preliminary analysis testing this assumption was conducted in 2008 by the CM LRS team and follow-on analysis is planned for Feb-March 2009
2. The wave model filters out energy content from waves that have a wave length less than the CM diameter. (Figure 4 in AMA, Inc. report, Appendix B)
 - Analysis to test this assumption is planned for Feb-March 2009 by the CM LRS team

	NASA Engineering and Safety Center Technical Report	Document #: NESC-RP-08- 00494	Version: 1.0
Title: Assessment of Orion Crew Module Ocean Wave Model			Page #: 23 of 158

3. Steady-state wind at 101 m altitude is an appropriate linkage between the Decision Support System (DSS) simulation to the wave model.
 - Assumes that the wind azimuth at 101 m is the reference for wave azimuth
 - Assumes that the 101 m winds can be extrapolated to the surface using the power law to derive wave conditions

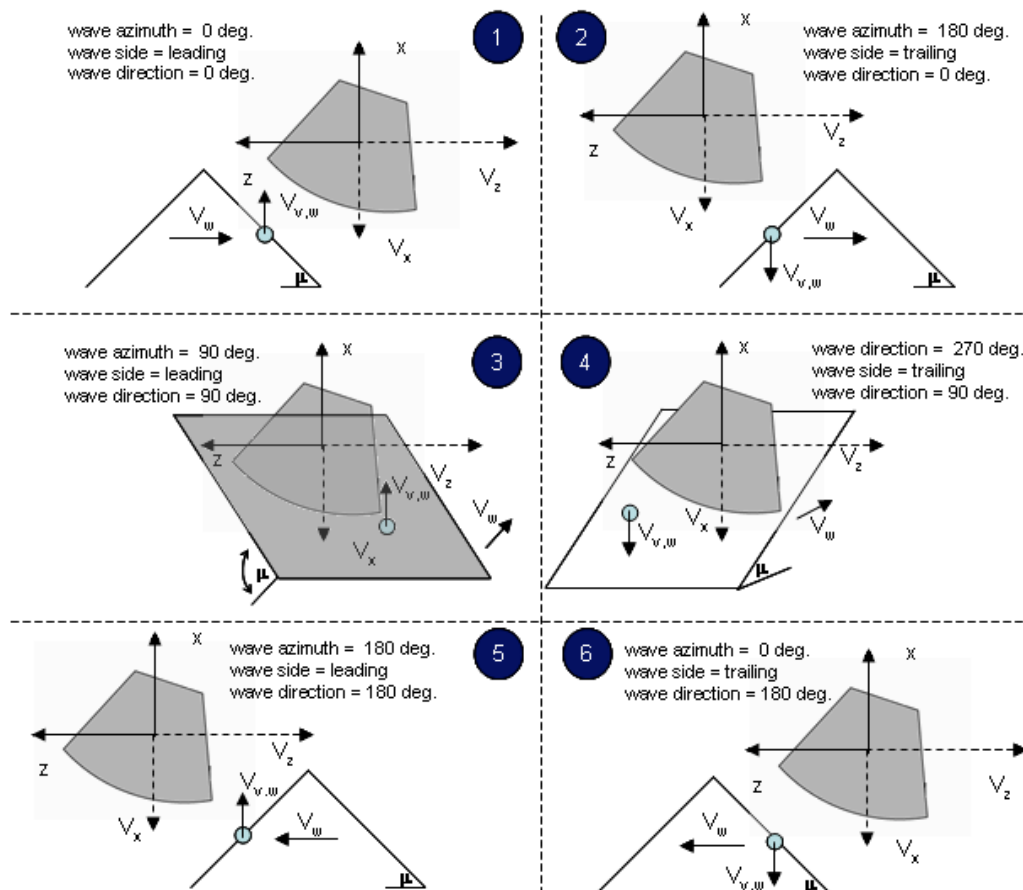



Figure 6.6-1. Crew Module Ocean Landing Scenarios (AMA, Inc. report, Appendix B)

	NASA Engineering and Safety Center Technical Report	Document #: NESC-RP-08- 00494	Version: 1.0
Title: Assessment of Orion Crew Module Ocean Wave Model			Page #: 24 of 158

6.7 Approaches to Model Assessment


The NESC assembled a team of experts with backgrounds in wave modeling, analytical/statistical methods and uncertainty, and buoy data and data sources. The NESC team reviewed the Orion CM Wave Model and generated questions prior to the review with AMA, Inc. The NESC team also requested an overview of the overall CM Landing Model Monte Carlo analysis process used to establish CM landing conditions, CxP DSNE, and nominal and off-nominal landing corridors. The January 2009 AMA, Inc. report review covered the development of the model, data sources, numerical methods, and underlying assumptions. Additionally, an overview of directional spectral analysis methods was presented by Scripps Institute of Oceanography. The NESC team compiled written findings and recommendations based on the AMA, Inc. report, contractor review, and Orion CM landing model. These findings and recommendations are provided in Section 8.0 of this NESC report.

7.0 Data Analysis of the AMA, Inc. Report

7.1 Interfaces to Overall Crew Module Landing Model

Determining the ocean waves, relative to the CM orientation, based upon only wind speed is assumed to be adequate for engineering design, despite a number of complicating factors such as fetch, swell, temperature gradient, and duration. The 10,000 CM orientations produced with the DSS package is treated separately from the 10,000 wave conditions produced with the AMA, Inc. model. Recall, the spectral wave function potentially could have been bounded with DSNE standards, but it was decided to not bound only one parameter while leaving the remaining unbounded for the purposes of Monte Carlo case generation. Similarly, some of the factors that go into the CM descent/trajectory are not included in the wave model which creates some asymmetry in assumptions. To ensure that the results of combining DSS and wave models adequately estimate the quantities of interest, the following conditions were considered:

- Variability of the wave behavior for a given wind speed is captured statistically (even at the low wind speed). As shown in Section 7.1.1, this can be accomplished by explicitly modeling record-to-record variability. This is different than the approach in the AMA, Inc. model that attempts to capture the variability across all wind speeds and later adjusts for the non-normality.
- For a given wind speed, this variability is statistically uncorrelated with the parameters that are used in DSS to simulate CM's flight dynamics. While it is likely the correlation is small, the issue may merit further investigation. It is important to note that it is a statistical correlation (and not causality) that needs to be ruled out.

	NASA Engineering and Safety Center Technical Report	Document #: NESC-RP-08- 00494	Version: 1.0
Title: Assessment of Orion Crew Module Ocean Wave Model			Page #: 25 of 158


After a discrete set of orientations is recovered from this process, the LS-DYNA™ package is then used to determine actual CM impact. Since the AMA, Inc. model is producing a single point result that is being coupled with a geometric result, there is ambiguity in the actual impact conditions. The slopes and vertical velocities predicted by the wave model will also likely be under-predicted due to the reliance on linear wave theory and other oceanographic effects. For these reasons, a sensitivity study with a finite set of deterministic impacts incorporating higher fidelity waves would help bound the expected error. This study could be achieved with some commercial software such as Fluent®/ABAQUS®/MPCII or CFX®/ANSYS®. One of potential issues for concern is the situation where only part of the CM contacts the wave surface upon initial impact (e.g., at the wave crest), which can subject the vehicle to additional rotational moments and cause a change in the effective orientation (including pitch).

7.1.1 Integrated Model and Overall Model Accuracy

The stated objectives of the wave model is to estimate slope, azimuth, and vertical velocity, represented in Section 7.1.1 as s , a , and v , respectively, of an impact point on the ocean surface. Buoy measurements were utilized for statistical characterization of these three parameters. Each buoy record effectively provides a snapshot of the ocean conditions at a given time and place. This snapshot is represented by a combination of sinusoidal waves, so that the quantities of interest can be inferred on a local (e.g., small) scale. More specifically, given a representative cumulative record length T_l (such as the one used for discrete Fourier transform), and assuming a uniform distribution of landing over T_l , it can be inferred the information about the moments of the corresponding physical quantity. In the case of a slope, the mean value is zero due to the symmetry considerations, and the variance σ_s^2 is estimated based on the discrete spectral density function (see Equation 14 of the AMA, Inc. report, Draft D). The corresponding properties of wave azimuth and vertical velocity are estimated similarly (resulting in zero means for both of these parameters).

Altogether six (three variance and three covariance) parameters provide the full description of the model at the local level. Each of these parameters can be interpreted as a physical parameter that characterizes the wave formation on a local time scale (a snapshot). Note the following on the slope characterization, with an understanding that similar analysis can be conducted for other parameters.

Consider multiple records from the same buoy that are collected over the cumulative record length T_g that is several magnitudes higher (e.g., years) than T_l : $T_g \gg T_l$. As a result, the sea conditions will change from record to record, and is σ_s^2 . For each of N records variance can be calculated as $V_{s1} \dots V_{sN}$. As correctly observed in the AMA, Inc. report, total variance can be calculated as:

	NASA Engineering and Safety Center Technical Report	Document #: NESC-RP-08- 00494	Version: 1.0
Title: Assessment of Orion Crew Module Ocean Wave Model			Page #: 26 of 158

$$V_{tot} = \sum_{i=1}^N \int_{-\infty}^{\infty} x^2 f_i(x) dx = \frac{1}{N} \sum_{i=1}^N V_i$$

Since the mean of the total slope distribution is zero, a normal distribution can be constructed in based on V_{tot} . Unfortunately, as observed in the AMA, Inc. report, the underlying distribution is not normal, and can lead to non-conservative estimates of the probability corresponding to a “3-sigma” slope. To compensate, correction factors to σ_s have been suggested (Table 5 of the AMA, Inc. report) that match the overall slope distribution in terms of slopes that are not exceeded with 99.7 percent probability. See Figure 7.1-1.

To understand the sources of the deviation from normal distribution qualitatively, consider a simple scenario of combining two records with variances $V_1 = 1.5$ and $V_2 = 0.5$, correspondingly,

$$V_{tot} = \frac{1}{2}(1.5 + 0.5) = 1$$

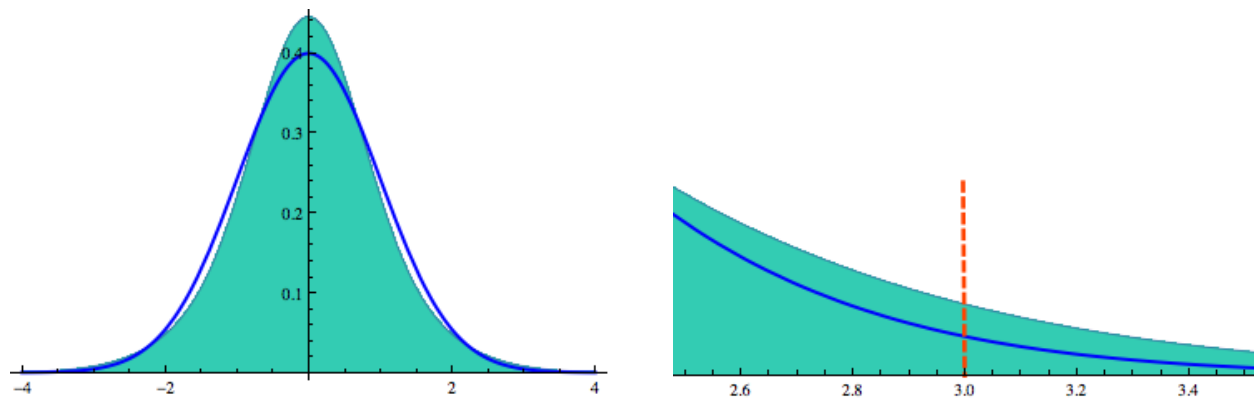



Figure 7.1-1. Probability Density Function for the Total Distribution (Blue Line Corresponds to a Standard Normal Distribution)

Calculating $P_{tot}(|x| \leq 3) = 0.9928$ can be contrasted to $P_{normal}(|x| \leq 3) = 0.9973$ for normal distribution with the same variance. It is also noted that standard deviation decreases slightly $\sigma_{tot} = 0.9659 < 1 = \sigma_{normal}$. To characterize the variability of σ_s or σ_s^2 for multiple records (i.e., variability of the ocean conditions at the time scale T_g), an appropriate statistical model can be selected. For the sake of specificity, in what follows modeling of σ_s is considered with understanding the choice between σ_s and σ_s^2 that can be made based on comparison between the data fits, which also depends on the selected parametric distribution. This selection is

	NASA Engineering and Safety Center Technical Report	Document #: NESC-RP-08- 00494	Version: 1.0
Title: Assessment of Orion Crew Module Ocean Wave Model			Page #: 27 of 158

complicated by the requirement of the values to be non-negative, so a normal distribution $\sigma_s = N[\mu_{\sigma_s}, \sigma_{\sigma_s}]$, here μ_{σ_s} and σ_{σ_s} , is the corresponding parameters of normal distribution will only be practical if negative values are highly unlikely (e.g., $\mu_{\sigma_s} > 3\sigma_{\sigma_s}$). In general, either lognormal distribution or truncated normal distribution can be used with the choice between the two driven by the data fit.

The following are alternative procedures for capturing direct record-to-record variability:

1. Obtain first two moments based on the individual records:

$$\mu_{\sigma} = \frac{1}{N} \sum_{i=1}^n \sigma_i, \quad \sigma_{\sigma} = \frac{1}{N-1} \sum_{i=1}^n (\sigma_i - \mu_{\sigma})^2$$

2. Use those moments to determine parameters of selected distribution: $\tilde{\mu}_{\sigma}$ and $\tilde{\sigma}_{\sigma}$
3. Evaluate overall slope probability distribution function. For the case of truncated normal distribution:

$$\tilde{f}(x) = \frac{1}{2\pi\tilde{\sigma}_{\sigma}\beta} \int_0^{\infty} \frac{1}{y} \exp\left(-\frac{x^2}{2y^2} - \frac{(y - \tilde{\mu}_{\sigma})^2}{2\tilde{\sigma}_{\sigma}^2}\right) dy$$

$$\beta = \int_0^{\infty} \exp\left(-\frac{(y - \tilde{\mu}_{\sigma})^2}{2\tilde{\sigma}_{\sigma}^2}\right) dy$$


It is important to note that for Monte Carlo simulation step 3 is not required: instead first σ_s is sampled in accordance with the parameters obtained in step 2, and the result is used to determine the parameter of normal distribution, which is then sampled to obtain a slope.

From this perspective, the assumption made in the AMA, Inc. report that total variability of the slope can be represented by a normal distribution is equivalent to setting σ_{σ_s} to zero. To demonstrate potential importance of large scale variability, refer to Figure 3 of the AMA, Inc. report. Because the low wind speeds demonstrate high variability, there could be a scenario with winds of 2.286 m/s where individual records indicate that σ_s is banded somewhere between 1.5 and 4.5 degrees with mean around 3 degrees. For this example, consider $\mu_{\sigma} = 3.0, \sigma_{\sigma} = 1.5$.

Following the outlined above procedures, calculate corresponding parameters of truncated to non-negative values normal distribution: $\tilde{\mu}_{\sigma} = 2.846, \tilde{\sigma}_{\sigma} = 1.647$. It is noted

that $\sigma_{eq} = \sqrt{V_{tot}} = 3.354 > \mu_{\sigma} = 3$. Comparing “3-sigma” slopes, observe:

$$P(s > 3\sigma_{eq}) = 0.00656 \text{ cf. } 0.00135.$$

	NASA Engineering and Safety Center Technical Report	Document #: NESC-RP-08- 00494	Version: 1.0
Title: Assessment of Orion Crew Module Ocean Wave Model			Page #: 28 of 158

Following the procedures outlined in the AMA, Inc. report, calculate correction factor (as in Table 3 of AMA, Inc. report), $\sigma_{scaled} = 4.057 = 1.21\sigma_{eq}$, the AMA, Inc. report indicates a 1.25 correction factor, so the studied effect is stronger. Figures 7.1-2a and b demonstrates the difference between the modeled distribution (green) and its approximations (blue is normal distribution based on total variance, and purple is the normal distribution with correction factor).

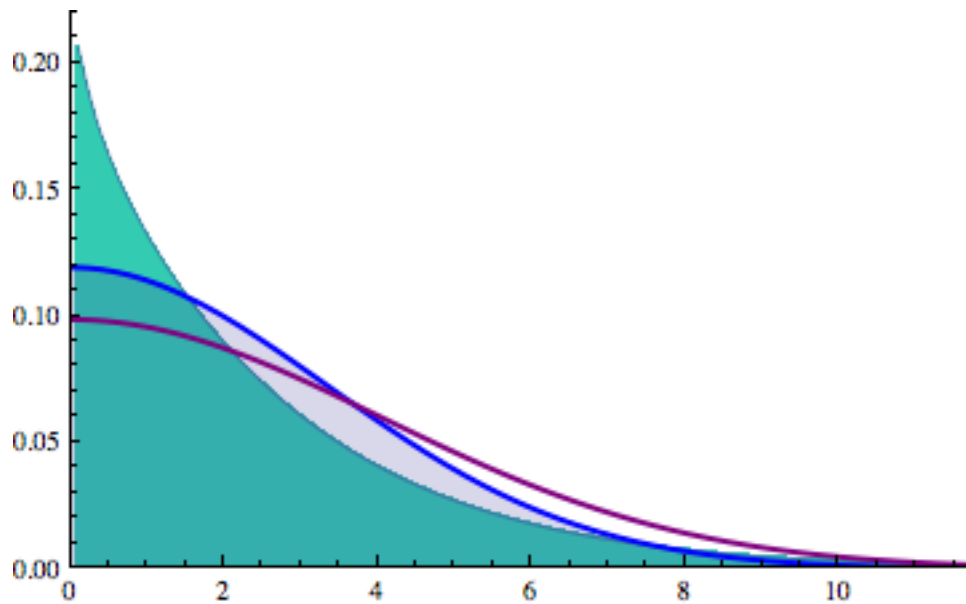



Figure 7.1-2a. Difference between the modeled distribution (green) and its approximations (blue is normal distribution based on total variance and purple is the normal distribution with correction factor).

	NASA Engineering and Safety Center Technical Report	Document #: NESC-RP-08- 00494	Version: 1.0
Title: Assessment of Orion Crew Module Ocean Wave Model			Page #: 29 of 158

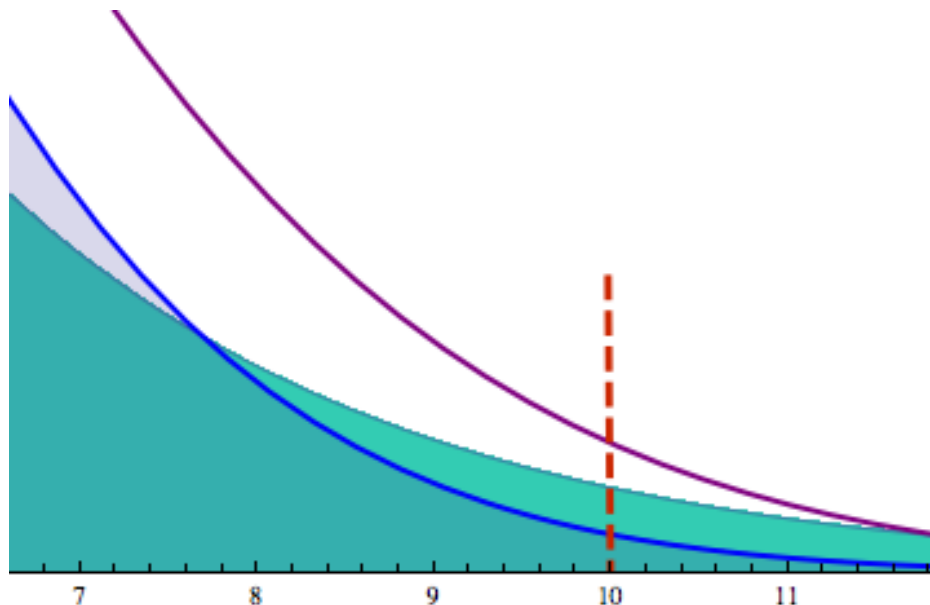



Figure 7.1-2b. (Zoom in of Figure 7.1-1a): Difference between the modeled distribution (green) and its approximations (blue is normal distribution based on total variance and purple is the normal distribution with correction factor).

Figure 7.1-2a and 7.1.2b show that distributions are significantly different.

In this context, it is concluded that the use of confidence intervals to account for variability of the slope at the global scale is not appropriate. Confidence intervals are useful in estimating the uncertainty about a physical parameter due to the lack of knowledge about the value of this parameter (so called epistemic uncertainty), most commonly due to the limited number of samples. As a result, as the sample size increases this uncertainty is reduced and the interval shrinks. All standard confidence interval estimations rely on this limiting property. In contrast, in this application, there is an inherent variability of the slope variance due to (global time scale) changes in sea conditions. This variability cannot be reduced with the increase of number of samples (individual records), and the use of confidence intervals is not appropriate, which explains the failure of the classical confidence intervals properly bound the observed data as was observed in the AMA, Inc. report. The AMA, Inc. report correctly states that providing a refined model for wave conditions and introducing some other explanatory variables will reduce this residual (unexplained) variability. However, creating such a model is challenging and, even if such a model is created, in order to use it as in input to Monte Carlo simulation, statistical representation of the input parameters would need to be provided. Therefore, it is simpler to provide a direct statistical characterization of the global scale variability.

	NASA Engineering and Safety Center Technical Report	Document #: NESC-RP-08- 00494	Version: 1.0
Title: Assessment of Orion Crew Module Ocean Wave Model			Page #: 30 of 158

In the current approach in which the variance of the slope is the primary Monte Carlo parameter, the as utilized confidence intervals are not an appropriate measure of accuracy. Including the global time scale variability results in a potentially 4.68 degree difference in equally likely wave slopes. As reported in Page 16 of the AMA, Inc. report, a difference of 4 degrees is significant to the designers. Indeed, this magnitude of difference occurred due to not accounting for wave direction in the Apollo Program model.

In addition, the second step of the model integration adjusts the 3-sigma slope to account for the non-normality of the effective variance that adjusts the effective slope variance. This special treatment of one of the variables is not done to the other variables used in the Monte Carlo analysis, perhaps biasing the outcome. The key point is to ensure all variables are treated similarly to produce a true Monte Carlo spread of cases when integrated with the similarly generated set of CM orientations.


7.1.2 Model Verification

The output from the AMA, Inc. wave model 99.7 percentile (3-sigma if normal) for slope and vertical velocity is used to define a plane for the impact analysis. This treatment has the advantage of being testable in a physical laboratory by dropping an instrumented command module from appropriate height and providing actual measurements of structural forces.

The AMA, Inc. Buoy-Based Wave Model was validated by comparing with both experimental and simulated data. The small wave tank data of Mase and Kirby could be replicated using a Computational Fluid Dynamics (CFD) Volume of Fluid (VOF) method to expand the scales to something more appropriate for the CM dimensions. Highly parallel computing currently can include the nonlinear effects currently unaccounted for in the model. The issue is determining the level of fidelity required for accurate CM impact analysis. In particular, the multi-wave simulated results shown in the last figure of the AMA, Inc., Report addendum showed the model was not converging with the data, and a reason for the discrepancy was not available.

Alternative approaches include:

- Define a boundary region that envelopes the landing region and utilize either the AMA, Inc. wind based model or actual buoy data to define point slope/velocity conditions.
- Apply a VOF method that includes atmospheric shear and directly solve the resulting nonlinear wave field within this region.
- Time-accurately model the impact of the CM into the ocean utilizing commercially available software
- Repeat for as many wind conditions as is practical to determine the statistical confidence of the current AMA/LS-DYNA™ impact results.

	NASA Engineering and Safety Center Technical Report	Document #: NESC-RP-08- 00494	Version: 1.0
Title: Assessment of Orion Crew Module Ocean Wave Model			Page #: 31 of 158

Overall, higher fidelity wave modeling and closer integration of the trajectory assumptions with the wave assumptions could improve the accuracy. By performing alternate verifications and impact sensitivities studies, it may be concluded the current approach is adequate, although it is not currently demonstrated.


7.1.3 Other Salient Model Assumptions

As noted in Section 6.6, Orion CM Model, the flat surface impact plane, wave high frequency cutoff value, and wind altitude extrapolation are assumptions that require further investigation.

The modeling analysis does not allow for the water surface to be represented by anything other than a flat surface impact plane (as shown in Figure 6.6-1). Although the model captures slope, vertical velocity and direction or azimuth, it is noted that the horizontal motion of the representative flat surface is not a predicted model variable. The present study does not provide information on the effect of the following: 1) landing on convex surface such as a wave crest; 2) landing on a concave wave form surface; and 3) landing on a rough surface, such as breaking waves, and its potential impact to Orion CM Water Landing dynamic analysis. While such questions may be beyond the scope of the wave model, the NESC team recognizes that these simplifying assumptions should be addressed as part of the design process.

Although the Apollo Program model assumed a cutoff frequency/wavelength relative to the vehicle diameter, the model assigned frequency of 0.56 Hz cutoff as associated with the larger Orion CM diameter may prove to be a limiting assumption with respect to design. The assumptions of a flat surface impact plane are related to establishing limits, either discrete or gradual, of the assigned frequency/wavelength cutoff. Sufficient analytical justification to defend the cutoff frequency has not been provided although it is addressed in Figure 4 in the AMA, Inc. report. It is recognized that the buoy data has a practical high frequency limit of measurement and that analytical methods must be employed to estimate the appropriate high frequency energy.

There are different methods of adjusting winds to the 10-m reference level in the source documents. For example, the 10-m wind in DSNE uses the method of Bidlot (2002) [ref. 7], while the AMA, Inc. report uses the method of Hsu, *et al.* (1994) [ref. 28], and the Orion CM Wave Model uses an undocumented method for the reduction of the 101-m wind (see Section 6.6) to the 10-m reference level. Some of the implications were discussed in this report, under the *Review of Wind Measurements from NDBC Buoys* section. Further avenues to explore would be the offshore wind power industry, which has been reinvigorated by recent energy concerns. The turbine hubs are generally at a height of 80 m, so studies of wind power potential have an interest in exploiting the more numerous low-level wind measurements to estimate wind power

	NASA Engineering and Safety Center Technical Report	Document #: NESC-RP-08- 00494	Version: 1.0
Title: Assessment of Orion Crew Module Ocean Wave Model			Page #: 32 of 158

at height. Examples of such studies are Giebel (2003) [ref. 22], Archer and Jacobson⁴ (2003 and 2004) [ref. 2, 3], Dvorak *et al.* (2007) [ref. 18], and van der Berg (2008) [ref. 54].

7.2 Use of Buoy Data to Drive the Monte Carlo Wave Model

The wave model developed to analyze Orion CM water landing conditions uses actual wind and wave measurements as input to the method. Given the critical nature of the wave measurements, it is important to fully understand what wave data is available, how this information may differ depending on the type of wave sensor and/or instrument platform used to collect the data, and how wave data varies geographically owing to changes in the wave climate.

7.2.1 Wave Data Availability


Ocean wave measurements collected by the NDBC, with pitch-roll buoys, and the CDIP, with translational Waverider® buoys, are used to derive the Monte Carlo Wave Model inputs (sea surface vertical velocity, slope, and azimuth). NDBC and CDIP are the primary collectors of wave data in the U.S. and their data archives represent the vast majority of in situ directional wave data that is available for research and design.

A critical initial assumption was that direct observations of the three Monte Carlo Model sea surface variables do not exist and therefore need to be derived from buoy measurement estimates of spectral wave energy $S(f)$ and the first four directional Fourier coefficients, $a_1(f)$, $b_1(f)$, $a_2(f)$, $b_2(f)$, also known as the “First 5” spectral wave parameters, at each wave frequency, f , of interest.

In reality, both pitch-roll and translational buoys measure time series of vertical displacement and sea surface slopes, or North-South and East-West buoy translation, that can be recast as continuous sea surface velocities, slopes, and azimuths. Historically, the time series were mainly of use to a limited number of wave researchers and the datasets were too large to transmit via satellite. As a result, NDBC has not routinely stored the time series, but instead processes this information down to the First 5 spectral data onboard the buoy for transmission and dissemination.

Alternatively, CDIP Waveriders® are Lagrangian “wave-followers” and continuously measure the x-y-z translation of the sea surface every 0.78 seconds with O(few cm) of accuracy. They have used FM data transmission to shore (and now also use Iridium satellite transmission) and can transmit both the time series and the processed First 5 parameters. The time series are


⁴ Archer and Jacobson’s research at Stanford University has been sponsored by NASA GRC led wind turbine development in the 1970s and early 1980s.

	NASA Engineering and Safety Center Technical Report	Document #: NESC-RP-08- 00494	Version: 1.0
Title: Assessment of Orion Crew Module Ocean Wave Model			Page #: 33 of 158

archived on the CDIP website and can be used to make continuous sea surface slopes and vertical velocity estimates without assuming the waves are linear.

This vast, but somewhat obscure, CDIP time series archive was overlooked in the current study and could significantly improve both the direct assessment of the three sea surface variables (in places where CDIP buoys exist) as well as validate the methodology used to estimate the statistical properties of these variables from First 5 data only, in regions covered by the more extensive NDBC buoy network. From a future operations point of view, CDIP buoys presently operate near Cape Canaveral, FL and offshore of CA, and can routinely provide real-time slope velocity, and azimuth statistics in these abort/recovery regions for mission managers. The following website was developed for this NESC assessment to illustrate the capability of obtaining the model data: (http://cdip.ucsd.edu/themes/user_groups/nasa). See Figure 7.2-1.

The NESC team noted that NASA may wish to consider sponsoring the deployment of a directional wave buoy in proximity to the nominal landing zone, or other locations of interest, that can be used for design verification and operational measurements.

	NASA Engineering and Safety Center Technical Report	Document #: NESC-RP-08- 00494	Version: 1.0
Title: Assessment of Orion Crew Module Ocean Wave Model			Page #: 34 of 158

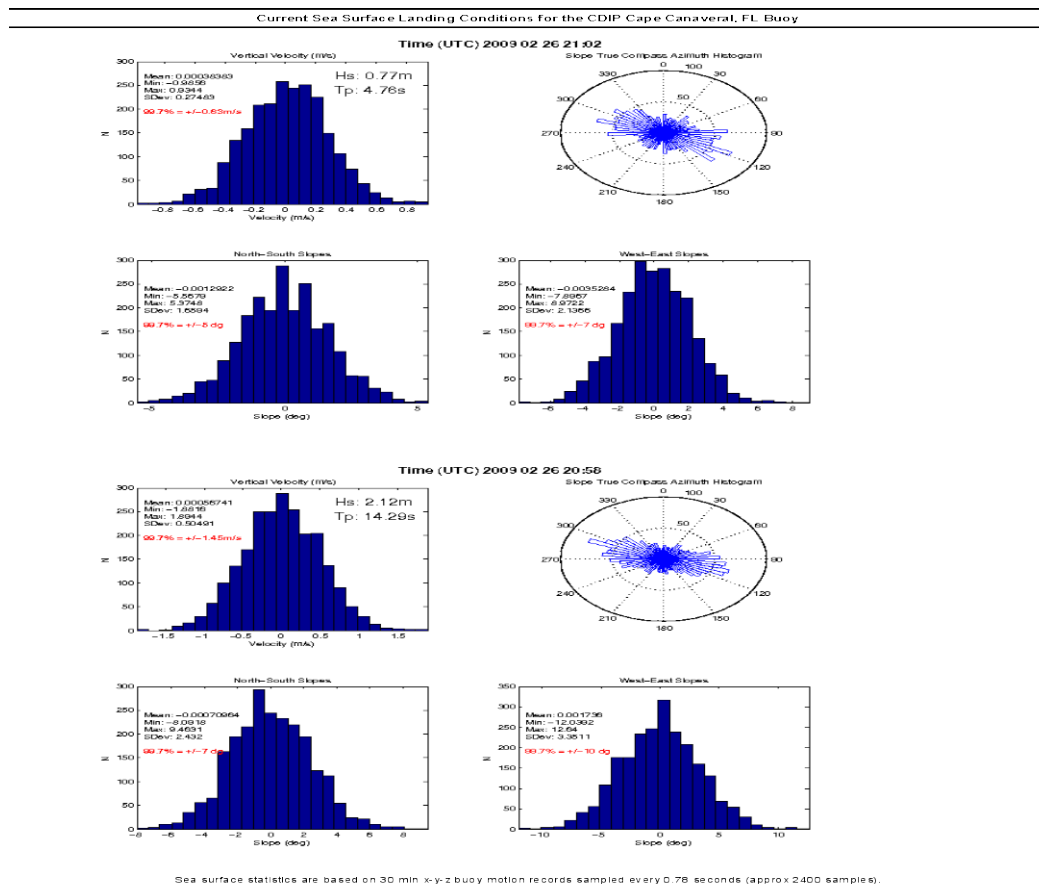



Figure 7.2-1. Current Sea Surface Landing Conditions for the CDIP Cape Canaveral, FL Buoy

7.2.2 Buoy Data Synthesis and Correlations: Slope, Vertical Velocity, and Azimuth

Operating under the assumption that no direct measurements of Monte Carlo Wave Model input parameters were available, they were derived from buoy First 5 spectral data, using linear wave theory, and the Maximum Likelihood Method (MLM) directional estimator. However, there are three ways this approach can potentially lead to underestimation of Monte Carlo input parameters.

First, NDBC buoys are known to overestimate directional spread owing to measurement noise (a combination of complicated buoy hull-wave-wind load response characteristics, and motion sensor fidelity) [ref. 43]. This is a documented trade-off on the part of NDBC to have a more stable platform and sufficient power to measure many other ocean and air variables (e.g., wind). The degree of spread overestimation is a function of the type of NDBC platform being used, and

	NASA Engineering and Safety Center Technical Report	Document #: NESC-RP-08- 00494	Version: 1.0
Title:	Assessment of Orion Crew Module Ocean Wave Model		Page #: 35 of 158

the type of motion sensor in the platform. Overestimates of spread lead to a more irregular/less coherent interpretation of the sea surface. This, in turn, leads to an underestimate of larger slopes for waves close to the peak wave direction, and a more modest overestimate of slopes of waves far from the peak direction. These spread errors result in underestimating the magnitudes of First 5 variables a_1 , b_1 , a_2 , and b_2 , which are used in estimating the slope and azimuth statistics for the Monte Carlo simulations. In cases where an NDBC sensor/platform combination has been compared to a Waverider® buoy, these biases can be removed to some degree. However, NDBC uses numerous types of directional wave sensors and platform configurations, and quantifying the First 5 accuracy of these combinations is beyond their current operational directive, so some of these biases will have to be dealt with in a more ad-hoc fashion.

Second, using linear theory to convert buoy energy spectra to slope spectra will underestimate the slope and vertical velocity. Wave field nonlinearities, particularly when a buoy is in an area of active wind-wave generation, will lead to steeper slope statistics than linear theory would predict. This is routinely observed in CDIP buoy data when the linear theory "check ratio" (ratio of horizontal to vertical buoy motion) falls below 1.0 at higher wave frequencies on windy days. Validation with measured velocities from the CDIP buoys could be used to correct for this underestimate.

Third, using the MLM directional estimator will overestimate directional spreads of the resulting data set (leading to slope under prediction as described above). The 2D energy density spectrum is defined as $S(f, \theta) = D(f, \theta)E(f)$, where $D(f, \theta)$ is the normalized directional distribution and $E(f)$ is the 1D energy density spectrum. The function $D(f, \theta)$ is normalized such

$$\text{that } \int_0^{2\pi} D(f, \theta) d\theta = 1.$$


There exists a separate directional distribution function for each frequency component that can be decomposed into a Fourier series:

$$D(f, \theta) = \frac{1}{\pi} \left[\frac{1}{2} + \sum_{n=1}^{\infty} \{a_n \cos(n\theta) + b_n \sin(n\theta)\} \right] \quad (\text{EQ. 2})$$

where

$$a_n(f) = \int_0^{2\pi} D(f, \theta) \cos n\theta d\theta, \quad (\text{EQ. 3})$$

$$b_n(f) = \int_0^{2\pi} D(f, \theta) \sin n\theta d\theta,$$

	NASA Engineering and Safety Center Technical Report	Document #: NESC-RP-08- 00494	Version: 1.0
Title: Assessment of Orion Crew Module Ocean Wave Model			Page #: 36 of 158

The first four Fourier coefficients (a_1 , b_1 , a_2 , b_2) can be inferred from the signals measured by a heave-pitch-roll directional buoy. This permits only an approximation from the truncated Fourier series (Longuet-Higgins et al. (1963) [ref. 36, 37], Kuik et al. (1988)) [ref. 33]:

$$D^*(f, \theta) = \frac{1}{\pi} \left[\frac{1}{2} + \sum_{n=1}^2 \{a_n(f) \cos(n\theta) + b_n(f) \sin(n\theta)\} \right] \quad (\text{EQ. 4})$$


Unfortunately, equation 3 has limited utility for describing $D(f, \theta)$, since it is only accurate if the unmeasured, higher order Fourier components are small. One possible manifestation of this inaccuracy is negative values of $D^*(f, \theta)$. Parametric models (such as the \cos^{2s} form) and data-adaptive methods have been developed to yield more natural (and thus presumably more accurate) representations of $D(f, \theta)$ given the measured low order moments. However, these models give details of $D(f, \theta)$ that are not actually determinable from buoy motion. Further, at least one commonly used data-adaptive method (the MLM) produces $D(f, \theta)$ inconsistent with the original cross-spectral matrix elements (Oltman-Shay and Guza 1984) [ref. 42]. More detail can be found on this topic in Cartwright (1967) [ref. 11], Steele et al. (1985) [ref. 45] and Benoit et al. (1997) [ref. 6].

Finally, other hull-mooring response problems can arise from time to time, which may require additional quality control prior to use in detailed sea surface studies such as this assessment. For example, the report is using station 41048 which is one of NDBC's 12-m hulls. The directional data above 0.20 Hz on 10- and 12-m hulls can be affected by currents because of a protruding retrieval pendant that acts like a rudder in strong currents resulting in motions at the wave frequencies (Steele, 1997) [ref. 46].

7.2.3 Atlantic and Pacific Wave Climates

The offshore wave climate along the U.S. coastline varies significantly between the Atlantic and Pacific and with latitude along both the East and West coasts. This variability requires consideration in design and operational wave modeling.


Buoys are point source measurements of wave conditions at that location. However, the generation, growth and propagation of surface gravity waves are based on “self-similarity” principles. This implies waves created in a small inland lake have similar characteristics to that of waves generated in the middle of the Pacific Ocean basin. At the boundary layer (air water interface) winds transfer momentum to the free surface and forms waves. Other mechanisms force the spectral shape, the downshifting in frequency, a limiting form of the spectra are part of this “self-similar” process. The overriding difference between the wave climate in an inland lake and the middle of the Pacific Ocean is to factor in the geographical variability. The length at

	NASA Engineering and Safety Center Technical Report	Document #: NESC-RP-08- 00494	Version: 1.0
Title: Assessment of Orion Crew Module Ocean Wave Model			Page #: 37 of 158

which the wind blows in the Pacific Ocean is orders of magnitude (for a small inland lake) greater and thus the wave climate is substantially higher. Also the forcing function or the wind conditions between these two areas are highly variable. Scaling of the winds to the wave energy or other variables can be performed. However, care must be taken in that the general characteristics of the geographical variability will differ.

Construction of a wave climate can be performed on various parameters. This analysis is simplified to one parameter, the SWH, because it is one of the primary criteria in the DSNE and it represents the integral property of the energy level of a given spectrum. Despite this simplification, the analysis will reflect the sensitivity geographical and temporal variations of the wave climate and is reflective of the variability of the key factors of interest of the wave model. The analysis is based on archived NDBC buoy data. Time periods selected were based on that data availability and consistency in the buoy location, measurement device, and analysis packages. The complete set of analysis graphics are provided in Appendix D.

The first assumption of geographical invariance in a wave climate is shown in the Figures 7.2-2 and 7.2-3. Figure 7.2-2 is derived from a NDBC buoy 44004, in the off-nominal path located east of Cape Hatteras in approximately 3200-m of water. The four panel plot provides the time variation in probabilities of SWHs less than 1-m; 1- to 2-m; 2- to 2-m and; 3- to 4-m for the period of 1990 through 2008. The figure shows the majority of the wave conditional probabilities at this particular location have SWHs less than 2-m. There are instances where the probabilities for the next two larger wave heights rarely exceed 0.35. Also, the probabilities for the 1- to 2-m SWHs are over the average invariant in time and average around 0.4. This means the wave climate will see SWHs of 1- to 2-m 40-percent of the time. It is also apparent wave heights less than 1-m are temporally variable not only seasonally but also from year to year. Using this argument a second set of data are derived from a NDBC buoy 46047 (1999-2008 record) located south of the Southern California Bight region. The highest probability of wave height conditions is contained in the class of SWHs between 1- and 2-m contrasting that of the previous example. The results for the class of heights between 2- and 3-m at this location again suggesting the population of larger SWH conditions will be greater than that at the location in the Atlantic. Differences in the wave climate at other sites in the Atlantic Ocean were analyzed and are provided in Appendix D. The general characteristics of the Atlantic sites suggest a gradient in a larger SWH population progressing from south-to-north. This is indicative of the trends of in the meteorological forcing, where Northeasters form in the south, increase in intensity, then migrates in a north easterly direction toward the North Atlantic. The largest SWHs are caused by tropical systems south of Cape Hatteras. The population of these events is not as persistent as in the case of Northeasters, and thus reduces the probability densities of larger SWHs.

	NASA Engineering and Safety Center Technical Report	Document #: NESC-RP-08-00494	Version: 1.0
Title: Assessment of Orion Crew Module Ocean Wave Model			Page #: 38 of 158

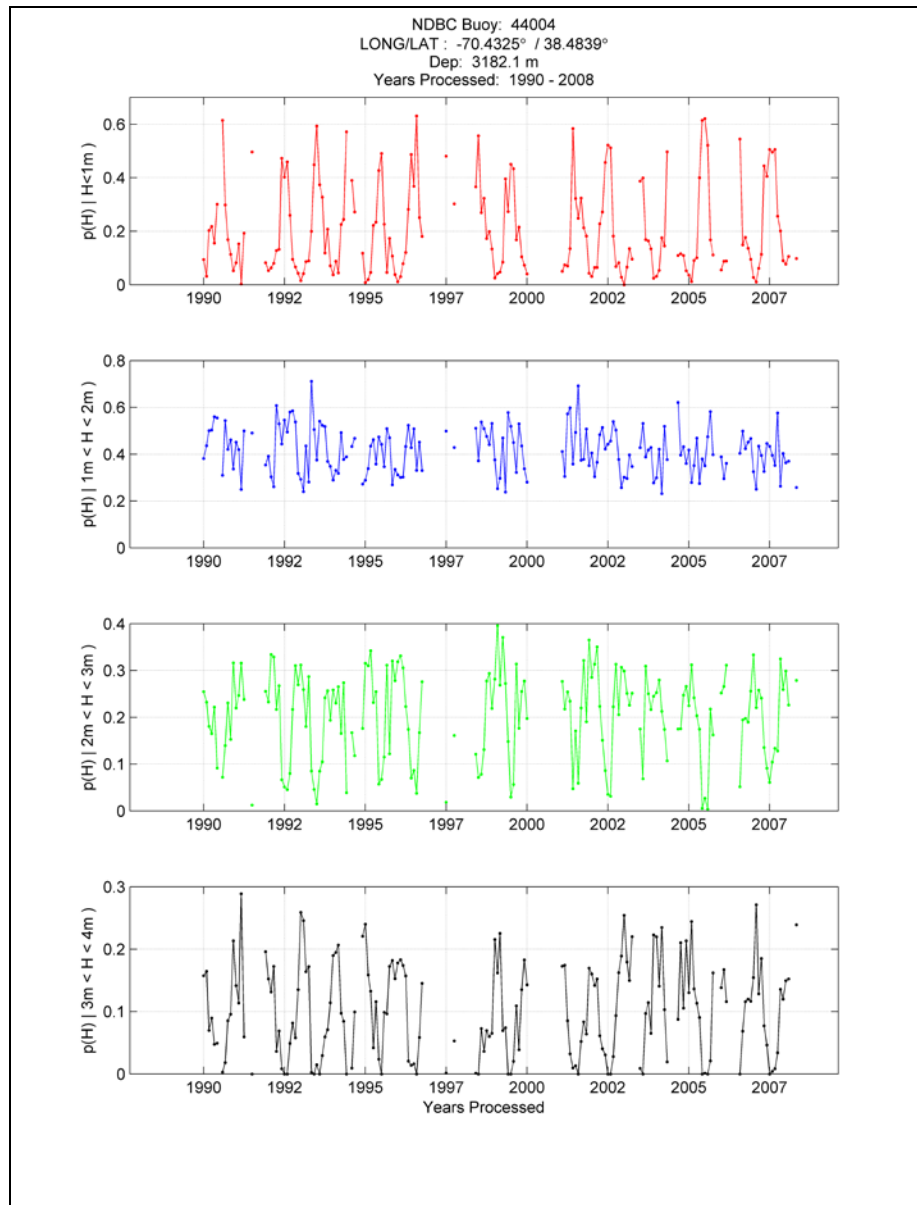



Figure 7.2-2. Classification of Wave Climate at NDBC Buoy 44004 at various Significant Wave Height Categories

The persistence of higher probabilities for larger SWHs at the Pacific buoy (46047, Figure 7.2-3) is influenced by its location. This buoy is positioned south of a well defined sheltered region defined by Point Conception. Winter and early spring storm waves generated from massive

	NASA Engineering and Safety Center Technical Report	Document #: NESC-RP-08- 00494	Version: 1.0
Title: Assessment of Orion Crew Module Ocean Wave Model			Page #: 39 of 158

synoptic-scale meteorological systems found in the North Pacific can impact the wave climate at 46047.

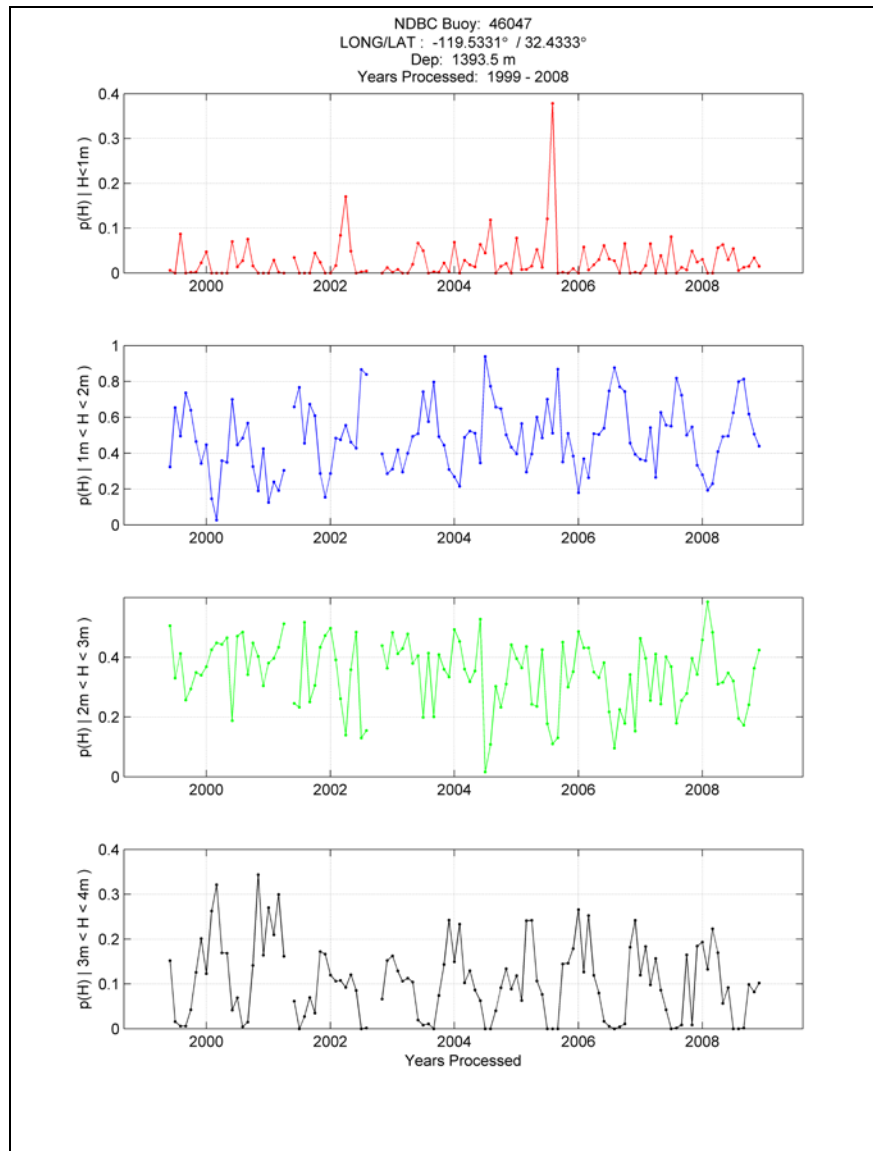



Figure 7.2-3. Classification of Wave Climate at NDBC Buoy 46047 at various Significant Wave Height Categories

Accompanying this wave energy are tropical systems moving off the Mexico/Central America region, propagating to the west and sending swells into the Southern California domain. These examples illustrate the differences in the wave climate from location to location, and application

	NASA Engineering and Safety Center Technical Report	Document #: NESC-RP-08- 00494	Version: 1.0
Title: Assessment of Orion Crew Module Ocean Wave Model			Page #: 40 of 158


of the Monte Carlo Wave Model must account for these differences. While these differences are great, there is an over-riding rule that all waves follow a self-similar process. It then becomes a question of what are the differences in the wave climate from location to location that will influence the results.

Not only does the wave climate vary geographically, but will vary temporally. The time scales can be rapid, as in the case of a storm evolution. The mid-level oscillation period can be defined as seasonal, where low significant wave heights occur in the summer months and become larger in the winter months. These differences can be seen in Figures 7.2-2 and 7.2-3 for the probability densities of the lowest wave height class ($H < 1\text{-m}$ top panel in both figures). The longest definable oscillation period is yearly up to decade changes in the wave climate. Yearly variations can be caused by an increase or decrease in extra-tropical or in storminess, added tropical systems, or a change in the jet stream that controls the path of the meteorological systems. Decadal changes are a result from El Niño and La Niña events typically affecting the wave climate along the Pacific Coast, and the Southern California Bight region. These effects are better reflected in the mean and variance of SWHs as illustrated in Figures 7.2-4 and 7.2-5 where the data are obtained from NDBC Buoy 44004 and 46047.

The short term temporal variations derived from an individual storm will not be evident in Figures 7.2-4 and 7.2-5 because of the averaging procedure used in the analysis. However, the monthly variations are evident where the mean SWHs oscillate between a low of 1-m to a maximum of nearly 4-m at 44004 (Figure 7.2-4). The monthly changes at 46047 are more variable, where the pattern from the highs of 3-m to the lows of about 1.25-m do not transition as smoothly as in the case at 44004. There is a consistent level of mid-wave heights that persist over time. There is also a well-defined dependency between the mean SWH and the variance. As the mean increases, so does the variance.

The longer term variation in the wave climate is also evident at both buoy locations. Tracking the upper limits of both mean SWH data, there is an apparent longer period oscillation and/or year to year variation. For the Pacific buoy 46047 it is the effects of El Niño, where the record is at 44004 (Atlantic buoy), the pattern reflects the storminess along with an influx of tropical systems.

This brief analysis shows that there are geographical and temporal variations in any set of buoy data. Limiting the data set to one specific location or for a short duration will have an effect on final results. There is no set method to choose the “typical” wave conditions or generalize the characteristic of a wave climate. Point source measurements reflect environmental conditions at that particular location. There is an overriding factor: wind wave growth and mechanisms are “self-similar”. However, that only applies to the local wave generation characteristics.

	NASA Engineering and Safety Center Technical Report	Document #: NESC-RP-08- 00494	Version: 1.0
Title: Assessment of Orion Crew Module Ocean Wave Model			Page #: 41 of 158

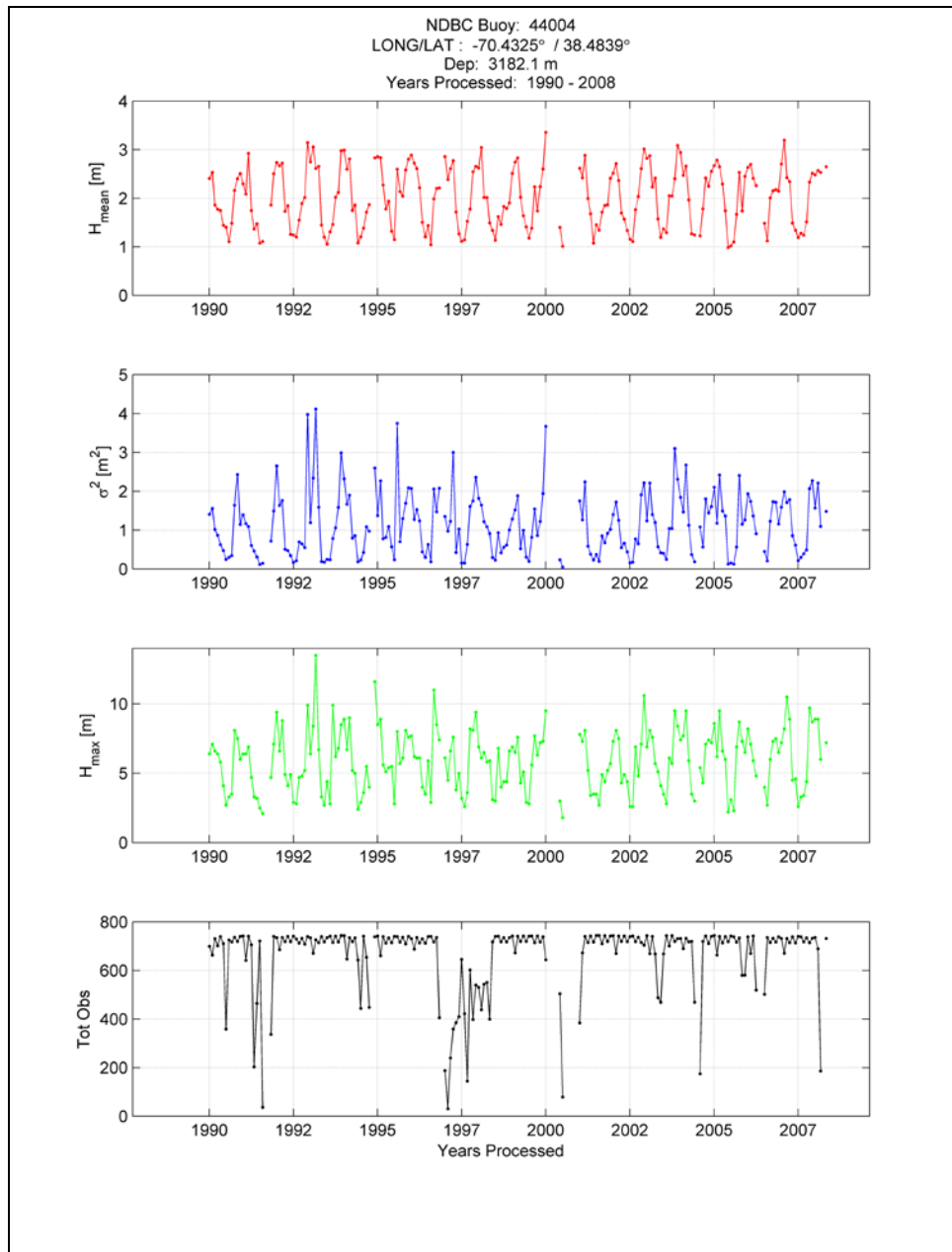



Figure 7.2-4. Monthly Averaged Mean Significant Wave Height, variance in the Mean, Maximum and Number of Observations at NDBC Buoy 44004

	NASA Engineering and Safety Center Technical Report	Document #: NESC-RP-08- 00494	Version: 1.0
Title: Assessment of Orion Crew Module Ocean Wave Model			Page #: 42 of 158

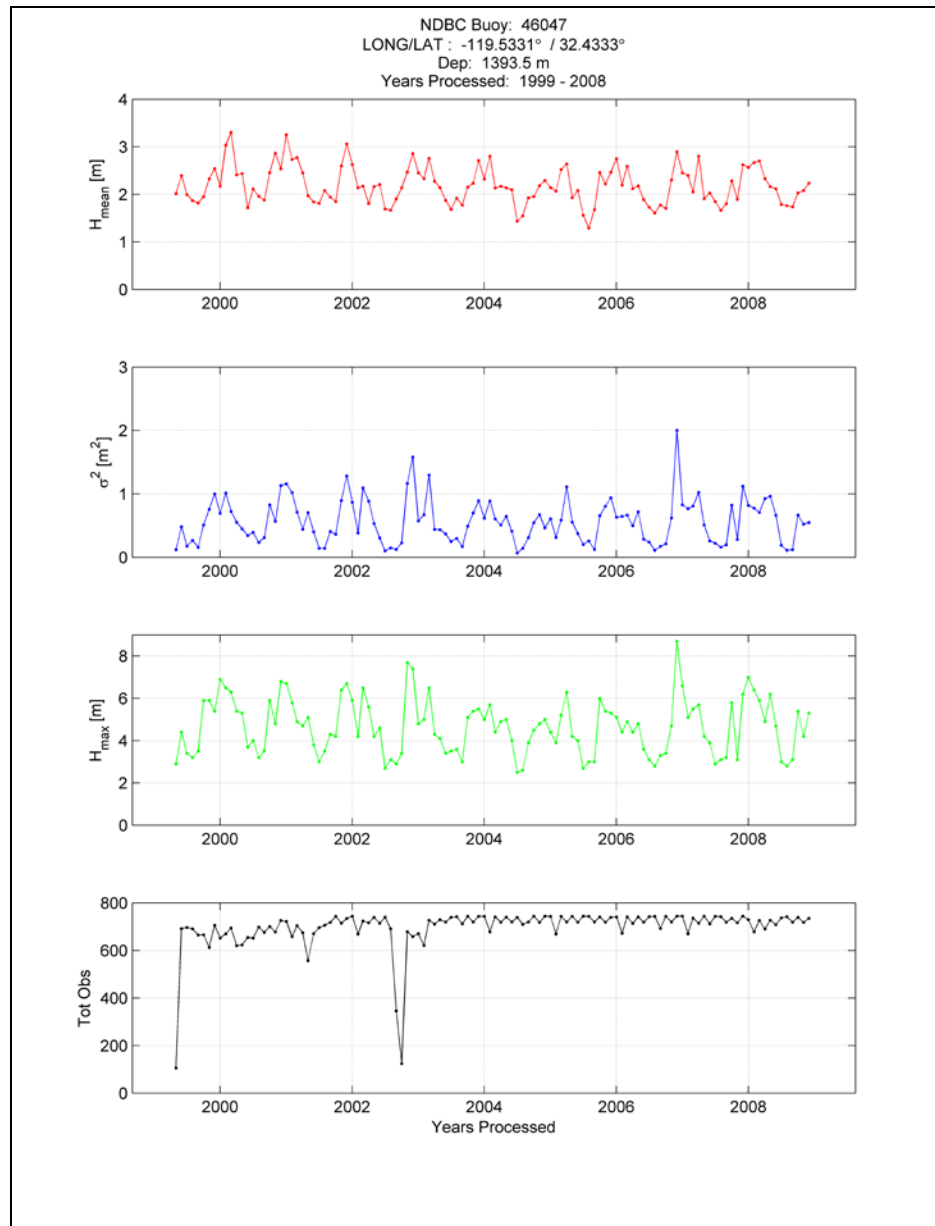



Figure 7.2-5. Monthly Averaged Mean Significant Wave Height, variance in the Mean, Maximum and Number of Observations at NDBC Buoy 46047

	NASA Engineering and Safety Center Technical Report	Document #: NESC-RP-08- 00494	Version: 1.0
Title: Assessment of Orion Crew Module Ocean Wave Model			Page #: 43 of 158

7.3 Oceanographic Considerations

7.3.1 Data Interpretation and Measurement Error

The NESC team observed that some of the scatter seen in Figure 3 and others in the AMA, Inc. report is due to measurement error. It was also observed that a larger part of the scatter is likely associated with other oceanographic effects not directly considered in the model. Even with error-free measurements, comparisons such as these will yield good agreement only if instantaneous wave conditions can be predicted using only the local, instantaneous wind speed. However, in the real ocean, wave conditions are a result a complex time and space integration of the wind field, with some other environmental factors, which have an additional (usually secondary) impact on the wave conditions. In the case of swell energy, the local instantaneous wind is not part of the time-space integration, implying that this wind is an especially poor predictor for that energy.


The time-space integration can be discussed in terms of fetch and duration, though in most circumstances, the environment is too irregular to assign a particular number to either. The fetch quantity is dictated by the size of the wind event and/or its orientation with respect to nearby land or ice. The duration is vaguely defined as the time period over which the wind speed and direction has not changed significantly.

7.3.2 Environmental Factors

Two environmental factors which can impact the local sea state are the bathymetry and currents. Locally, these two variables can make a wave of a given frequency more or less steep. Related effects are shoaling and refraction, which are non-local, since they are produced by gradients in bathymetry and currents. The result is that a statistical model developed using data from a buoy in a region of high current shear would not be representative of nearby locations. A similar conclusion could be made for a buoy near shoals or otherwise irregular bathymetry.

A theoretical and practical discussion of the effects of ocean currents and vessel movement on steepness is provided in Britton and Lily, 1981[ref. 9] where seas moving against the current cause an increase in steepness (Figure 7.3-1, left). The impact of current steepening is that for a given wind speed different slopes can be measured based on the alignment of the wave-generating wind with the current leading to greater record-to-record variability. Strong currents are needed in order to effect significant steepening, but such currents may be present in the Gulf Stream (off the North American Eastern seaboard), the Kuroshio (off the coast of Japan), or the Agulhas (off the coast of South Africa).

Similarly, vessels, or in this case the Orion CM, whose direction of movement opposes the direction of the waves can result in a relative steeping of the slope (Figure 7.3.1, right), or

	NASA Engineering and Safety Center Technical Report	Document #: NESC-RP-08- 00494	Version: 1.0
Title: Assessment of Orion Crew Module Ocean Wave Model			Page #: 44 of 158

dampening of the slope if the movement follows the direction of the waves. This observation is the source of the mariners wish for *fair winds and following seas*. The steepening is effected by expanding the denominator of the AMA, Inc. report's Equation 19 to be the sum of the wave phase speed and ocean current speed and vessel, or Orion CM, speed relative to the wave direction.

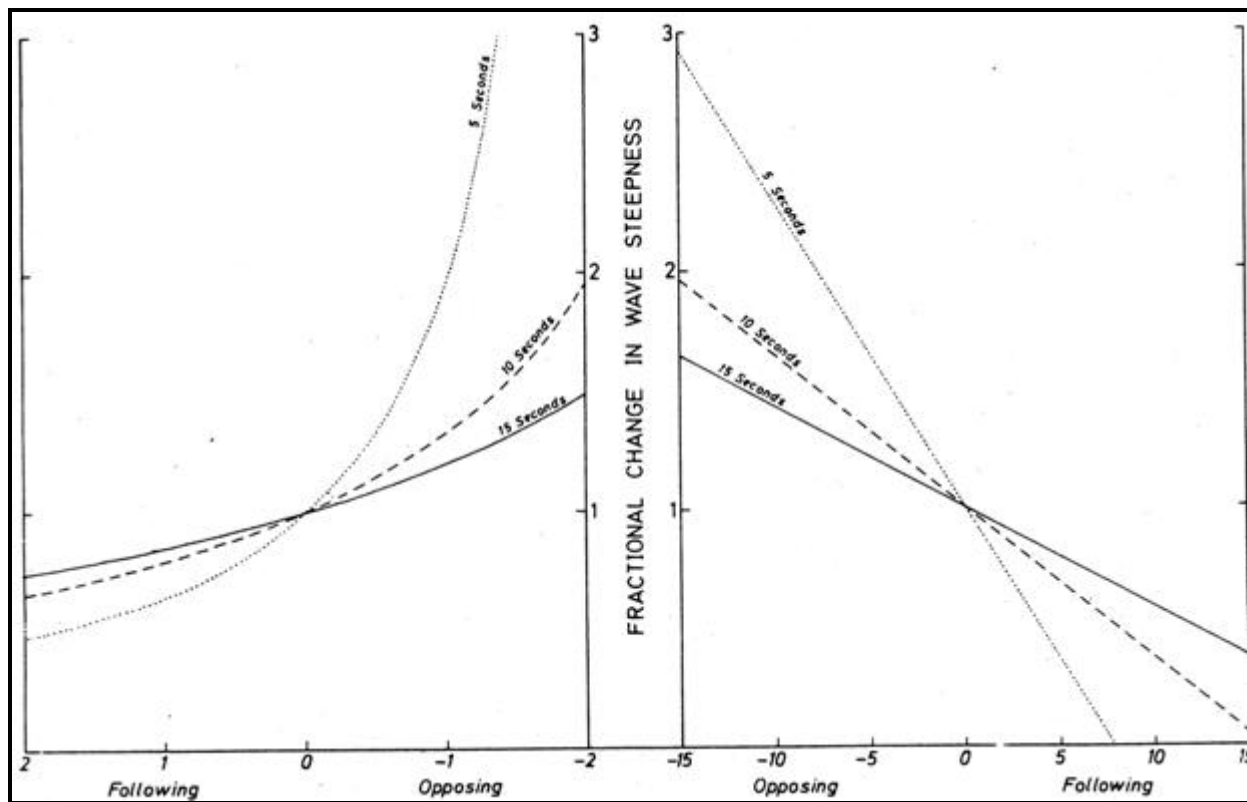



Figure 7.3-1. Steepness Factors with Currents and Following or Opposing Seas (left) and for Opposing and Following Vessel Speed (right) (speeds in knots) [ref. 9]

Another effect is air-sea temperature differences (stability). This is usually considered a lower order effect, but may become important insofar as the CM landing model assumes that wind speed is the only meteorological variable that affects the both vehicle descent and the sea state as noted in Section 7.1.

The surf zone (see Section 12.0, Definition of Terms) and its unique characteristics are not considered in the wave model. The surf zone is usually narrow, (100 m) or less, and therefore, surf zone landings may be regarded as a low probability. However, it is expected that

	NASA Engineering and Safety Center Technical Report	Document #: NESC-RP-08- 00494	Version: 1.0
Title: Assessment of Orion Crew Module Ocean Wave Model			Page #: 45 of 158

accommodation of surf zone for off-nominal conditions (e.g., launch abort) be accounted for in the CM landing analysis.

The continental shelf is relatively wide in some regions (e.g., 150-180 km near Savannah, Georgia). Therefore, it is appropriate to include scenarios for landing in intermediate depth waters (see Section 12.0, Definition of Terms) in off-nominal contingency planning.

The assumption of deep water is not necessary and may introduce error in coastal areas. It is noted that buoy 44008 is in 59.1 m water depth. For this and other non-deep locations, using the deep water assumption will result in non-conservative estimates of slope. Since slope variance is typically dominated by higher frequencies, this error is not necessarily large.

The more general, arbitrary-depth form of all relevant equations should be used in the AMA Inc. Report and in the software. Use of the general form will be especially appropriate when adding coastal buoys to the model dataset. The linear dispersion relation for arbitrary water depth is $\omega^2 = gk \tanh kh$. Note that in the NESC team's recommended changes to Equations 16, 17, 19, 25 and 26 given in the AMA, Inc. report, the more general forms are used (see Section 8.3, R-7).

7.3.3 Breaking Waves for Crew Module's Off-nominal and Nominal Water Landing

The current wave model does not consider the presence of steepness limited breaking waves in the open ocean and its potential impact to Orion CM Water Landing dynamic analysis. Ideally, the CM will be scheduled to have water landing in areas where sea states and winds are nominal as defined by DSNE. It is expected that breaking waves are not to be active and should have an insignificant presence. However, there is a possibility that the CM could be forced to land in areas where sea states and winds are off-nominal as defined by DSNE. It is also expected that the presence of breaking waves could be appreciable. The quantification of presence of breaking waves can be effected based on whitecap coverage per unit area. The whitecap coverage at sea due to breaking waves is a power law function of wind speed expressed as

$$P_w(\%) = A(U_{10})^B$$

where U_{10} is wind speed at 10 m height in m/s, A and B are empirically determined constants. However, the estimation of whitecap coverage based on the wind speed-dependent relation could vary due to other factors such as wave age, air stability, and fetch. Hwang and Sletten (2008) [ref. 29] suggested that the whitecap coverage proposed by Monahan (1971) [ref. 39] can approximate the upper limit envelope, which is

$$P_w(\%) = 0.00135(U_{10})^{3.4}$$



NASA Engineering and Safety Center Technical Report

Document #:
**NESC-RP-08-
00494**

Version:
1.0

Title:

Assessment of Orion Crew Module Ocean Wave Model

Page #:
46 of 158

The possible maximum encounter probability of breaking wave at sea then can be estimated based on this equation. For example, at wind speed of 10 m/s, the probability of encountering breaking wave is 3.4 percent. This breaking wave occurrence probability could increase by 4 times to 13.5 percent as the wind speed increases to 15 m/s. See Figure 7.3-2.

Wind Speed (U_{10} m/s)	2	5	10	15	20
Breaking waves probability (percent)	0.14	0.3	3.4	13.5	35.8

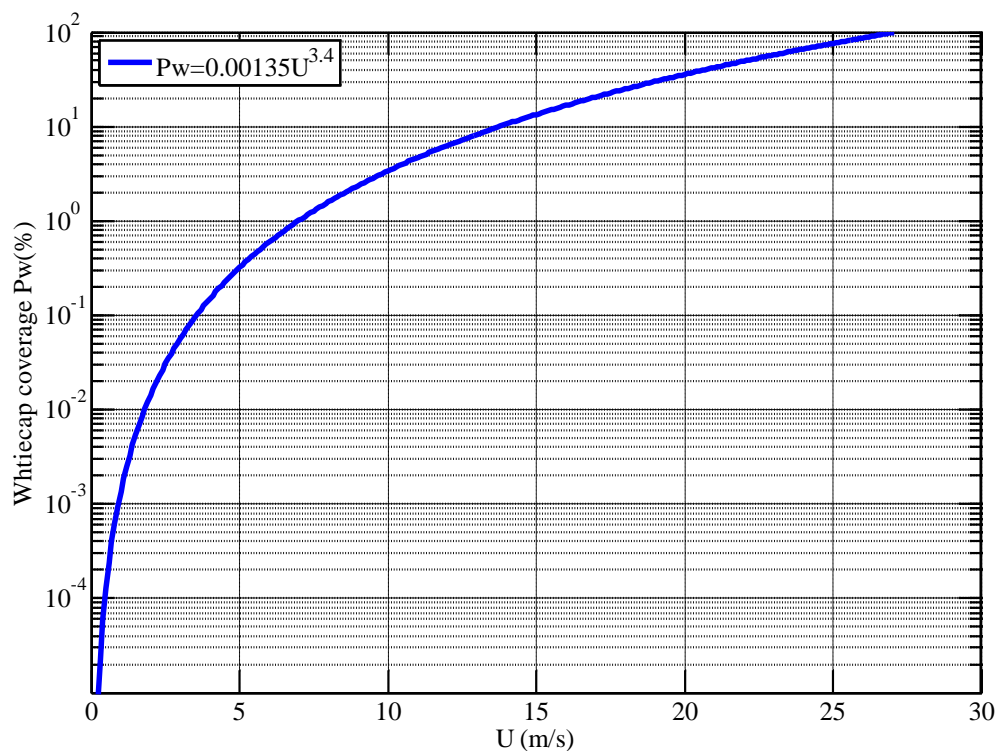



Figure 7.3-2. Whitecap Coverage as a Function of Wind Speed

	NASA Engineering and Safety Center Technical Report	Document #: NESC-RP-08- 00494	Version: 1.0
Title: Assessment of Orion Crew Module Ocean Wave Model			Page #: 47 of 158

8.0 Findings, Observations, and Recommendations

8.1 Findings

- F-1. The new material in the AMA, Inc. report (added after 1/20/09, discussed in Section 7.1.2, and listed in Appendix C of this report) compares the predicted slope variance derived from buoy wave spectra against the variance from directly simulated wave slopes that are propagated in both time and space.

In most cases, there was good agreement. However, in perhaps the most important test using buoy directional wave spectrum data, Test Case 5, the upwind-downwind slope variances of simulated wave slope data at a single location in time do not converge to the expected variances that were directly computed from buoy spectra (See Figure 9 in Appendix C). Specifically, it appears the variance of the simulated slopes is smaller than that predicted from spectra. The AMA, Inc. report did not give a further explanation for this anomaly. Moreover, since the Monte Carlo impact analysis will be based upon a single physical location in the ocean and buoy data, this test is most relevant and unfortunately demonstrates the most error in the expected wave slope.

- F-2. In the AMA, Inc. report, the assumption of deep water is not always valid when calculating the wave number (k).


This would impact equations used to calculate slope variance.

- F-3. Slope, azimuth, and vertical velocity of waves do not follow normal distribution due to the record-to-record variability of the variance computed for individual buoy records.


Ad hoc correction factors (such as those provided in Table 5 of AMA, Inc. report for correcting wave slope and vertical velocity) used to match the proper distribution with a normal one at a single point corresponding to 99.7 percent probability is an inefficient way to model this non-normality, as the other points from the distribution will not be modeled correctly. Calling this probability 3-sigma is inappropriate since the underlying distribution is non-normal.

- F-4. Classical χ^2 confidence intervals cannot be used to model the record-to-record variability described in F-3.

The intervals quantify the lack of knowledge in estimating statistical parameters of a single distribution, and this uncertainty tends to zero as the number of samples increases. In contrast, the record-to-record variability is physical in nature and is not reduced as the number of samples increases. In general, confidence intervals do not provide a direct way to express overall distributions for Monte Carlo simulation of CM landing condition.

	NASA Engineering and Safety Center Technical Report	Document #: NESC-RP-08- 00494	Version: 1.0
Title: Assessment of Orion Crew Module Ocean Wave Model			Page #: 48 of 158

- F-5. The CDIP archives of x-y-z time series data from Waverider® buoys provide a direct measure of vertical velocities, slopes, and wave azimuths, but were not included in the AMA Inc. report analyses or verification.
- F-6. There are long-term variations in the wave climate that were not considered in the AMA, Inc. report.
- Applications of only one-year of data will introduce errors compared to a mean climatic condition. Additionally, geographic variability introduces similar errors.*
- F-7. There are different methods of adjusting winds to the 10-m reference level in the source documents, none of which incorporates atmospheric stability, the wind speed dependency of the drag coefficient, or wave-wind interaction (Fairwell et al., 2003) [ref. 21].
- Specifically:*
- DSNE Ground Winds at Landing Site (AMA, Inc. report Section 3.5.8) uses an uncited adjustment to 10-m that uses a power law method with a power of 0.14, and assumes neutral atmospheric stability.*
 - C-ERA40 (wave and spectra used in the DSNE (AMA, Inc. report Section 3.5.18) adjusted buoy winds to 10 m using the method of Bidlot, et al. (2002) [ref. 7], which is a logarithmic profile and assumes neutral atmospheric stability. This method should not be used above 20-m (CERC, 1984).*
 - AMA, Inc. report Equation 5 and the Orion CM Wave Model (the output of the DSS is extrapolated from 101 to 10-m, (see Appendix A) use the method of Hsu et al. (1994) [ref. 28], which is a power law method with a power of 0.11. Hsu et al. (1994) is empirically derived from data in the Gulf of Mexico and the Atlantic Ocean under near neutral atmospheric stability and higher winds. The adjustments also introduce further uncertainties in the 10-m winds in addition to the +/- 1.0 m/s accuracy of buoy measured wind speeds at the anemometer height.*
- F-8. It is evident that: a) estimation of $D(f, \theta)$ is not necessary, so the process could be simplified, and b) the Maximum Likelihood Estimator in particular introduces error.
- In the December 19, 2008 AMA, Inc. report (provided in Appendix B), Equations 16, 17, 19, 25, and 26 uses $D(f, \theta)$, which is a directional distribution estimated from the Fourier coefficients provided by the data centers. There are a number of directional estimators available for doing this. In the study, the MLM (sometimes called “Maximum Likelihood Estimator”) is used [Capon et al., (1967), ref. 10 and Oltman-Shay and Guza, (1984), ref. 43].*

	NASA Engineering and Safety Center Technical Report	Document #: NESC-RP-08- 00494	Version: 1.0
Title: Assessment of Orion Crew Module Ocean Wave Model			Page #: 49 of 158

F-9. Although the Apollo Program model assumed a cutoff frequency/wavelength relative to the CM diameter, the model assigned frequency/wavelength cutoff associated with the larger Orion CM diameter may prove to be a limiting assumption with respect to design.

Sufficient analytical justification to defend the cutoff frequency has not been provided.

F-10. Refraction and shoaling will tend to broaden or skew the probability density function (pdf) of wave related parameters such as slope variance and imply the validity would be greatly localized.

For example, abort scenarios into coastal waters will require different modeling techniques that account for the high spatial variability. (Note that this is a separate and much more difficult issue versus simply removing deep water assumption).

F-11. The surf zone and its unique wave characteristics are not considered in the wave model.

8.2 Observations

The following NESC observations are made:

O-1. In the AMA, Inc. report, the high frequency tails of NDBC spectra are extrapolated with an f^{-4} tail.

This will result in a high (conservative) estimate of the slope variance and vertical velocity, since in nature, the tail decays more rapidly than this for some of the frequency range. Specifically, Kahma and Calkoen (1992) have found that from just above the spectral peak to $3f_p$, a f^{-4} power-law relationship is observed, and past $3f_p$, a f^{-5} relationship is observed.

O-2. The use of linear theory to estimate the ocean wave field will result in an underestimation of slopes and vertical velocities.


The linear assumption will impact the inputs to the landing Monte Carlo model yielding non-conservative bias.

O-3. NDBC buoys overestimate First 5 directional spread owing to measurement noise (a combination of complicated buoy hull-wave-wind load response characteristics, and motion sensor fidelity).

This is a documented trade-off on the part of NDBC to have a more stable platform and sufficient power to measure many other important ocean and air variables (e.g., wind).

O-4. Scatter in plots such as Figures 3 and 10 in the AMA, Inc. report is probably due to instrument error and omission of oceanographic effects such as fetch, duration, wind rotation, and currents.

See further discussion above in Section 7.3, "Oceanographic Considerations".

	NASA Engineering and Safety Center Technical Report	Document #: NESC-RP-08- 00494	Version: 1.0
Title: Assessment of Orion Crew Module Ocean Wave Model			Page #: 50 of 158

- O-5. There is higher variability of slope and vertical velocity at low wind speed conditions (AMA, Inc. report, Figures 3 and 19).

It is the NESC team's interpretation that this is due to the dominance of the swell, not associated with local winds.

- O-6. The assumption that horizontal wind velocity is the sole atmospheric factor coupling flight dynamics and wave characteristic is not verified.

Statistical correlation between other atmospheric conditions used in the CM flight dynamic model and wave conditions might impact the results of combined simulation.

- O-7. The AMA, Inc. report uses the NDBC hourly 8-minute wind speeds of the observation hour.

The NDBC wind observations are not contemporaneous with NDBC wave measurements. In most cases, winds are taken from minute 42 to minute 50 past the hour while wave measurements are generally made from minute 20 to minute 40 past the hour for 20-minute records and from minute 00 to minute 40 for 40-minute records. Also, wind waves do not respond instantaneously to wind speeds (Hanson and Phillips, 1999).

- O-8. The assumption of flat surface neglects the potential effects related to a curved impact surface (e.g., wave form) and may be critical to establishing limits, either discrete or gradual, of the assigned frequency/wavelength cutoff.

Sufficient analytical justification to defend the cutoff frequency has not been provided.

- O-9. The current wave model does not consider the presence of breaking waves that potentially exist in nominal and off-nominal conditions.

- O-10. Readability of the AMA, Inc. report is complicated by the interspersed supporting and exploratory analyses.


It is not clear which buoys were selected for which analyses.

- O-11. NASA may consider sponsoring the deployment of a directional wave buoy in proximity to the nominal landing zone, or other locations of interest, that can be used for design verification and operational measurements.

8.3 Recommendations

The following NESC recommendations are made to the Orion Project:

- R-1.** Record-to-record variability should be directly modeled by fitting a distribution either for variance or standard distribution (using the values from the individual records as samples) that would statistically characterize this variability for a given wind condition. (*F-3, F-4*)

	NASA Engineering and Safety Center Technical Report	Document #: NESC-RP-08- 00494	Version: 1.0
Title: Assessment of Orion Crew Module Ocean Wave Model			Page #: 51 of 158

For example, the wave slope could be characterized by a normal distribution with standard deviation σ_s that itself is a random variable that follows an appropriate distribution (for example, it can be a lognormal or truncated normal distribution). In a Monte Carlo simulation this representation can be easily implemented by drawing a random sample from σ_s (in accordance with the specified distribution) and then use this standard deviation to generate a slope sample. In this case, the two parameters μ_{os} and σ_{os} fully represent the underlying distribution (unlike the use of σ_s and the corresponding correction factor that only represent one point on the distribution correctly). All other parameters of interest (i.e., azimuth and vertical velocity, as well as the correlations among the slope and these two parameters) can be modeled in a similar manner.

- R-2.** CDIP Waverider® buoy (x-y-z time series) data should be included to provide a direct statistical assessment of the three primary wave parameters and to validate the Monte Carlo Model. *(F-5, O-2)*
- R-3.** Use of the buoy data in the Monte Carlo model should include, at the minimum, three to five years of temporal wave data and should consider multiple geographic locations for landing/abort scenarios. *(F-6, F-10)*
- R-4.** Explicit modeling of record-to-record variability eliminates need of confidence intervals calculated in the AMA, Inc. report and should be removed. *(F-4)*

The need for additional physical parameters to explain variability of wave slope, azimuth, and vertical velocity for a given wind condition as discussed in the AMA, Inc. report is eliminated since this variability is explicitly taken into account in a statistical fashion regardless of its physical source.


- R-5.** Investigate the sensitivity to varied methods in determining the 10-m winds model input, their underlying assumptions, and their possible contributions to the uncertainty of the 10-m winds model input. *(F-7)*

A consistent method should be applied across CxP documents.

- R-6.** Investigate averaging the wind speeds over the 3 hours of and prior to the wave measurements to reduce record-to-record variability. *(O-4, O-5, O-7)*

For example improved correlations between wind speed and wave spectra at the higher frequencies (0.20 to 0.35 Hz) can be achieved by time averaging the wind speeds over a 3-hour period (Lang, 1987, ref. 37, and Palao and Gilhousen, 1993).

- R-7.** Replace AMA, Inc. report Equations 16, 17, 19, 25, and 26 with equations used to measure directional Fourier coefficients directly, thereby eliminating the need for the MLM (or any other) directional estimator. *(F-8)*

	NASA Engineering and Safety Center Technical Report	Document #: NESC-RP-08- 00494	Version: 1.0
Title: Assessment of Orion Crew Module Ocean Wave Model			Page #: 52 of 158

For example, below illustrates how the aforementioned equations in Section 7.2.2 can be modified such that they use the Fourier coefficients provided by the data centers.

Old:

$$\sigma_{ud}^2 = \sum_{j=1}^m \left[\sum_{i=2}^n \left[\left(\frac{\omega_i^2}{g} \right)^2 D_i(\theta_j) S(f_i) df_i \cos^2(\theta_j - \theta_{wind}) \right] d\theta_j \right] \quad [16]$$

$$\sigma_c^2 = \sum_{j=1}^m \left[\sum_{i=2}^n \left[\left(\frac{\omega_i^2}{g} \right)^2 D_i(\theta_j) S(f_i) df_i \sin^2(\theta_j - \theta_{wind}) \right] d\theta_j \right] \quad [17]$$

New:

$$\sigma_{ud}^2 = 0.5 \int_{f_1}^{f_2} k^2 S(f) [1 + \cos(2\theta_{wind}) a_2(f) + \sin(2\theta_{wind}) b_2(f)] df$$

$$\sigma_c^2 = 0.5 \int_{f_1}^{f_2} k^2 S(f) [1 - \cos(2\theta_{wind}) a_2(f) - \sin(2\theta_{wind}) b_2(f)] df$$

Old:

$$\sigma_{ud,c}^2 = \sum_{j=1}^m \left[\sum_{i=2}^n \left[\left(\frac{\omega_i^2}{g} \right)^2 D_i(\theta_j) S(f_i) df_i \sin(\theta_j - \theta_{wind}) \cos(\theta_j - \theta_{wind}) \right] d\theta_j \right] \quad [19]$$


New:

$$\sigma_{ud,c}^2 = 0.5 \int_{f_1}^{f_2} k^2 S(f) [\cos(2\theta_{wind}) b_2(f) - \sin(2\theta_{wind}) a_2(f)] df$$

Old:

$$\sigma_{ud, wvv}^2 = \sum_{j=1}^m \left[\sum_{i=2}^n \left[-\left(\frac{\omega_i^3}{g} \right) D_i(\theta_j) S(f_i) df_i \cos(\theta_j - \theta_{wind}) \right] d\theta_j \right] \quad [25]$$

$$\sigma_{c, wvv}^2 = \sum_{j=1}^m \left[\sum_{i=2}^n \left[-\left(\frac{\omega_i^3}{g} \right) D_i(\theta_j) S(f_i) df_i \sin(\theta_j - \theta_{wind}) \right] d\theta_j \right] \quad [26]$$

	NASA Engineering and Safety Center Technical Report	Document #: NESC-RP-08- 00494	Version: 1.0
Title: Assessment of Orion Crew Module Ocean Wave Model			Page #: 53 of 158

New:

$$\sigma_{ud, wvv}^2 = - \int_{f_1}^{f_2} \omega k S(f) [\cos(\theta_{wind}) a_1(f) + \sin(\theta_{wind}) b_1(f)] df$$

$$\sigma_{c, wvv}^2 = - \int_{f_1}^{f_2} \omega k S(f) [\cos(\theta_{wind}) b_1(f) - \sin(\theta_{wind}) a_1(f)] df$$

θ_{wind} is of Cartesian convention, with ‘toward East’ being zero, so if the buoy center provides data in terms of nautical “from North” convention, a conversion is required.

$$\theta_{wind, cartesian} = 270^\circ - \alpha_{wind, nautical}$$

NDBC provides $\alpha_1, r_1, \alpha_2, r_2$ instead of a_1, b_1, a_2, b_2 .

Transformation $a_1 = r_1 \cos \theta_1$, $b_1 = r_1 \sin \theta_1$, etc. is required.

Also, recall from above that $\alpha_1 = 270^\circ - \theta_1$; $\alpha_2 = 270^\circ - \theta_2$


The results derived from these equations will be slightly different from the current results because the MLM directional estimator used to estimate $D(\theta)$ in the AMA, Inc. report does not exactly fit the buoy's a's and b's. As a consistency check, the results of the new and old equations can be compared by using the MEM directional estimator (not MLM) with the old equations. MEM (Maximum Entropy Method, Lygre and Krogstad 1986) returns $D(\theta)$ that fits a's and b's exactly, so both sets of equations should yield identical results. This only has to be performed for a single buoy record to ensure the revised equations are correct. This consistency check should require minimal effort, since it only involves calling a different MATLAB function with identical arguments (MEM instead of MLM).

- R-8. Material that is not used in the final model should be moved to the AMA, Inc. report Appendices. **(O-10)**

This would include sections where it is demonstrated that particular steps can be safely omitted/simplified. Thus, readers will have faster comprehension of what the model actually does. Identifying which buoys (e.g., depicted in a table) are used for a particular analysis would allow traceability of data for the reader.

- R-9. Use an alternate method of verification to check specific cases in the model (e.g., Test Case 5, Figures 9 and 10 of Appendix C) with a higher fidelity ocean wave simulation. **(F-1)**

Commercially-available software such as Fluent can simulate ocean wave/atmospheric interface problems under assumed wind conditions. It would be possible to simulate both

	NASA Engineering and Safety Center Technical Report	Document #: NESC-RP-08- 00494	Version: 1.0
Title: Assessment of Orion Crew Module Ocean Wave Model			Page #: 54 of 158

the buoy floating in the ocean and the AMA, Inc. model. In essence, the x-y-z position data is known everywhere with this approach and may help clear up some of the concerns raised in the aforementioned test.

- R-10. Conduct an analysis to determine which frequency/wavelengths are important to the module structural design with considerations for Orion CM diameter, curved wave surfaces, and breaking waves associated with nominal and off-nominal sea states. **(F-9, O-8, O-9)**

Accuracy would be improved by providing a smoother transition from waves that affect the landing to waves that do not affect the landing using weights, as opposed to a simple assigned frequency/wavelength cutoff.

- R-11. Account for the shallow water depth and surf zone and their unique wave characteristics in the structural analysis and the overall Orion CM landing analysis. **(F-11)**

- R-12. Use the more general, arbitrary-depth form of all relevant equations in the AMA, Inc. report and in the software. **(F-2)**

The linear dispersion relation is $\omega^2 = gk \tanh kh$ and simple functions are available to calculate k using this relation.

9.0 Alternate Viewpoints

There were no alternate viewpoints during the course of this assessment.

10.0 Other Deliverables

There are no other deliverables after the final report and the stakeholder outbriefing are completed and approved by the NRB and key stakeholders.


11.0 Lessons Learned

When encountering new disciplines outside of NASA's experience base, the use of other Government organizations, with domain specific knowledge early in the design process, may yield improved solutions to a specific problem. This is mainly due to domain experience, access to non-public information, and alternate stakeholder products and networks.

12.0 Definition of Terms

Coastal Regions

Variously defined, used here as minimally within 100 km of shoreline, and extending further to 300 m depth contour in areas where continental shelf is broad; often includes deep water.

	NASA Engineering and Safety Center Technical Report	Document #: NESC-RP-08- 00494	Version: 1.0
Title: Assessment of Orion Crew Module Ocean Wave Model			Page #: 55 of 158

Corrective Actions

Changes to design processes, work instructions, workmanship practices, training, inspections, tests, procedures, specifications, drawings, tools, equipment, facilities, resources, or material that result in preventing, minimizing, or limiting the potential for recurrence of a problem.

Deep Water

Depths for which $kh > \pi$, where k is wave number.

Directional Estimator (also known as a “Data-Adaptive Method”)

An algorithm that uses low order moments of an unknown directional distribution $D(\theta)$ to produce an estimate of said distribution. The low order moments are typically derived from observations and there exists a set of moments for each frequency band.

Fetch

Horizontal distance available for wave generation by wind.

Finding

A conclusion based on facts established during the assessment/inspection by the investigating authority.

Intermediate Water Depth

Depths for which $0.25 < kh < \pi$

Lessons Learned


Knowledge or understanding gained by experience. The experience may be positive, as in a successful test or mission, or negative, as in a mishap or failure. A lesson must be significant in that it has real or assumed impact on operations; valid in that it is factually and technically correct; and applicable in that it identifies a specific design, process, or decision that reduces or limits the potential for failures and mishaps, or reinforces a positive result.

Observation

A significant factor established during this assessment that supports and influences the conclusions reached in the statement of Findings and Recommendations.

Problem

The subject of the independent technical assessment/inspection.

	NASA Engineering and Safety Center Technical Report	Document #: NESC-RP-08- 00494	Version: 1.0
Title: Assessment of Orion Crew Module Ocean Wave Model			Page #: 56 of 158

Recommendation

An action identified by the assessment/inspection team to correct a root cause or deficiency identified during the investigation. The recommendations may be used by the responsible C/P/P/O in the preparation of a corrective action plan.

Record

The measured observation corresponding to a single time and location.

Refraction and Shoaling

Modifications of the wave field associated with spatial gradients in bathymetry or surface currents.

Root Cause


Along a chain of events leading to a mishap or close call, the first causal action or failure to act that could have been controlled systemically either by policy/practice/procedure or individual adherence to policy/practice/procedure.

Sea State

A description of the properties of sea surface waves at a given time and place. This might be given in terms of the wave spectrum, or more simply in terms of the SWH and some measure of the wave period (Glickman, 1999); and/or the World Meteorological Organization (WMO) codes for sea state (WMO, 1995) Code Table 3700):

Table 1: WMO Code Table 3700 (Sea State)

<i>Code Figure</i>	<i>Descriptive terms</i>	<i>[Wave] Height* in metres</i>
<i>0</i>	<i>Calm (glassy)</i>	<i>0</i>
<i>1</i>	<i>Calm (rippled)</i>	<i>0 – 0.1</i>
<i>2</i>	<i>Smooth (wavelets)</i>	<i>0.1 – 0.5</i>
<i>3</i>	<i>Slight</i>	<i>0.5 -1.25</i>

	NASA Engineering and Safety Center Technical Report	Document #: NESC-RP-08- 00494	Version: 1.0
Title: Assessment of Orion Crew Module Ocean Wave Model			Page #: 57 of 158

<i>Code Figure</i>	<i>Descriptive terms</i>	<i>[Wave] Height* in metres</i>
4	<i>Moderate</i>	1.25 - 2.5
5	<i>Rough</i>	2.5 - 4
6	<i>Very rough</i>	4 - 6
7	<i>High</i>	6 - 9
8	<i>Very high</i>	9 – 14
9	<i>Phenomenal</i>	Over 14

Notes:

(1) * These values refer to well-developed wind waves of the open sea. While priority shall be given to the descriptive terms, these height values may be used for guidance by the observer when reporting the total state of agitation of the sea resulting from various factors such as wind, swell, currents, angle between swell and wind, etc.

(2) The exact bounding height shall be assigned for the lower code figure; e.g., a height of 4 m is coded as 5.


Comment: This is not the same as Beaufort force, or Beaufort number. A number denoting the speed (or “strength”) of wind according to the Beaufort wind scale (WMO, 1995 - Appendix E). The Beaufort scale (codes) uses descriptive terms to describe ranges of wind speed, while the Sea State Codes use descriptive terms to describe a range of wind wave heights.

Shallow Water Depth

Depths for which $kh < 0.25$

Significant Wave Height (SWH)

The average of the highest 1/3 of waves in a time series. Traditionally, this measure of waveheight is believed close to the waveheight reported by trained visual observation. Outside the surf zone, it is very close to the “zero moment waveheight” calculated by integration of a surface elevation variance spectrum, such as reported by wave buoys.


	NASA Engineering and Safety Center Technical Report	Document #: NESC-RP-08- 00494	Version: 1.0
Title: Assessment of Orion Crew Module Ocean Wave Model			Page #: 58 of 158

Surf Zone

Definition varies, some use $h < 2H_s$ where h is local mean water depth and H_s is significant waveheight.

13.0 List of Acronyms


AMA	Analytical Mechanics Associates, Inc.
ARES	Acquisition and Reporting Environmental System (NDBC Payload System)
ARS	Angular-Rate-Sensor
ATLAS	Autonomous Temperature Line Acquisition System
C-ERA40	European Center for Medium-Range Weather Forecast
CDIP	Coastal Data Information Program
CERC	Coastal Engineering Research Center (US Army Corps of Engineers)
CM	Crew Module
COARE	Coupled Ocean Atmosphere Response Experiment
CxP	Constellation Program
DACT	Data Acquisition Control and Telemetry
DDWM	Digital Directional Wave Module
DSNE	Design Specification for Natural Environments (Constellation Program)
DSS	Decision Support System
DWA	Directional Wave Analyzer (DACT)
DWPM	Directional Wave Processing Module
GRC	Glenn Research Center
GSPB	General Service Buoy Payload
Hippy	Heave, Pitch, and Roll Sensor
IAHR	International Association of Hydraulic Engineering and Research
IOOS	Integrated Ocean Observing System
JSC	Johnson Space Center
LaRC	Langley Research Center
LRC	Landing and Recovery System (Orion)
MARS	Management Analysis and Reporting System
MLM	Maximum Likelihood Method
MO	Magnetometer-Only
MOS	Model Output Statistics
MTSO	Management and Technical Support Office
NASA	National Aeronautics and Space Administration
NDBC	National Data Buoy Center
NDWPM	Non-Directional Wave Processing Module
NESC	NASA Engineering and Safety Center
NOAA	National Oceanic and Atmospheric Administration

	NASA Engineering and Safety Center Technical Report	Document #: NESC-RP-08- 00494	Version: 1.0
Title: Assessment of Orion Crew Module Ocean Wave Model			Page #: 59 of 158

NOMAD	Navy Oceanographic Meteorological Automatic Device
NWS	National Weather Service
NRB	NESC Review Board
pdf	Probability Density Function
PTF	Power Transfer Function
QUARTOD	Quality Assurance of Real-Time Ocean Data
TAO	Tropical Atmosphere Ocean Array
VEEP	Value Engineered Environmental Payload
VOF	Volume of Fluid
WA	Wave Analyzer (DACT)
WDA	Wave Data Analyzer
WMO	World Meteorological Organization
WPM	Wave Processing Module

13.1 Nomenclature


$V_s = \sigma_s^2$	slope variance (square of standard deviation) for an individual record
T_z	mean zero-downcrossing period
β	parameter used to normalize $\tilde{f}(x)$, so its integral equals to 1
$\tilde{f}(x)$	probability density function for truncated normal distribution
V_{tot}	total slope variance for combined records
P_{tot}	probability for combined records, in this context it is the probability of exceeding slopes of a given magnitude
μ_{σ_s} and σ_{σ_s}	first two moments (mean and standard deviation) representing the record-to-record variability of slope's standard deviation
$\tilde{\mu}_\sigma$ and $\tilde{\sigma}_\sigma$	parameters of truncated normal distributions that match required μ_{σ_s} and σ_{σ_s}
α_i	direction from which waves come measured clockwise from true North
H_{m0}	zero moment waveheight
$D(f, \theta)$	directional spectrum normalized at each frequency
m_0, m_2	zeroth and second spectral moment
a_i and b_i	Fourier coefficients
C and Q	co- and quad-spectra, respectively
$D^*(f, \theta)$	truncated Fourier series for wave directional distribution
$E(f)$	spectral density of the water surface vertical motion (i.e., the nondirectional wave spectrum)
f	frequency,
f_c	upper frequency limit

	NASA Engineering and Safety Center Technical Report	Document #: NESC-RP-08- 00494	Version: 1.0
Title: Assessment of Orion Crew Module Ocean Wave Model			Page #: 60 of 158


f_p	peak frequency
G	constant for a particular buoy deployment
h	water depth
H_s	significant waveheight (see Definition of Terms, Section 12.0)
K	empirical correction constant
k	wavenumber, 2π /wavelength,
$P_w(\%)$	percent whitecap coverage
r_1 and r_2	parameters representing the directional energy spreading in the corresponding direction, and are know as the first and second normalized polar coordinates from Fourier coefficients, respectively.
$S(f, \theta)$	two-dimensional energy density spectrum
$S_{0.01}$ and $S_{0.02}$	acceleration spectral energy at $f = 0.01$ and 0.02 Hz, respectively.
$S_h(f)$	spectrum of the buoy heave motion
$S_w(f)$, $E(f)$, $C_{11}(f)$	spectral density of the water surface vertical motion (i.e., the nondirectional wave spectrum)
U_{10}	wind speed at 10 m height
θ	direction of wave propagation (counterclockwise from east by convention),
θ_1 and θ_2	mean and principal wave directions, respectively
μ	mean value
σ	standard deviation
ω	angular frequency, $2\pi f$

14.0 References


1. Anguelova, M. D., and F. Webster (2006), Whitecap coverage from satellite measurements: A first step toward modeling the variability of oceanic whitecaps, *J. Geophys. Res.*, 111, C03017, doi:10.1029/2005JC003158.
2. Archer, C. L., and M. Z. Jacobson, 2003: Spatial and temporal distribution of U.S. winds and wind power at 80 m derived from measurements, *J. Geophys. Res.*, 108(D9), 4289. [Available on-line at: http://www.stanford.edu/group/efmh/winds/winds_jgr.pdf].
3. Archer, C. L., and M. Z. Jacobson, 2004: Corrections to “Spatial and temporal distribution of U.S. winds and wind power at 80 m derived from measurements”, *J. Geophys. Res.*, 109(D20116), doi:10.1020/2004JD005099, 2004.
4. Barbre, B.J., and Keller, V.W., Sea State and Weather Assessment Capability for NASA's Constellation Program
<http://naca.larc.nasa.gov/search.jsp?R=1027347&id=1&q=N%3D4294650006>

	NASA Engineering and Safety Center Technical Report	Document #: NESC-RP-08- 00494	Version: 1.0
Title: Assessment of Orion Crew Module Ocean Wave Model			Page #: 61 of 158


5. Barrick, D.E, Lipa, B.J., and Steele, K.E., 1989, Comments on Theory and application of calibration techniques for an NDBC directional wave measurements buoy by K.E. Steele, et al.: nonlinear effects, *Journal of Ocean Engineering*, IEEE, Vol. 14(3), pp. 268-272.
6. Benoit, M., P. Frigaard, H. A. Schäffer, 1997: Analysing multidirectional wave spectra: a tentative classification of available methods. Proc. Int. Assoc. Hydraulic Res.: Multidirectional Waves and Their Interaction with Structures, San Francisco, CA, National Research Council of Canada, 131-157.
7. Bidlot, J. R., D. J. Holmes, P. A. Wittmann, R. Lalbeharry, and H. S. Chen, 2002: Intercomparison of the performance of operational wave forecasting systems with buoy data. Wea. Forecasting, 17, 287–310. [Available on-line at: <http://ams.allenpress.com/archive/1520-0434/17/2/pdf/i1520-0434-17-2-287.pdf>].
8. Bose, David M., “Monte Carlo Ocean Wave Modeling”, Analytical Mechanics Associates, Inc., Report No.: 08-09, Rev. D., December 19, 2008.
9. Britton, G.P. and Lily, K.E. (ed.), 1981: *An Introduction to Sea State Forecasting*, NOAA.
10. Capon, J., R.J. Greenfield, R.J. Kolker, 1967: Multidimensional maximum-likelihood processing of a large aperture seismic array. Proc. IEEE, 55, 192-211. Capon, J., R.J. Greenfield, R.J. Kolker, 1967: Multidimensional maximum-likelihood processing of a large aperture seismic array. Proc. IEEE, 55, 192-211.
11. Cartwright, D.E., 1963: The use of directional spectra in studying the output of a wave recorder on a moving ship, In *Ocean Wave Spectra*, Prentice Hall, 203-218.
12. CERC (Coastal Engineering Research Center), 1984: *Shore Protection Manual*, Vol. 1, Department of the Army, US Army Corps of Engineers, pp. 3-26.
13. Chaffin, J., Bell, W., O'Neil, K., and Teng, C.C., 1994, “Design and Testing of the NDBC Wave Processing Module,” *Proceedings of WAVES '93*, New Orleans, Louisiana, pp. 277 - 286.
14. Constellation Program Design Specification for Natural Environments (DSNE) CxP 70023, Revision A, Change 001, National Aeronautics and Space Administration Release Date: November 7, 2008.
15. Corliss, J. Overview of the Monte Carlo Analysis Process used to Establish Crew Module Water Landing Conditions January 8, 2008, NASA LaRC, Revision: Draft
16. Cote, L.J., et al., “The directional spectrum of a wind generated sea as determined from data obtained by the Stereo Wave Observation Project”. *Meteorological Papers*, New York University College of Engineering, 2(6), 88 pp., 1960.

	NASA Engineering and Safety Center Technical Report	Document #: NESC-RP-08- 00494	Version: 1.0
Title: Assessment of Orion Crew Module Ocean Wave Model			Page #: 62 of 158


17. Cummings, A. D., et al., "Concepts and Procedures Used to Determine Certain Sea Wave Characteristics", NASA Technical Note D-6961, 1972.
18. Dvorak, M.J., Jacobson, M.Z., Archer, C.L., 2007: California offshore wind energy potential. *Proceedings from Windpower 2007: American Wind Energy Association Windpower 2007 Conference & Exhibition*, June 36, 2007, Los Angeles, CA: AWEA. [Available on-line at: <http://www.stanford.edu/~dvorak/papers/offshore-wind-ca-analysis-awea-2007.pdf>]
19. Earle, M.D., and Bush, K.A., 1982, "Strapped-down Accelerometer Effects on NDBC Wave Measurements," in *Proceedings of Oceans '82*, pp. 838-843.
20. Earle, M.D., Steele, K.E., and Hsu, Y.H.L., 1984, "Wave Spectra Corrections for Measurements with Hull-fixed Accelerometers," in *Proceedings of Oceans '84*, pp. 725-730.
21. Fairall, C.W., E.F. Bradley, J.E. Hare, A.A. Grachev, and J.B. Edson, 2003: Bulk Parameterization of Air–Sea Fluxes: Updates and Verification for the COARE Algorithm, *Jrnl. Clim.*, V.16(4), pp.571-591. [Available on-line at: <http://ams.allenpress.com/archive/1520-0442/16/4/pdf/i1520-0442-16-4-571.pdf>].
22. Giebel, G., 2003: *The State-Of-The-Art in Short-Term Prediction of Wind Power, A Literature Overview, Version 1.1*, European Commission, Project ANEMOS, 36 pp. [Available on-line at: http://anemos.cma.fr/download/ANEMOS_D1.1_StateOfTheArt_v1.1.pdf].
23. Gilhousen, D., 1999: Improvements in National Buoy Center Measurements, *Achievements in Marine Climatology*, Val Swail, ed., Environment-Canada, Toronto, 79-89. [Available on-line at: <http://www.ndbc.noaa.gov/improvements.shtml>].
24. Gilhousen, D.B., 1987: A field evaluation of NDBC moored buoy winds. *Jrnl. Atmos. Ocean. Techn.*, 4, 94-104. [Available on-line at: <http://ams.allenpress.com/archive/1520-0426/4/1/pdf/i1520-0426-4-1-94.pdf>]
25. Gilhousen, D.B., 2006: A Complete Explanation of Why Moored Buoy Winds are Less than Ship Winds, *Mariners Weather Log*, V. 50(1). [Available on-line at: http://www.vos.noaa.gov/MWL/apr_06/winds.shtml].
26. Glickman, T.S., 1999: *Glossary of Meteorology*, American Meteorological Society, 851 pp. [Available on-line at: <http://amsglossary.allenpress.com>].
27. Howes, D.B., and Whitnah, A. M., "Analytical Model for Determining Spacecraft Impact Velocity and Orientation Relative to an Impact Surface", NASA Technical Note D-6325, 1971.

	NASA Engineering and Safety Center Technical Report	Document #: NESC-RP-08- 00494	Version: 1.0
Title: Assessment of Orion Crew Module Ocean Wave Model			Page #: 63 of 158

28. Hsu, S., E.A. Meindl, and D.B. Gilhousen, 1994: Determining the Power-Law Wind-Profile Exponent under Near-Neutral Stability Conditions at Sea, *Jrnl. Appl. Meteor.*, V33(6), pp. 757–765. [Available on-line at: <http://ams.allenpress.com/archive/1520-0450/33/6/pdf/i1520-0450-33-6-757.pdf>]
29. Hwang, P. A., and M. A. Sletten (2008), Energy dissipation of wind-generated waves and whitecap coverage, *J. Geophys. Res.*, 113, C02012, doi:10.1029/2007JC004277.
30. IAHR, 1989: List of Sea–State Parameters, *Journal of Waterway, Port, Coastal and Ocean Engineering*, Vol. 115, No. 6, pp. 793-808.
31. Kahma, K. K., and C. J. Calkoen, 1992: Reconciling discrepancies in the observed growth of wind-generated waves. *J. Phys. Oceanogr.*, **22**, 1389-1405.
32. Kinsman, B., 1984: *Wind Waves: Their Generation and Propagation on the Ocean Surface*, Dover, New York, 676 pp.
33. Kuik, A.J., G. van Vledder, L.H. Holthuijsen, 1988: A method for the routine analysis of pitch-and-roll buoy wave data. *J. Phys. Oceanogr.* 18, 1020-1034.
34. Lang, N., 1987: The Empirical Determination of a Noise Function for NDBC Buoys with Strapped-down Accelerometers, in *Proceedings of Oceans '87*, Vol. 1, Halifax, N.S., Canada, pp. 225-228.
35. Liu, W. T., K. B. Katsaros, and J. A. Businger, 1979: Bulk Parameterizations of Air-Sea Exchanges of Heat and Water Vapor Including Molecular Constraints at the Interface, *Jrnl. Atmos. Scie.*, Vol. 36, 1722-1735. [Available on-line at: <http://ams.allenpress.com/archive/1520-0469/36/9/pdf/i1520-0469-36-9-1722.pdf>].
36. Longuet-Higgins, M.S., Cartwright, D.E. and Smith, N.D., 1963, Observations of the directional spectrum of sea waves using the motions of a floating buoy, In *Ocean Wave Spectra*, Prentice Hall, 111-136.
37. Longuet-Higgins, M.S., Cartwright, D.E., and Smith, N.D., 1963. Observations of the Directional Spectrum of Sea Waves Using the Motions of a Floating Buoy, in *Proceedings of Ocean Wave Spectra*, published by Prentice-Hall, pp. 111-136.
38. Lygre, A., H.E. Krogstad, 1986: Maximum entropy estimation of the directional distribution in ocean wave spectra. *J. Phys. Oceanogr.* 16, 2052-2060.
39. Monahan, E. C. (1971), Oceanic Whitecaps, *J. Phys. Oceanogr.*, 1, 139–144.
40. NDBC, 1996: *NDBC Technical Document 96-01, Nondirectional and Directional Wave Data Analysis Procedures*, [Available on-line at: <http://www.ndbc.noaa.gov/wavemeas.pdf>].

	NASA Engineering and Safety Center Technical Report	Document #: NESC-RP-08- 00494	Version: 1.0
Title: Assessment of Orion Crew Module Ocean Wave Model			Page #: 64 of 158


41. NDBC, 2003: *NDBC Technical Document 03-02, Handbook of Automated Data Quality Control Checks and Procedures of the National Data Buoy Center* [Available on-line at: <http://www.ndbc.noaa.gov/handbook.pdf>].
42. Oltman-Shay, J. and R.T. Guza, 1984: A data-adaptive ocean wave directional-spectrum estimator for pitch and roll type measurements. *J. Phys. Oceanogr.* 14, 1800-1810.
43. O'Reilly, W. C.; Herbers T. H. C.; Seymour R. J.; and Guza R. T. A Comparison of Directional Buoy and Fixed Platform Measurements of Pacific Swell and *J. Atmos Ocean. Technol.*, 13, (1), pp231-238, 1996.
44. Spera, D.A. and T.R. Richards, 1979: *Modified Power Law Equations for Vertical Wind Profiles*, NASA TM-79275, 14 pp. [Available on-line at: http://ntrs.nasa.gov/archive/nasa/casi.ntrs.nasa.gov/19800005367_1980005367.pdf].
45. Steele, K.E. J.C. Lau, and Y.L. Hsu, 1985: Theory and application of calibration techniques for an NDBC directional wave measurements buoy. *IEEE Journ. Oceanic Eng.*, **10(4)**, 382-396.
46. Steele, K.E., 1997: Ocean Current Kinematic Effects on Pitch-Roll Buoy Observations of Mean Wave Direction and Nondirectional Spectra, *Journal of Atmospheric and Oceanic Technology*, V14(2), pp.278-291. [Available on-line at: <http://ams.allenpress.com/archive/1520-0426/14/2/pdf/i1520-0426-14-2-278.pdf>].
47. Steele, K.E., and M.D. Earle, 1991: Directional Ocean Wave Spectra Using Buoy Azimuth, Pitch, and Roll Derived from Magnetic Field Components, *Journal of Ocean Engineering, IEEE*, Vol. 16, pp. 427-433.
48. Steele, K.E., Teng, C.C., and Wang, D.W., 1992: "Wave Direction Measurements Using Pitch-Roll Buoys," *Journal of Ocean Engineering, IEEE*, Vol. 19, No. 4, pp. 349-375.
49. Steele, K.E., Wang, D.W., Earle, M.D., Michelena, E.D., Dagnall, R.J., 1998: "Buoy Pitch and Roll Computed Using Three Angular Rate Sensors", *Journal of Coastal Engineering, IEEE*, Vol. 35, pp. 123-139.
50. Taylor, P.K., E. Dunlap, F.W. Dobson, R. J. Anderson, and V. R. Swail, 2002: On the Accuracy of Wind and Wave Measurements from Buoys, *Data Buoy Cooperation Panel (DBCP) Technical Documents 21-2002*. [Available on-line at: http://www.jcommops.org/dbcp/doc/DBCP-21/DOCS_DBCP21/27%20Taylor.doc].
51. Teng, C.C., Remond, F., and Dagnall, R., 1991: "Field Evaluation of the Magnetometer-Only Directional Wave System from Buoys," *Proceedings of MTS '91*, New Orleans, Louisiana, pp. 1216 - 1224.
52. Thuillier R.H, and Lappe, U.O, 1964: Wind and temperature profile characteristics from observations on a 1400 ft tower, *J. App. Met.*, V3, 299-306.

	NASA Engineering and Safety Center Technical Report	Document #: NESC-RP-08- 00494	Version: 1.0
Title: Assessment of Orion Crew Module Ocean Wave Model			Page #: 65 of 158

53. Teng, C.C., 2002: Wave measurements from NDBC buoys and C-MAN stations, *Proc. Oceans 2002 MTS/IEEE*, V.1, pp. 517-524.
54. van den Berg, G. P., 2008: Wind turbine power and sound in relation to atmospheric stability, *Wind Energy*, 11(2), 151, pp. 151-169.
55. Whitnah, A.M. and Howes, D.B., "Statistics Concerning the Apollo Command Module Water Landing, Including the Probability of Occurrence of Various Impact Conditions, Successful Impact, and Body X-Axis Loads", NASA Technical Memorandum X-2430, 1971.
56. WMO, 1995: WMO PUBLICATION No. 306 - MANUAL ON CODES, Volume I.1 - Part A - Alphanumeric Codes, World Meteorological Organization, Geneva. [Available on-line at: <http://www.wmo.int/pages/prog/www/WMOCodes/Manual/Volume-I-selection/ManualCodesSel.html>].
57. WMO, 1998: Guide to Wave Analysis and Forecasting, WMO-No. 702, World Meteorological Organization, Geneva.

Volume II: Appendices

- A. Overview of the Monte Carlo Analysis Process used to Establish Crew Module Water Landing Conditions, January 8, 2008
- B. Monte Carlo Ocean Wave Modeling, Rev. D, December 2008
- C. Wave Simulations (AMA, Inc. Report, Section 3.1.2)
- D. Spatial-Temporal Variability
- E. NDBC Wave Measurements (Data Format)
- F. CDIP Wave Measurements (Data Format)

	NASA Engineering and Safety Center Technical Report	Document #: NESC-RP-08- 00494	Version: 1.0
Title: Assessment of Orion Crew Module Ocean Wave Model			Page #: 66 of 158

Appendix A. Overview of the Monte Carlo Analysis Process used to Establish Crew Module Water Landing Conditions

January 8, 2008
 Jim Corliss / NASA LaRC
 Revision: Draft

STEP 1: Conduct Descent and Landing Flight Dynamics Monte Carlo Analysis


The Orion Guidance, Navigation & Control (GN&C) group conducts a Monte Carlo analysis that establishes the distribution of Crew Module landing conditions for dispersed vehicle and atmospheric conditions. The descent and landing Monte Carlo analysis is conducted using a simulation program called DSS. The dispersed vehicle conditions include, among other things, variations on Crew Module mass properties and parachute aerodynamic parameters (e.g., drag coefficient). The dispersed atmospheric conditions include variations on atmospheric density, horizontal winds, and vertical winds, usually as a function of altitude, and are provided by the Global Reference Atmosphere Model (GRAM). The Monte Carlos currently being provided by the GN&C group typically contain 10,000 to 12,000 individual cases that uniformly span the calendar year.

Separate descent and landing Monte Carlos are conducted for various landing scenarios, including:

- a) Planned re-entry landings for either ISS or lunar missions at the primary water landing site near San Clemente Island, CA;
- b) Ascent abort landings along the Atlantic seaboard of the Eastern United States;
- c) Pad abort landings off-shore or on land near the Kennedy Space Center Pad 39 complex; and
- d) Contingency land landings

The output of the descent and landing Monte Carlo analysis is a set of tabulated data that defines the Crew Module attitudes and velocities for each Monte Carlo case. The DSS Monte Carlo output that is relevant to establishing the actual landing conditions includes the following Crew Module data:

- Vertical velocity

	NASA Engineering and Safety Center Technical Report	Document #: NESC-RP-08- 00494	Version: 1.0
Title: Assessment of Orion Crew Module Ocean Wave Model			Page #: 67 of 158

- Horizontal velocity and heading
- Pitch, yaw, and roll attitudes
- Steady-state wind speed at 101 meter altitude (used for establishing ocean wave conditions as described in the following steps, the altitude of 101 meters is used because it is the altitude at which the steady-state winds correlate best to the Crew Module horizontal velocity)


STEP 2: Select a Landing Scenario and Extract/Expand DSS Data

The descent and landing Monte Carlo analyses described in Step 1 are conducted over a wide range of horizontal wind conditions, and are also conducted with either three main parachutes (nominal) or with two main parachutes (off-nominal failure mode). Through past analyses the Orion Project has determined that several specific landing scenarios result in water landing loads that drive the vehicle design. These scenarios are:

- a) Landing near San Clemente Island with two main parachutes in maximum nominal winds (8.2 m/s steady-state wind at 10 m altitude)
- b) Landing near San Clemente Island with two main parachutes in lower nominal winds (~2.3 m/s steady-state wind at 10 m altitude) at which the Crew Module roll control capability is not available. The Crew Module roll control capability degrades as the horizontal velocity decreases, and with a surface wind of 2.3 m/s it is anticipated that the roll control will not function.
- c) An ascent abort water landing along the Atlantic seaboard with three main parachutes and maximum specified abort winds of 13.9 m/s at 10 m altitude).

Other landing scenarios are evaluated as part of the Crew Module design process, but for the sake of this overview we will limit the discussion to these three scenarios.

Since the descent and landing Monte Carlo analyses are conducted over a wide range of horizontal wind conditions, specific data for each of the aforementioned landing scenarios must be extracted from the DSS output. For example, when we evaluate the landing conditions for scenario (a) above, we will extract all of the DSS Monte Carlo data with steady-state wind speeds of 8.2 ± 1.0 m/s at the 10 m altitude. We use a range of ± 1.0 m/s because the published accuracy of the NOAA buoy wind measurements is ± 1.0 m/s. Note that since the DSS output currently only provides the steady-state wind speeds at 101 m altitude, we extrapolate the DSS-provided wind down to 10 m altitude using a power law with an exponent of 0.11.

	NASA Engineering and Safety Center Technical Report	Document #: NESC-RP-08- 00494	Version: 1.0
Title: Assessment of Orion Crew Module Ocean Wave Model			Page #: 68 of 158

At the conclusion of this process, depending on the landing scenario selected, the subset of data that is extracted from the DSS Monte Carlo typically contains between 500 and 2000 individual landing cases. This data set is then expanded to 10,000 cases through a process of deriving probability distributions for each landing parameter (velocity, attitude, etc.) and then using these distributions to generate a larger data set.

STEP 3: Establish Ocean Wave Conditions

At this point in the process we have a data set of 10,000 landing cases for a given landing scenario. Each landing case is defined by a specific set of Crew Module landing velocities and attitudes, and a steady-state horizontal wind speed at 10 m altitude. Using the 10 m wind speed as the input, the process described in Section 3.0 of the wave model document [Monte Carlo Ocean Wave Modeling, D. Bose, Rev. D] is used to cast a water slope, water slope azimuth, and water vertical velocity for each of the 10,000 landing cases.

With the ocean wave data established for each landing case, the distribution of Crew Module water landing conditions can now be derived, which includes:


- Relative vertical velocity (sum of Crew Module descent velocity and water the wave vertical velocity)
- Crew Module horizontal velocity and heading relative to the wave face (note that while the water may have a small component of horizontal velocity we ignore this component because it is typically small compared to the Crew Module's horizontal velocity)
- Crew Module pitch, yaw, and roll attitudes

The distribution of these landing parameters is then used to establish the relevant landing cases that will be evaluated through LS DYNA water impact analysis.

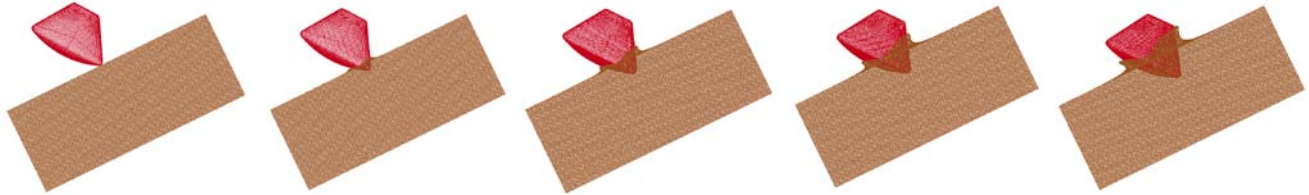
STEP 4: LS DYNA Water Impact Analysis

The LS DYNA Crew Module impact analysis is not part of the process to establish landing conditions, but a brief description is provided here for additional information.

LS DYNA is a widely used non-linear impact analysis code that Orion uses to evaluate the landing accelerations, crew loads, and structural loads when the Crew Module


	NASA Engineering and Safety Center Technical Report	Document #: NESC-RP-08- 00494	Version: 1.0
Title: Assessment of Orion Crew Module Ocean Wave Model			Page #: 69 of 158

impacts the water. A set of snap shots from an example water impact analysis is shown below.




Two general assumptions are made as part of the LS DYNA analysis that may be relevant to the NESC wave model review.

1. The wave model generates a distribution of “point” water slopes. In other words, the distribution of slopes represents the probability that the slope of the water surface will be a specific value at any point across the water surface. When we conduct the LS DYNA analysis we take this point water slope and treat it as an “infinite” flat surface with the point slope as indicated in the above images.
2. We assume that waves with a wave length less than the diameter of the Crew Module are negligible in terms of their effect on landing loads, and we “filter out” these waves and their slopes as discussed in the wave model document.

	NASA Engineering and Safety Center Technical Report	Document #: NESC-RP-08- 00494	Version: 1.0
Title: Assessment of Orion Crew Module Ocean Wave Model			Page #: 70 of 158

Appendix B. Monte Carlo Ocean Wave Modeling, Rev. D

	NASA Engineering and Safety Center Technical Report	Document #: NESC-RP-08- 00494	Version: 1.0
Title: Assessment of Orion Crew Module Ocean Wave Model			Page #: 71 of 158

Monte Carlo Ocean Wave Modeling

Prepared by:

David M. Bose
Analytical Mechanics Associates, Inc.

DRAFT

AMA Report No.: 08-09, rev D
NASA Contract BPA NNL04AA03Z
NNL07AB53T - AMA Task 9005-174
December 19, 2008



	NASA Engineering and Safety Center Technical Report	Document #: NESC-RP-08- 00494	Version: 1.0
Title: Assessment of Orion Crew Module Ocean Wave Model			Page #: 72 of 158

Table of Contents

1.0	BACKGROUND.....	4
1.1	THE APOLLO MODEL	4
1.2	ADVANCES IN WAVE THEORY	5
1.3	BUOY MEASUREMENTS.....	6
2.0	MODEL OVERVIEW.....	8
2.1	MODEL REQUIREMENTS.....	8
2.2	MODELING APPROACH.....	10
2.3	FUNDAMENTALS OF LINEAR WAVE THEORY.....	11
2.4	WAVE SLOPE	12
2.4.1	<i>Nondirectional Slope Variance</i>	<i>12</i>
2.4.2	<i>Frequency Limits.....</i>	<i>13</i>
2.4.3	<i>Frequency Extrapolation.....</i>	<i>14</i>
2.4.4	<i>Upwind-downwind and Crosswind Components of Wave Slope.....</i>	<i>16</i>
2.4.5	<i>Independence and Normality of Upwind-downwind and Crosswind Slopes.....</i>	<i>19</i>
2.4.6	<i>Confidence Intervals.....</i>	<i>22</i>
2.5	WAVE VERTICAL VELOCITY.....	26
2.5.1	<i>Correlation to Wave Slope.....</i>	<i>27</i>
2.5.2	<i>Confidence Intervals.....</i>	<i>30</i>
2.6	WAVE DIRECTION AND WAVE AZIMUTH.....	31
2.7	3-SIGMA ADJUSTMENTS.....	32
3.0	THE INTEGRATED MODEL.....	33
3.1	MODEL VERIFICATION	35
3.1.1	<i>Wave Vertical Velocity Variance.....</i>	<i>35</i>
3.1.2	<i>Slope Variance using Simulated Data.....</i>	<i>36</i>
3.1.3	<i>Overall Model Assumptions</i>	<i>37</i>
4.0	SUMMARY AND CONCLUSIONS.....	45
5.0	ACKNOWLEDGEMENTS.....	45
6.0	REFERENCES	46

	NASA Engineering and Safety Center Technical Report	Document #: NESC-RP-08- 00494	Version: 1.0
Title: Assessment of Orion Crew Module Ocean Wave Model			Page #: 73 of 158

This document provides an overview of the wave model developed for Crew Module (CM) Landing Monte Carlo analysis performed by Analytical Mechanics Associates, Inc. in support of contract NNL07AB53T, "Dynamic Analysis of the Orion Crew Module (CM) Retro Rocket Landing System".

Section 1.0 provides background on the modeling effort. Details of key components of the model, including underlying assumptions are provided in Section 2.0. Section 3.0 summarizes the complete Monte Carlo model and presents results of simulation trials. A summary and list of conclusions are outlined in Section 4.0. Finally, acknowledgements are noted in Section 5.0 followed by a list of references.

Nomenclature

Parameters, notations, abbreviations and key terms used in this document are defined below.

μ	total wave slope angle [rad]
μ_{ud}	upwind-downwind component of wave slope angle [rad]
μ_c	crosswind component of wave slope angle [rad]
ψ	direction the wave is oriented relative to the direction of the horizontal wind [rad]
I	nondirectional wave slope variance respectively [unitless]
$\sigma_{ud}, \sigma_{ud}^2$	standard deviation and variance of the upwind-downwind wave slope [unitless]
σ_c, σ_c^2	standard deviation and variance of the crosswind wave slope [unitless]
$\sigma_{ud,c}$	covariance of upwind-downwind and crosswind wave slopes [unitless]
ρ	correlation coefficient of upwind-downwind and crosswind wave slopes [unitless]
$\sigma_{w,v}^2$	variance of wave vertical velocity [m ² /s ²]
$\sigma_{ud,wv}$	covariance of upwind-downwind slope and wave vertical velocity [m/s]
$\sigma_{c,wv}$	covariance of crosswind slope and wave vertical velocity [m/s]
$\rho_{ud,wv}$	correlation coefficient of upwind-downwind wave slope and wave vertical velocity [unitless]
$\rho_{c,wv}$	correlation coefficient of crosswind wave slope and wave vertical velocity [unitless]
V_{wind}	10-meter wind speed [m/s]
$V_{wind,5m}$	5-meter wind speed (typical anemometer height associated with NDBC buoy data)
V_w, c	wave speed or wave celerity [m/s]
$V_{w,v}$	component of wave speed in the vertical direction [m/s]
K_{age}	wave age, defined as the ratio of wave speed to wind speed
PM	refers to Pierson-Moskowitz
NDBC	refers to the National Oceanic and Atmospheric Administration's National Data Buoy Center
CDIP	refers to the Coastal Data Information Program
η	surface elevation of a wave form (height relative to sea level) [m]
H	wave height measured from trough to peak [m]
k	wave number [m ⁻¹]
L	wave length [m]
ω, f, T	wave frequency [rad/s], wave frequency [Hz], wave period [sec]
t	time [sec]
ϕ	wave phase angle [rad]
g	gravitational acceleration [m/s ²]
m_0	zeroth spectral moment [m ²]
S	wave spectral density [m ² /Hz]
df	bandwidth of a frequency band [Hz]
D	wave energy directional spreading function [unitless]
θ	wave direction [rad]
θ_w	wind direction [rad]
$d\theta$	width of directional bands [rad]


	NASA Engineering and Safety Center Technical Report	Document #: NESC-RP-08- 00494	Version: 1.0
Title: Assessment of Orion Crew Module Ocean Wave Model			Page #: 74 of 158

Figure 1 illustrates the relationship between wave azimuth (ψ), total (μ), upwind-downwind (μ_{ud}) and crosswind wave slopes (μ_c). The horizontal frame is aligned with the wind, with the x_h in the direction of the wind, z_h pointing toward the earth's center and y_h rounding out the right-handed system. The plane tangent to the wave represents a rotation ψ about the z_h , followed by a rotation of μ about the resulting y_h . Projections of the horizontal frame vectors x_h and y_h onto the tangent plane result in the vectors i_{ud} and i_c respectively. The angles between x_h and i_{ud} and y_h and i_c represent μ_{ud} and μ_c .

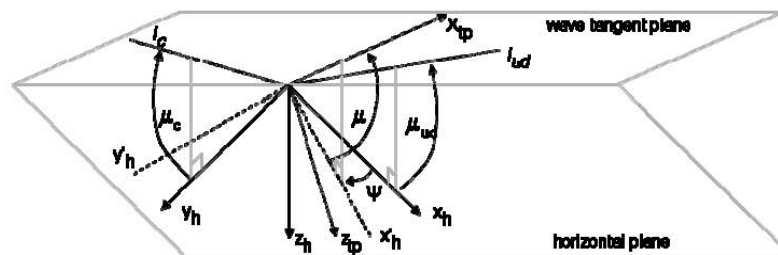


Figure 1. Definition of Wave Slopes, adapted from Cummings et al. [1972]

1.0 Background


Certain abort scenarios shall result in Crew Module (CM) landings in the open ocean. For the purposes of CM design assumptions, in particular structural loads, it is important to understand the potential landing conditions in terms of CM velocity and attitude relative to the ocean surface. To establish statistical estimates of these conditions, AMA, in conjunction a group of consultants and peer reviewers (see Acknowledgements), developed a Monte Carlo analysis tool. A key component of this analysis capability is a wave model, which estimates the slope, direction, and vertical velocity of an impact point on the ocean surface.

1.1 The Apollo Model

Wave modeling for the purposes of CM ocean landing analysis is not a unique endeavor. Apollo engineers faced the same problem. Their model and the underlying technical approach are nicely summarized in Cummings et al. [1972]. For the purposes of this paper, the model and techniques described in that document will be referred to as the Apollo model. A brief summary is provided below. Some of the assumptions and modeling concepts described provide the foundation for the current effort. For details of the Apollo model, please refer to [1].

In terms of wave slope, the Apollo model derived a total slope variance assuming the Neumann spectrum, a semi-empirical expression for the frequency spectrum of fully developed seas developed in the early 1950's. Other than frequency, the only other variable in the Neumann spectrum is wind speed. After some manipulation, the Neumann spectrum can be used to create a wave slope spectrum. After calculating the total slope variance at two wind speeds, a linear expression for total nondirectional wave slope variance (I) was created, where the wind speed in this equation has units of knots.

$$I = (0.808 \times 10^{-3} V_{\text{wind}} - 0.00581)^{1/2} \quad [1]$$

	NASA Engineering and Safety Center Technical Report	Document #: NESC-RP-08- 00494	Version: 1.0
Title: Assessment of Orion Crew Module Ocean Wave Model			Page #: 75 of 158

Since the Neumann spectrum provides no directional distribution of wave energy, the Apollo model adopts a directional breakdown of slope variance based on the findings of the Stereo Wave Observation Project (SWOP), see Cote et al. [1960]. In short, the SWOP data showed that the upwind-downwind and crosswind components of total variance were roughly 0.625 and 0.375 respectively, which gives,

$$\sigma_{ud}^2 = 0.625 I \quad [2]$$

$$\sigma_c^2 = 0.375 I \quad [3]$$

With these variances in hand, a wave slope can be estimated in a Monte Carlo fashion using:

1. upwind-downwind component of wave slope, μ_{ud} , using σ_{ud} .
2. crosswind component of wave slope, μ_c , using σ_c .
3. computing the total wave slope according to the expression $\mu = \tan^{-1}(\sqrt{\tan^2 \mu_{ud} + \tan^2 \mu_c})$.

The Apollo model does not address wave vertical velocity directly although a procedure for estimating wave speed is defined. Essentially a wave age is determined based on probability distributions that vary by wind speed. Wave speed is then calculated as the product of wave age and wind speed. The correlation of wave speed with wave slope is captured by limiting the determination of wave age to three regions of the probability distribution based on the upwind-downwind component of wave slope. The underlying assumption here is that steep wave slopes are an indication of younger waves which are slower. Although not part of the Apollo model, wave vertical velocity can be estimated from the wave slope and the wave horizontal velocity as simply,


$$V_{w,v} = \pm K_{age} V_{wind} \tan(\mu) \quad [4]$$

where the sign depends on whether the point is on the leading or trailing side of the wave.

The final aspect of the Apollo model is the wave direction, which is measured relative to the prevailing wind. The model adopts a cumulative probability distribution for wave direction that approximates a \cos^2 distribution on the interval of $\pm \pi/2$. Wave direction is loosely correlated to wave age by limiting the determination of wave direction to 3 overlapping regions of the probability distribution. The region from which a wave direction is cast is specified by the wave age determined in the calculation of wave horizontal velocity. Since wave age is correlated to the upwind-downwind component of wave slope, wave direction is also loosely correlated to upwind-downwind wave slope. Basically, older waves are assumed to be more likely to be aligned with the direction of the wind whereas younger, steeper waves exhibit more deviation.

1.2 Advances in Wave Theory

After review of the wave model by the team, most notably oceanography consultants Dr. James Kaihatu of Texas A&M University and Dr. William Perrie of the Bedford Institute of Oceanography, several opportunities of improvement to the Apollo model were identified. For the most part, these opportunities align with the advances in wave theory and ocean engineering, which have taken place since the time of the Apollo model was developed.

	NASA Engineering and Safety Center Technical Report	Document #: NESC-RP-08- 00494	Version: 1.0
Title: Assessment of Orion Crew Module Ocean Wave Model			Page #: 76 of 158

The Pierson-Moskowitz (PM) spectrum, [Pierson and Moskowitz, 1964], provides a characterization of the energy in fully developed seas, which is specified by a single parameter, namely the wind speed (at an elevation of 19.5 meters). To this day, the PM-spectrum remains the standard for describing fully developed seas. The PM-spectrum, however, is limited in that true ocean conditions rarely reach a fully developed sea state, energy due to swell is not captured, and the PM-spectrum is not valid for fetch-limited growing waves.

The JONSWAP spectrum, by Hasselmann et al. [1973], was developed based on experiments conducted in the North Sea for fetch-limited and duration-limited growing wave spectra. Energy spectra calculated from these experiments were found to converge to the PM-spectrum in the limit as the spectra approach the fully developed sea state. The JONSWAP spectrum improved the comparisons between measured and theoretical spectra by essentially adding a peak enhancement factor to the PM spectrum. However, it is difficult to determine the enhancement factor a-priori (i.e. in the absence of measured data).

Another limitation of both the PM and JONSWAP spectrums is that they do not capture bimodal spectra, which commonly occur when wave fields have strong swell components resulting in a low frequency energy peak. Although there have been advances in theoretical modeling to address bimodal spectra (see e.g. Ochi and Hubble [1976]; Torsethaugen and Haver [2004]; Resio and Perrie [2008]) their usefulness depends on the availability of measurements required to fully specify the spectrum. A good summary of standard and modified wave spectrum formulations can be found in Michel [1999], Long and Resio [2007].

The availability of ocean measurements (e.g. buoy data) is, perhaps, the most significant advancement since the time the Apollo model was developed. The wealth of data that is available via online data archives as well as real time data servers is astounding. In the early phases of the modeling effort described in this paper, buoy data were used to verify the suitability of assumed wave spectra like the PM-spectrum. However, it became apparent that the best answers would come from simply using the buoy data since measured data carries none of the limitations described above.


1.3 Buoy Measurements

The National Oceanic and Atmospheric Administration's (NOAA) National Data Buoy Center (NDBC) designs, develops, operates, and maintains a network of data collecting buoys in support of the missions of the National Weather Service and NOAA. Public access to the data is facilitated through a self service website which includes links to detailed documentation regarding the processing of buoy data (www.ndbc.noaa.gov). The network of buoys spans the globe with concentrations of buoys deployed off all coasts of the United States. Key data products provided by the buoys include:

Standard Meteorological Data: typical atmospheric conditions including wind speed, standard wave parameters including significant wave height, mean wave direction, dominant and zero crossing wave periods.

Detailed Wave Data: wave parameters broken down into components attributed to swell and wind waves respectively.

Spectral Wave Data: nondirectional wave energy across a set of discrete frequency bins. Directional buoys include directional spreading data. Frequency bins range from 0.03 to 0.485 Hz.

	NASA Engineering and Safety Center Technical Report	Document #: NESC-RP-08- 00494	Version: 1.0
Title: Assessment of Orion Crew Module Ocean Wave Model			Page #: 77 of 158

NDBC buoys referenced in this paper include:

6-meter Nomad Buoy:

Cape May: 200NM East of Cape May, NJ

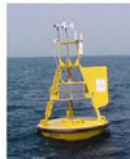
ID: 44004
Depth: 3182.1 m
Payload: 6-meter Nomad / ARES



3-meter Discus Buoys:

Cape Cod: SE Cape Cod 30NM East of Nantucket, MA

ID: 44018
Depth: 74.4 m
Payload: ARES



Nantucket: NANTUCKET 54NM Southeast of Nantucket

ID: 44008
Depth: 59.1 m
Payload: ARES

Santa Rosa: South Santa Rosa Island, CA

ID: 46069
Depth: 1004.6 m
Payload: ARES

Tanner Banks: TANNER BANKS - 121NM West of San Diego, CA

ID: 46047
Depth: 1393.5 m
Payload: ARES

12-meter Discus Buoy:

West Bermuda: W Bermuda

ID: 41048
Depth: 5261 m
Payload: ARES




Buoy images courtesy of NOAA's National Data Buoy Center (www.ndbc.noaa.gov).

All NDBC buoys with the exception of the Cape May buoy provide directional spreading information. All NDBC buoys capture wind speed at a height of 5-m above the surface with the exception of the West Bermuda buoy which measures winds at 10 meters. For consistency all wind speeds utilized and reported in this effort were adjusted to the 10 meter reference height using the following power rule provided by the NASA Marshall E&C SIG:

$$V_{wind} = V_{wind,5m} \left(\frac{10}{5}\right)^{.11} \quad [5]$$

Another source of buoy data is provided by the Coastal Data Information Program (CDIP), (<http://cdip.ucsd.edu/>). CDIP buoys provide much the same data as those of NDBC. An advantage of the CDIP buoys is that they are designed to more accurately capture wave energy at higher frequencies. The frequency range of the CDIP buoys has an upper limit of 0.58 Hz.

	<p align="center">NASA Engineering and Safety Center Technical Report</p>	<p>Document #: NESC-RP-08- 00494</p>	<p>Version: 1.0</p>
<p>Title: Assessment of Orion Crew Module Ocean Wave Model</p>			<p>Page #: 78 of 158</p>

One CDIP buoy was utilized in this effort, namely:

CDIP Buoy 067: San Nicholas Island, Owned and maintained by Scripps Institution of Oceanography

Depth: 335 m

Configuration/Payload: Waverider



The wealth of buoy data available today presents a huge advantage over the tools/data available to the engineers working on the Apollo program. As will become evident in the next section, buoy data will provide the foundation for improvements made to the Apollo model.

2.0 Model Overview


2.1 Model Requirements

Output of the integrated wave model is used in ocean landing Monte Carlo analysis to compute surface-relative landing conditions including relative vehicle attitude as well as relative velocity. Specific wave model outputs used in landing analysis include:

1. **Wave slope:** a nonnegative angle defining the inclination of the wave plane relative to the local horizontal [rad].
2. **Wave azimuth:** the orientation of the wave plane as measured by the rotation of the wave plane about the vertical axis [rad] relative to the wind direction.**
3. **Wave vertical velocity:** the velocity of the impact point on the wave's surface in the vertical, inertial direction, positive up [ft/s].

** Note that the definition of wave azimuth may differ in landing simulations.

The coordinate frame assumed by the wave model is illustrated below along with specific landing scenarios. Note that this coordinate frame may not align with that employed by the landing simulations.

	<p>NASA Engineering and Safety Center Technical Report</p>	<p>Document #: NESC-RP-08- 00494</p>	<p>Version: 1.0</p>
<p>Title: Assessment of Orion Crew Module Ocean Wave Model</p>			<p>Page #: 79 of 158</p>

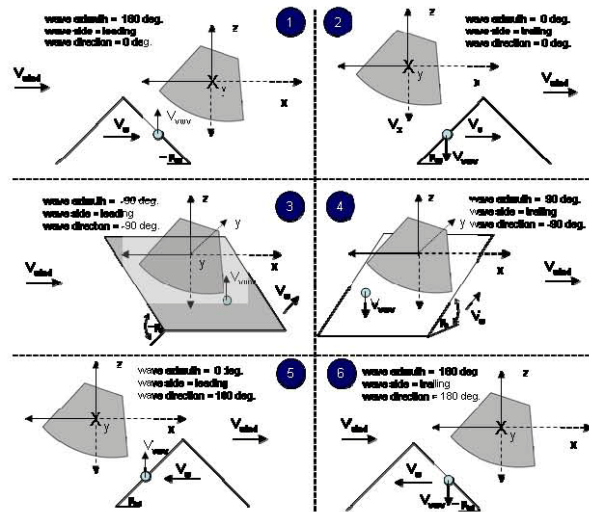



Figure 2. CM Ocean Landing Scenarios

The CM nominally has a 28 degree hang angle, pitch down relative to its horizontal direction of travel, nominally in the direction of the prevailing wind. In Figure 2, the CM is moving left to right as it falls toward the wave. The relative impact angles and velocity will depend on the three wave model outputs noted above, namely wave slope, wave azimuth, and wave vertical velocity. Sets of these outputs are produced by the wave model for each Monte Carlo case. Six potential scenarios illustrated in Figure 2 are described below. The frequency of these scenarios will depend on the wind speed as well as the Monte Carlo seed provided to the wave model.

- Scenario 1:** The CM lands on the leading side of the wave (downhill). The wave slope is aligned with the wind resulting in a negative upwind-downwind wave slope and a zero crosswind slope. The wave is moving up to meet the CM at impact. The CM's horizontal velocity reduces normal velocity (relative velocity of the CM normal to the wave surface) whereas the wave's vertical velocity increases it.
- Scenario 2:** The CM lands on the trailing side of the wave (uphill). The wave slope is aligned with the wind resulting in a positive upwind-downwind wave slope and a zero crosswind slope. The wave is moving down, away from the CM, at impact. The CM's horizontal velocity increases normal velocity whereas the wave's vertical velocity reduces it.
- Scenario 3:** The CM lands abeam to the leading side of the wave (breach). The wave slope is perpendicular to the wind resulting in a zero upwind-downwind wave slope and a negative crosswind slope. The wave is moving up to meet the CM at impact. The CM's horizontal velocity has no impact on the normal impact velocity. The wave's vertical velocity increases the normal velocity.
- Scenario 4:** The CM lands abeam to the trailing side of the wave (breach). The wave slope is perpendicular to the wind resulting in a zero upwind-downwind wave slope and a positive

	NASA Engineering and Safety Center Technical Report	Document #: NESC-RP-08- 00494	Version: 1.0
Title: Assessment of Orion Crew Module Ocean Wave Model			Page #: 80 of 158

crosswind slope. The wave is moving down, away from the CM, at impact. The CM's horizontal velocity has no impact on the normal impact velocity. The wave's vertical velocity decreases the normal velocity.

Scenario 5: The CM lands on the leading side of the wave (uphill). The wave slope is aligned with the wind resulting in a positive upwind-downwind wave slope and a zero crosswind slope. The wave is moving opposite to the wind leading to a positive wave vertical velocity. The CM's horizontal velocity and the wave's vertical velocity both increase normal velocity.

Scenario 6: The CM lands on the trailing side of the wave (downhill). The wave slope is aligned with the wind resulting in a negative upwind-downwind wave slope and a zero crosswind slope. The wave is moving opposite to the wind leading to a negative wave vertical velocity. The CM's horizontal velocity and the wave's vertical velocity both decrease normal velocity.

2.2 Modeling Approach

As mentioned above, the wave model supports Monte Carlo simulation analysis. Additionally, the modeling approaches outlined in this and subsequent sections may be applicable to the establishment of operational procedures for performing near or real-time predictions of launch availability.

An underlying assumption for the wave model is that landing occurs in deep water. In deep water, waves are unaffected by the ocean bottom. When waves travel in areas of shallow water, they are affected. Free orbital motion of the water is disrupted, and water particles in orbital motion no longer return to their original position. In very shallow water, waves become higher and steeper, ultimately assuming a familiar sharp-crested wave shape.


Deep water is typically characterized by conditions where the water depth is greater than 0.5 times the wave length of the waves. For the buoys noted in the previous section, the shallowest is the Nantucket buoy at 59.1 meters. At this depth, waves with frequencies below 0.11 Hz do not qualify as deep water waves under the classic definition. However, frequencies most relevant to wave slope are above this frequency. Hence, all the buoys used in the analysis described herein are considered to be in deep water.

At a high level, the wave model is comprised of three main components:

1. Wave slope
2. Wave Vertical Velocity
3. Wave Azimuth

The data analysis flow supporting development of these components is as follows:

1. Identify a period of record on which to ground the wave model and a set of applicable buoys.
2. Download historical data from the NDBC website (<http://www.ndbc.noaa.gov/hmd.shtml>) for records during this period of record. Required data is captured in the following files:
 - a. Standard meteorological data: contains wind speed, wind direction and significant wave height.
 - b. Spectral wave density data: contains spectral density data
 - c. Spectral wave (alpha1) direction data: contains first of four data pieces capturing the directional spreading of the wave energy (mean wave direction)

	NASA Engineering and Safety Center Technical Report	Document #: NESC-RP-08- 00494	Version: 1.0
Title: Assessment of Orion Crew Module Ocean Wave Model			Page #: 81 of 158

- d. Spectral wave (alpha2) direction data: contains second of four data pieces capturing the directional spreading of the wave energy (principal wave direction).
 - e. Spectral wave (r1) direction data: contains third of four data pieces capturing the directional spreading of the wave energy (first normalized polar coordinate).
 - f. Spectral wave (r2) direction data: contains fourth of four data pieces capturing the directional spreading of the wave energy (second normalized polar coordinate).
3. Clean and align data. Missing or corrupt data in the NDBC buoy records are indicated by '99' or '999', depending on the specific parameter. Records with these types of entries are removed. Moreover, records in the various data files, for example standard meteorological and wave density files, may not be in the same order or may not contain the same set of records. A date and time stamp in each record is used during this step to align the data sets.
 4. Estimate nondirectional slope and wave vertical velocity variance for each record using the wind speed from the standard meteorological data (WSPD), as well as spectral density from the wave density data. Note that the frequencies associated with the wave density data are indicated in the header of the data file. The first frequency bin is considered by NDBC as a noise bin and is not included in this analysis. Wind speed 10-meters above sea level is also estimated in this step.
 5. Estimate the breakdown of the nondirectional slope variance into upwind-downwind and crosswind components using the same data as in step 4 but with wind direction (VD) as well as the four data sets defining the directional spreading of each record (alpha1, alpha2, r1 and r2).
 6. Estimate the correlation of wave vertical velocity and wave slope components using the same data used in steps 4 and 5.

Additional analysis details related to these 6 steps and the development of the three main components of the model are provided in the sub-sections to follow. A detailed description of the final, integrated model is provided in Section 3.0.

2.3 Fundamentals of Linear Wave Theory


Linear or small amplitude wave theory is commonly attributed to Airy who, in 1845, derived the first equations for waves assuming two-dimensional ideal fluid flow. Linear wave theory is applicable to conditions where wave height is small compared to wavelength and water depth. Under these assumptions, a single wave has the form:

$$\eta = \frac{H}{2} \cos(kx - \omega t + \phi) \quad [6]$$

where η is the elevation of a point on the surface measured from sea-level, H is the wave height measured trough to crest, k is the wave number, x is a coordinate indicating the horizontal location of a point on the wave, t is time, and ω is the wave's temporal frequency. For completeness, a phase angle, ϕ , is also included. Alternative formulations of the small amplitude wave form can be written in terms of L , wavelength, and T , wave period, with:

$$L = \frac{2\pi}{k}, \text{ and} \quad [7]$$

$$T = \frac{2\pi}{\omega} \quad [8]$$

	NASA Engineering and Safety Center Technical Report	Document #: NESC-RP-08- 00494	Version: 1.0
Title: Assessment of Orion Crew Module Ocean Wave Model			Page #: 82 of 158

The horizontal speed of the wave, referred to as wave celerity (c), is simply $\frac{L}{T}$. For deep water waves, Airy showed that wavelength and therefore wave celerity is specified by wave period alone.

$$L = \frac{gT^2}{2\pi} \quad [9]$$

$$c = \frac{L}{T} = \frac{gT}{2\pi} \quad [10]$$

For a more complete derivation of the linear wave equations, see for example Reeve et al [2004].

2.4 Wave Slope

The wave slope of a wave form as described in equation [6] is,

$$\frac{d\eta}{dx} = k \frac{H}{2} \sin(kx - \omega t + \phi) = k\eta_{\phi=\phi-\pi/2} \quad [11]$$

Recognizing that the ocean's surface is not characterized by a single wave but rather by a wave field, the slope at any given point can be written as,

$$\frac{d\eta}{dx}(x,t) = \sum_i k_i \frac{H_i}{2} \sin(k_i x - \omega_i t + \phi_i) \quad [12]$$

2.4.1 Nondirectional Slope Variance


Mathematically, the variance of a periodic function can be computed simply as the integral of its energy spectrum. For example, the variance of elevation in a wave field can be computed as:

$$m_0 = \sum_i S(f_i) df_i \quad [13]$$

where f refers to frequency in Hz ($\frac{\omega}{2\pi}$), $S(f_i)$ is the discrete spectral density function, in m^2/Hz , commonly provided by buoys, and df_i is the bandwidth in Hz of each of the frequency bands for which the energy spectrum is provided. Also referred to as the zeroth spectral moment, m_0 , is used to estimate the wave parameter Hm_0 , referred to as significant wave height ($Hm_0 = 4\sqrt{m_0}$).

Recognizing that the wave slope function, differs from the wave elevation function only by a factor of k and a 90 degree phase shift, wave slope variance can be computed as:

$$I = \sum_i k_i^2 S(f_i) df_i \quad [14]$$

	NASA Engineering and Safety Center Technical Report	Document #: NESC-RP-08- 00494	Version: 1.0
Title: Assessment of Orion Crew Module Ocean Wave Model			Page #: 83 of 158

Here λ refers to the nondirectional wave slope variance since wave directional spreading is not yet considered (see Section 2.2.4). Nondirectional 1-sigma wave slopes computed from year-2007 and 2008 records of the Cape May buoy are illustrated below. Plotted along with the 1-sigma slopes is the effective 1-sigma slope line. This is estimated by segmenting the variances computed for each record by 10-meter wind speed. Bin widths of 1.524 m/s (5 ft/s) were used. Once segmented, the effective variance was computed as the mean of the variances in each bin.

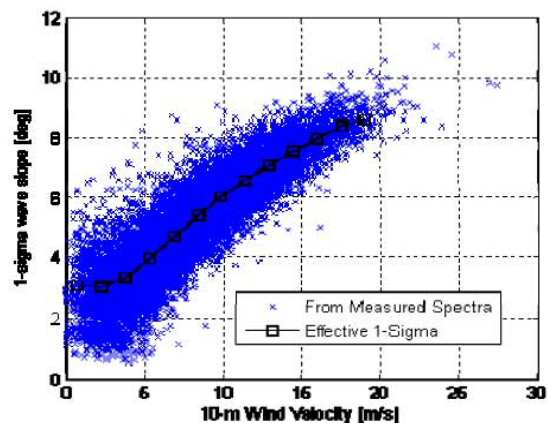


Figure 3. Nondirectional 1-sigma Slopes, Cape May, 2007-2008


There is a clear trend as 1-sigma wave slopes increase with the 10-meter wind velocity. At lower wind speeds (< 5 m/s), swell is a more significant component of the wave field as demonstrated by the leveling off of the effective 1-sigma slope line.

Note: the frequency bin centered at 0.02 Hz in the spectra reported by NOAA's NDBC buoys is treated as a noise bin and is not used in the calculation of wave parameters reported by NDBC. Following this approach, the 0.02 Hz bin was excluded from the calculation of wave slope variances.

2.4.2 Frequency Limits

An upper limit is placed on the frequencies included in the slope variance calculation. This limit is implemented in order to restrict contributions to slope variance to only those waves that are significant in scale relative to the Crew Module. Following Cummings et al. [1972], this limit is selected to include waves with a wavelength greater than or equal to the diameter of the Crew Module. Assuming a 5-meter capsule the frequency limit is roughly 0.56 Hz, which corresponds to a period of 1.8 seconds.

The impact associated with including waves of higher frequencies is illustrated in the Figure 4. Here, an example wave spectrum is broken down into wave field components then plotted atop a notional cross-section of the Crew Module. Each component of the wave field represents the accumulation of

	NASA Engineering and Safety Center Technical Report	Document #: NESC-RP-08- 00494	Version: 1.0
Title: Assessment of Orion Crew Module Ocean Wave Model			Page #: 84 of 158

energy in 6 of 12 frequency bins, each 0.1 Hz in width. The green dashed lines are simply the zero-crossing lines of each wave form. The blue lines represent $\pm \frac{1}{2}$ theoretical wave length of waves at that given frequency. The distance between the two blue lines is the total wavelength, which, at 0.54 Hz, is just greater than the diameter of the capsule. The maximum wave slope associated with each wave component is also indicated in this figure and varies from 2.0 deg. in the lowest frequency bin to 19.6 deg. in the highest. Although the higher frequency waves are much smaller in scale than the Crew Module, they are significant contributors to the total slope variance.

To the right of the wave components are three plots illustrating the spectral density, wave heights, and slope variances of this example. In comparison to other buoy records this is a rather benign sea state. However, if all frequencies are included in the slope variance calculation the estimated 1-sigma slope would be 9.5 deg. The issue lies in the fact that the slope spectrum carries a k^2 factor which translates to a factor of ω^4 . If, at high frequencies, the spectral density does not decay faster than ω^4 , the total slope variance will continue to increase as higher and higher frequencies are included. As a result, the total slope variance is sensitive to the selected upper limit on frequency.

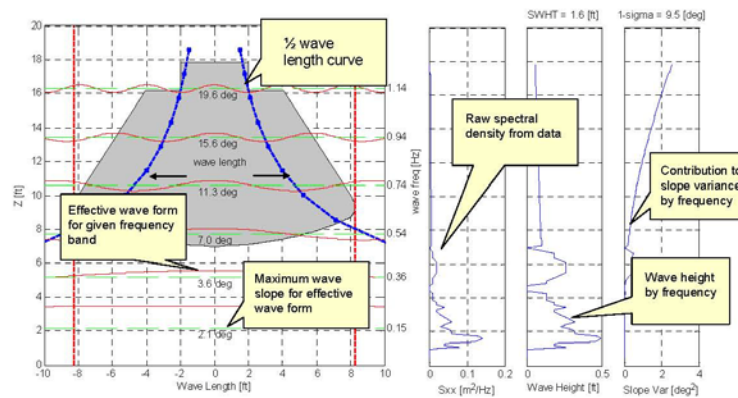



Figure 4. An Illustration of the Wave Scales

2.4.3 Frequency Extrapolation

As described in the previous section, a frequency limit of 0.56 Hz was chosen for slope variance calculations. NOAA provides a great number of buoys from which to access spectral measurements. However, those measurements have upper limits of 0.40 or 0.485 Hz, depending on the data acquisition system. All of the NDBC buoys referenced in this paper have a bandwidth of 0.485 Hz. In either case, extrapolation of the reported spectral densities is required to reach the 0.56 Hz limit.

In addition to the issue of buoy bandwidth there is some question as to how well the NDBC buoys resolve energy at the higher frequencies of the band. This question arises mainly due to the size of the NDBC buoys and the associated reduction in sensitivity caused by their mass properties and mooring characteristics. Although NDBC attempts to adjust measured data for frequency-dependent effects of buoy response, an investigation into this subject was warranted.

	NASA Engineering and Safety Center Technical Report	Document #: NESC-RP-08- 00494	Version: 1.0
Title: Assessment of Orion Crew Module Ocean Wave Model			Page #: 85 of 158

To aid in this investigation, data was taken from CDIP buoy 067 for all of 2007. This is an ideal buoy for this analysis since it is a Datawell's Waverider buoy, which provides accurate measurement of waves up to a frequency of 0.58 Hz. The 067 buoy is also located in deep water, close to a potential Crew Module landing site. The only drawback of 067 is that it does not provide a measure of wind speed. To get around this shortcoming, the wind velocity at 067 was assumed to be the average of the winds measured at NDBC's South Santa Rosa Island and Tanner Banks buoys.

Figure 5 and Figure 6 illustrate a comparison of spectral densities at these two NDBC buoys compared to those measured at CDIP buoy 067. Spectral densities are fairly consistent across the three buoys until about 0.4 Hz. Above this frequency, the spectral densities of the NDBC buoys roll off at a faster rate compared to buoy 067. This same behavior was seen when comparing buoy 067 to the Nantucket and Cape May buoys, which is further indication that this difference is not related to buoy location but rather an artifact of the measurement system (buoy configuration and payload).

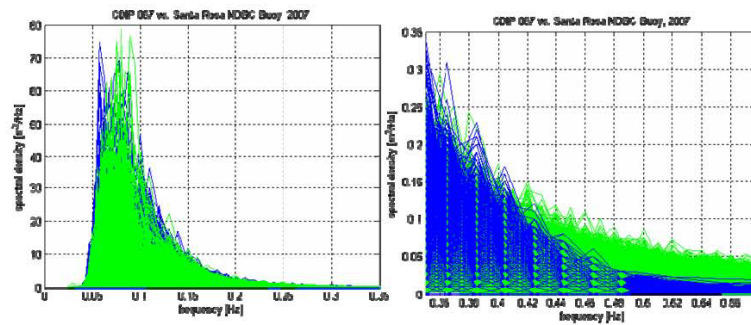


Figure 5. Spectral Densities of CDIP Buoy 067(green) and NOAA's NDBC Buoy 46069 (blue)

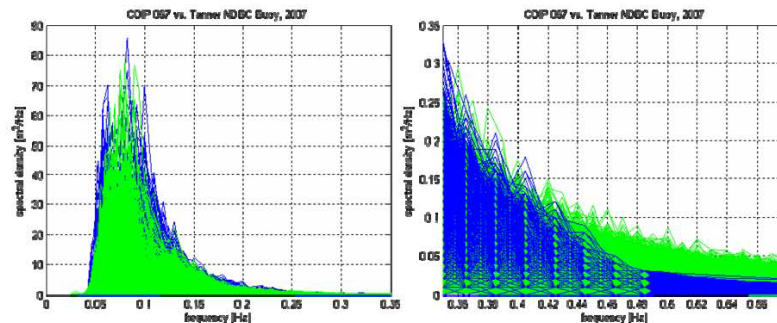



Figure 6. Spectral Densities of CDIP Buoy 067 (green) and NOAA's NDBC Buoy 46047 (blue)

	<p align="center">NASA Engineering and Safety Center Technical Report</p>	<p>Document #: NESC-RP-08- 00494</p>	<p>Version: 1.0</p>
<p>Title: Assessment of Orion Crew Module Ocean Wave Model</p>			<p>Page #: 86 of 158</p>

The NDBC adjustments do not appear to fully recover the energy at higher frequencies. Unfortunately, CDIP buoys are not found in many deep water locations. As such, an extrapolation approach was defined such that NDBC buoys could be used with increased confidence. Many different approaches can be employed for extrapolating the data. Here, a simple approach is adopted following the advice of oceanographic experts. Specifically, an f^{-4} tail is appended to the measured spectrum starting at 0.40 Hz. When overlaying the resulting spectra on those of the 067 buoy it is clear that this approach provides reasonable results.

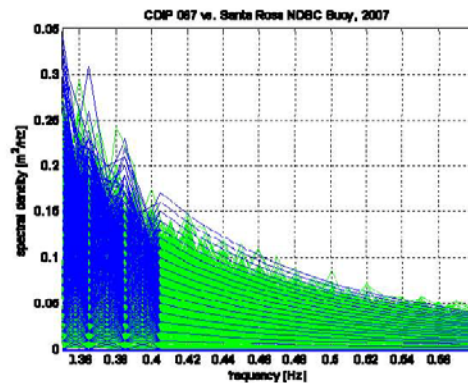



Figure 7. Spectral Density Comparisons Using f^{-4} Extrapolation (Green: CDIP 067)

2.4.4 Upwind-downwind and Crosswind Components of Wave Slope

The nondirectional slope spectrum is the accumulation of slope energy across all wave directions. It is not a valid representation of total slope spectrum since slopes from waves moving in different directions are not purely additive. The only case where the nondirectional slope spectrum does represent the total slope is the case where all waves are aligned in a single direction. In reality the wave field is made up of multiple, independent waves traveling in many different directions. Although a significant portion of the wave field may be aligned with the prevailing wind, particularly in the presence of high winds, there typically is a component in the crosswind direction. Recall that the Apollo model assumed a breakdown of upwind-downwind and crosswind slope variance components of 0.625 and 0.375 respectively.

Figure 8 below illustrates the impact of breaking the slope variance into these components through a 10,000 case Monte Carlo simulation assuming a 6.5 degree 1-sigma nondirectional slope. The slopes that are computed simply using the nondirectional slope variance have considerably more slopes near zero and a 99.7-percentile slope of roughly 19.4 degrees. In contrast, the distribution of slopes computed using the Apollo model breakdown peaks around 5 degrees and has a 99.7-percentile slope that is 15.6 deg. This 4 degree difference is significant to designers of the CM, so further investigation of the directional breakdown is warranted.

	NASA Engineering and Safety Center Technical Report	Document #: NESC-RP-08- 00494	Version: 1.0
Title: Assessment of Orion Crew Module Ocean Wave Model			Page #: 87 of 158

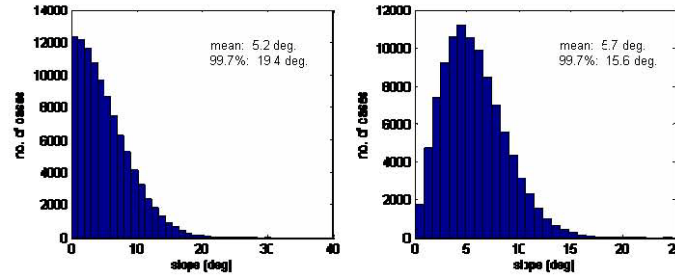


Figure 8. Slopes Resulting from Nondirectional Slope Variance (left) and an Assumed Breakdown (right)

To investigate the breakdown of nondirectional slope variance, buoys with directional spreading data were used. In the Atlantic, these buoys include the Nantucket, Cape Cod, and West Bermuda buoys. At each frequency, directional spreading is defined by four parameters capturing a Fourier series truncated to two terms. Mathematically, the spreading function is defined by Earle [1996] as:

$$D_i(\theta_j) = 1/\pi [1/2 + r_{1,i} \cos(\theta_j - \alpha_{1,i}) + r_{2,i} \cos(2(\theta_j - \alpha_{2,i}))] \quad [15]$$

where $D_i(\theta_j)$ is the spreading function associated with the i th frequency bin, θ_j represents the direction associated with the j th directional bin and,


- $r_{1,i}$ is the 1st normalized polar coordinate of the Fourier coefficients for frequency bin i
- $r_{2,i}$ is the 2nd normalized polar coordinate of the Fourier coefficients for frequency bin i
- $\alpha_{1,i}$ is the mean direction of the waves for frequency bin i
- $\alpha_{2,i}$ is the principal direction of the waves for frequency bin i (direction with the most energy)

where the α 's represent the direction the waves are coming from, measured clockwise from true North.

Applying the spreading function to the wave spectra at the aforementioned buoys it is possible to estimate the upwind-downwind and crosswind components of wave slope directly. Essentially the equation for the nondirectional slope variance is expanded to include integration over the directional dimension with,

$$\sigma_{ud}^2 = \sum_{j=1}^m \left[\sum_{i=2}^n \left(\frac{\omega_i^2}{g} \right)^2 D_i(\theta_j) S(f_i) df_i \cos^2(\theta_j - \theta_{wind}) \right] d\theta_j \quad [16]$$

$$\sigma_c^2 = \sum_{j=1}^m \left[\sum_{i=2}^n \left(\frac{\omega_i^2}{g} \right)^2 D_i(\theta_j) S(f_i) df_i \sin^2(\theta_j - \theta_{wind}) \right] d\theta_j \quad [17]$$

	NASA Engineering and Safety Center Technical Report	Document #: NESC-RP-08- 00494	Version: 1.0
Title: Assessment of Orion Crew Module Ocean Wave Model			Page #: 88 of 158

where θ_j is the direction of the wind is coming from measured clockwise from true North, and $d\theta_j$ is the width of the j -th directional bin. Some care needs to be taken in computing a discretized version of the spreading function such that,

$$\sum_{j=1}^m [D_i(\theta_j) d\theta_j] = 1.0, \text{ for all } i \quad [18]$$

An artifact of implementing the spreading function with a truncated Fourier series is that it is possible to get unrealistic, negative values of $D_i(\theta_j)$. There have been several techniques developed in the oceanographic community to leverage the Fourier coefficients reported by buoys while avoiding the issue of negative energies. These include the Maximum Likelihood Method (MLM) and the Maximum Entropy Method (MEM), see Earle et al. [1999]. Ultimately, the choice of which method to use is left to the analyst. The MLM method provides improved directional resolution over the Fourier coefficients without producing artificial double peaks in the spreading function, which is possible with the MEM approach. After discussion with project consultants, the MLM approach was chosen.

Figure 9 illustrates results for upwind-downwind and crosswind slope variances for three different buoys including a 1st order fit. These calculations do not include extrapolated spectra.

It is interesting to note that the slopes of the fit lines are very consistent with those reported in Cote et al. [1960] (0.625 – 0.375). In terms of total slope, it is conservative to assume a larger contribution from one component over the other. This was demonstrated above when comparing slopes generated from the nondirectional variance to those generated with an assumed breakdown.

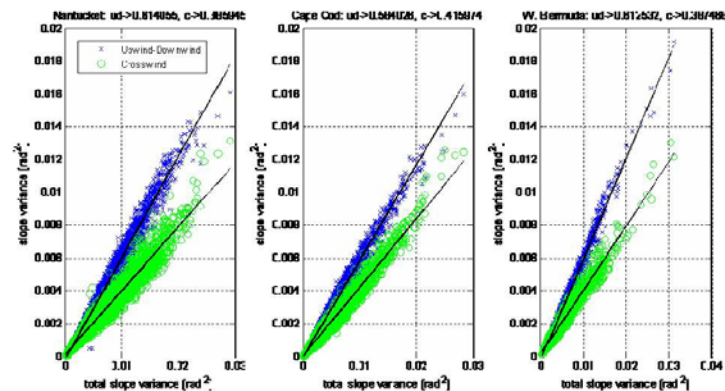



Figure 9. Upwind-downwind and Crosswind Slope Variance Components for 3 Buoys

Examining the breakdown of slope variance against wind speed it is evident that the 0.625 – 0.375 breakdown is a good, if not conservative fit at higher wind speeds. At low wind speeds the effective breakdown between upwind-downwind and crosswind slope variance tends toward 0.50. This makes sense, since at low wind speeds swell is a more significant contributor to the wave spectrum. At very high wind speeds, the breakdown starts to decrease. This may be an artifact of the low number of

	NASA Engineering and Safety Center Technical Report	Document #: NESC-RP-08- 00494	Version: 1.0
Title: Assessment of Orion Crew Module Ocean Wave Model			Page #: 89 of 158

samples is this region. However, this effect may also be real as the very high wind velocities may be associated with significant storms. In such cases, it is possible to get significant swell moving away from the storm which does not align with the local wind velocity. Investigating this behavior in more detail was beyond the scope of this effort.

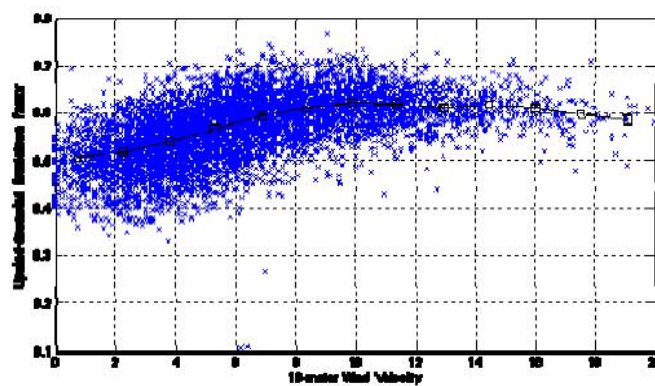



Figure 10. Ratio of Upwind-downwind and Crosswind Slope Variance

2.4.5 Independence and Normality of Upwind-downwind and Crosswind Slopes

An assumption of the Apollo model is that the upwind-downwind and crosswind components are independent zero mean, Gaussian random variables. Although these assumptions may not hold for a limited number of waves they are reasonable assumptions when wave energy is spread over multiple directions. Figure 11 illustrates slopes from a sample spectrum with each histogram demonstrating slope distribution as more and more frequency bins are included in the wave field. The record chosen was that with the highest calculated correlation coefficient between upwind-downwind and crosswind slopes for 2007 records of the Nantucket buoy. In other words, this record demonstrates the most alignment between waves. Even in this scenario, the slope distribution takes on a bell shape as more and more bins are included in the wave field. Strictly speaking, the distribution is not Gaussian as the range of slopes is bounded and there is more probability density at the tails of the distribution than seen in a true normal distribution. This is evident in the normal probability plot provided in Figure 12. For our purposes, however, a Gaussian assumption is reasonable since it does accurately represent roughly 90% of the slopes and is conservative in terms of the 99.7% slope.

	NASA Engineering and Safety Center Technical Report	Document #: NESC-RP-08- 00494	Version: 1.0
Title: Assessment of Orion Crew Module Ocean Wave Model			Page #: 90 of 158

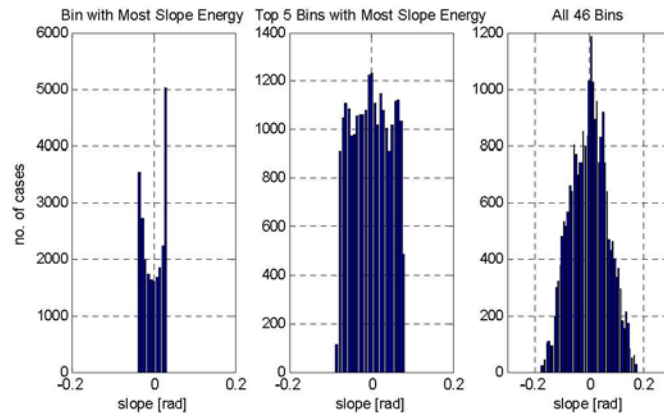


Figure 11. Slope Distribution for 1, 5, and 46 Frequency Bins

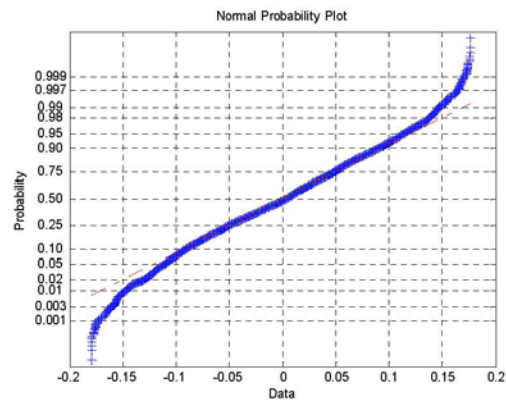



Figure 12. Normal Probability Plot

Correlation between upwind-downwind and crosswind slopes can be investigated by computing the covariance between these two slope components.

	NASA Engineering and Safety Center Technical Report	Document #: NESC-RP-08- 00494	Version: 1.0
Title: Assessment of Orion Crew Module Ocean Wave Model			Page #: 91 of 158

$$\sigma_{ud,c}^2 = \sum_{j=1}^m \left[\sum_{i=2}^n \left[\left(\frac{\omega_i^2}{g} \right)^2 D_i(\theta_j) S(f_i) df_i \sin(\theta_j - \theta_{wind}) \cos(\theta_j - \theta_{wind}) \right] d\theta_j \right] \quad [19]$$

From the covariance, a correlation coefficient may be computed according to,

$$\rho = \frac{\sigma_{ud,c}^2}{\sigma_{ud} \sigma_c} \quad [20]$$

Figure 13 illustrates correlation coefficients as a function of 10-meter wind speed for year-2007 records at the Nantucket buoy (approximately 6700 records). Coefficients range from +/- 0.5 with an absolute average around 0.1.

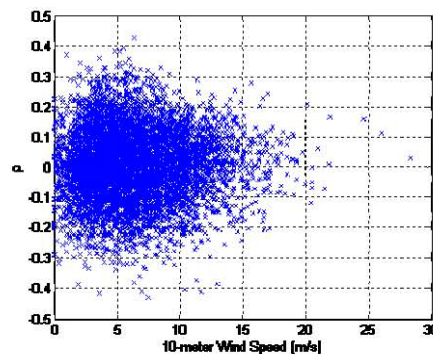



Figure 13. Correlation Coefficient of Upwind-downwind and Crosswind Slopes

To understand the impact of correlation on slope estimates a series of simulations were performed. Each simulation analyzed slopes associated with records in each of the 10-m wind speed bins described earlier. For each record, slopes were estimated three different ways, namely:

1. Computed upwind-downwind and crosswind breakdown with computed correlation.
2. Computed upwind-downwind and crosswind breakdown with no correlation.
3. Assumed upwind-downwind and crosswind breakdown with no correlation.

The computed nondirectional slope variance of each record was used in each of these 3 scenarios. The assumed slope variance breakdown used in method 3 was taken from Figure 10. Records from 2007 for the Nantucket buoy were used. Results are tabulated below in Table 1. Slopes from method 1 represent the "truth" estimates. The total 99.7% slope represents the 99.7% slope across all records using the specified method. Note that values populating Table 1 are the results of one simulation case but are representative.

	NASA Engineering and Safety Center Technical Report	Document #: NESC-RP-08- 00494	Version: 1.0
Title: Assessment of Orion Crew Module Ocean Wave Model			Page #: 92 of 158

10-meter Wind Speed [m/s]	Total 99.7% Slope Method 1 [deg]	Total 99.7% Slope Method 2 [deg]	Difference 1-2 [deg]	Total 99.7% Slope Method 3 [deg]	Difference 1-3 [deg]
[13.72 - 15.24]	17.3842	17.2852	0.099	17.302	0.0822
[4.57 - 6.10]	9.4447	9.3889	0.0559	9.3721	0.0726
[0.00 - 1.52]	8.5422	8.517	0.0252	8.5023	0.04

Table 1. Errors in 99.7% Slope Estimates for Key Modeling Assumptions

Differences between methods 1 and 2 indicate the error in assuming upwind-downwind and crosswind slope components are uncorrelated. This error is roughly 0.1 deg at high wind speed and decreases as wind speed declines.

Differences between methods 1 and 3 represent the error in assuming both a breakdown in nondirectional slope variance (i.e. the effective breakdown from Figure 10) as well as uncorrelated slope components. Errors with this method are similar to those seen in method 1, indicating that the assumed breakdown, on average, adds very little error.

Given the low errors seen in method 3, the simplifying assumptions associated with that approach were adopted. It should be noted that while errors in the total 99.7% slope are reasonably small when considering slopes across all the records in a given velocity bin, they are larger on a record by record basis. The maximum error seen in method 3 for any single record in these trials was roughly 0.6 deg. This may be significant when applying these methods to a limited number of records. In such cases, it is recommended that the computed breakdown and correlations for each individual record be used.

2.4.6 Confidence Intervals

2.4.6.1 Confidence Interval about the Slope Variance of an Individual Record

From Jenkins and Watt [1968], the standard formulae for estimating upper (L_v) and lower limits (l_v) defining confidence intervals are given by:


$$l_v = \frac{v}{X_v^2(\alpha/2)} \quad [20]$$

and

$$L_v = \frac{v}{X_v^2(1-\alpha/2)} \quad [21]$$

where v is the number of degrees of freedom and X represents the chi-square distribution function. The resulting overall confidence interval around the nondirectional slope variance is then $[l_v < I < L_v]$.

Since the nondirectional slope variance is essentially a sum over all frequency bins, the degrees of freedom, v , represents the total degrees of freedom of a particular record, TDF. In computing confidence intervals for significant wave height, Earle [1996] notes that TDF is computed as:

	NASA Engineering and Safety Center Technical Report	Document #: NESC-RP-08- 00494	Version: 1.0
Title: Assessment of Orion Crew Module Ocean Wave Model			Page #: 93 of 158

$$TDF = \frac{2 \left(\sum_{i=1}^N S(f_i) \right)^2}{\sum_{i=1}^N S^2(f_i)} \quad [22]$$

Since we are computing the TDF related to the slope variance calculation we replace $S(f_i)$ with $k_s^2 S(f_i)$. Figure 14 illustrates 90% confidence bounds (L_v , h_v) for nondirectional slope variance calculations for wind velocities in the [13.7 – 15.24] m/s range at the Nantucket buoy in 2007. The 90% bounds correspond to roughly -25% to +40%.

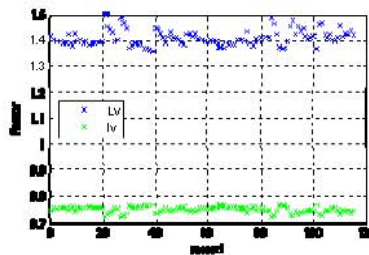



Figure 14. 90% Confidence Intervals on Nondirectional Slope Variance at High Wind Speeds

2.4.6.2 Confidence Interval about Effective Slope Variance (average in a given wind speed bin)

Conventional wisdom would dictate that the confidence interval about the effective slope variance would be computed the same way as for an individual record but with the degrees of freedom set to the sum of the degrees of freedom associated with the records used to compute the effective variance. However, tests of the confidence intervals computed in this manner consistently fail (i.e. are too tight), particularly at lower wind speeds. The most likely reason for this is that the wind-speed only model of slope variance is missing something. Figure 15 illustrates wave slope data against both wind speed and significant wave height. Judging by the orientation of the contours, significant wave height does provide additional insight into slope variance, particularly for low wind speeds. At higher wind speeds, for example greater than 10 m/s, the contours are much flatter, indicating that wind speed is the more dominant driver at these conditions.

	NASA Engineering and Safety Center Technical Report	Document #: NESC-RP-08- 00494	Version: 1.0
Title: Assessment of Orion Crew Module Ocean Wave Model			Page #: 94 of 158

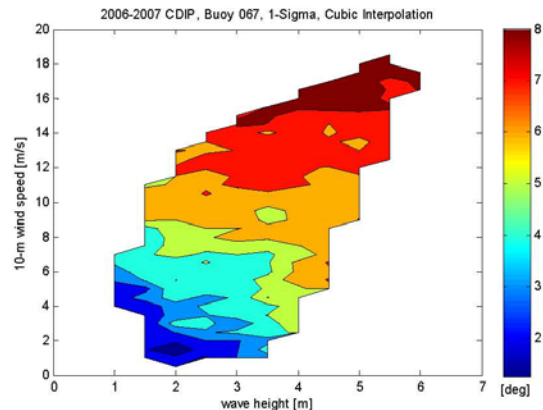


Figure 15. Slope Variance by Wind Speed and Significant Wave Height

Although it is possible to improve model fidelity by adding significant wave height into the formulation, the added fidelity is not worth the added complexity. This decision can be revisited should model variation prove problematic to the CM design effort.

In the mean time, confidence intervals around the model of effective variance were estimated using the bootstrapping technique, which uses observed variances as the approximating distribution (see Reference [16]). 1,000 bootstrap samples were used with Matlab's studentized bootstrap method (bootci), which was found to provide the most robust confidence intervals. The level of significance was set to 5%. Figure 16 through Figure 18 through illustrate the confidence intervals over the wind speed range for one year of data (2007-2008) at the Nantucket and Cape Cod buoys. Table 2 provides the confidence intervals relative to the nominal prediction (i.e. the effective variance).

Note that the confidence intervals are wider at the tails. At lower wind speeds the confidence intervals expand because the distribution of effective variance across buoy records is wider than at higher wind speeds. At higher wind speeds the wider confidence intervals are due to the small number of records available with these wind speed characteristics. Judging from this information, caution should be taken when using the effective variances calculated above 18 m/s.



NASA Engineering and Safety Center Technical Report

Document #:
**NESC-RP-08-
00494**

Version:
1.0

Title:

Assessment of Orion Crew Module Ocean Wave Model

Page #:
95 of 158

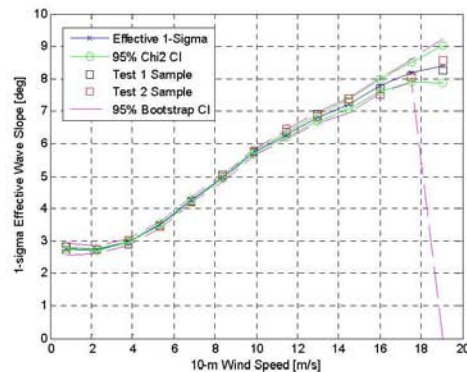


Figure 16. Confidence Intervals around Effective Nondirectional Slope Variance

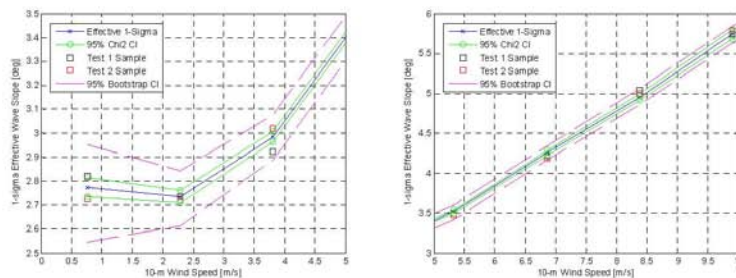


Figure 17. Confidence Intervals at Low Wind Speeds (< 10 m/s)

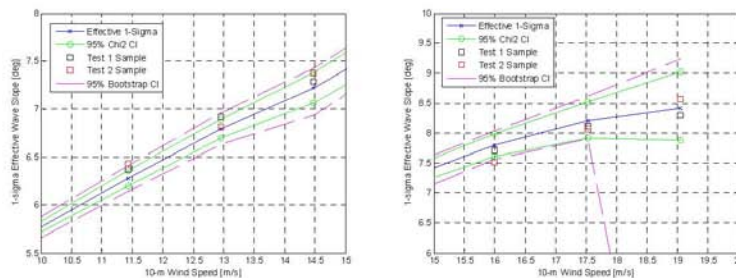



Figure 18. Confidence Intervals at High Wind Speeds (> 10 m/s)

	NASA Engineering and Safety Center Technical Report	Document #: NESC-RP-08- 00494	Version: 1.0
Title: Assessment of Orion Crew Module Ocean Wave Model			Page #: 96 of 158

Wind Speed [m/s]	Lower Limit (95%)	Upper Limit (95%)
0.762	0.8414	1.1321
2.286	0.9118	1.0808
3.81	0.9362	1.0604
5.334	0.9434	1.05
6.858	0.9572	1.0406
8.382	0.9584	1.0404
9.906	0.9626	1.0367
11.43	0.957	1.0438
12.954	0.9519	1.0502
14.478	0.9234	1.0573
16.002	0.9415	1.0625
17.526	0.9276	1.1003
19.05	0.0	1.2047

Table 2. Confidence Intervals relative to Effective Variance

2.5 Wave Vertical Velocity


Wave vertical velocity refers to the velocity of a particle on the surface of the water in the direction normal to the plane tangent to sea level. In deep water, the horizontal motion of a particle on the surface can be ignored allowing for calculation of wave vertical velocity for a single wave form as simply,

$$d\eta / dt = -\omega \frac{H}{2} \sin(kx - \omega t + \phi) = -\omega \eta_{\phi=\phi-\pi/2} \quad [23]$$

Similar to the calculation of slope variance, we recognize that it is possible to build a wave vertical velocity spectrum from the measured energy spectrum and compute the variance as,

$$\sigma_{wyy}^2 = \sum_i (\omega_i)^2 S(f_i) df_i \quad [24]$$

Essentially, this is the equation for the 2nd spectral moment, m_2 , expressed in units of m^2/s^2 . Applying this equation to year-2007 records of the Nantucket buoy results in the variance estimates illustrated in Figure 19. Here, the effective 1-sigma curve was calculated in the same way as described in the wave slope section. At low wind speeds the effective 1-sigma wave vertical velocity is roughly 0.3 m/s. As wind speed increases, the effective variance grows, reaching roughly 0.9 m/s at a wind speed of 15 m/s.

	NASA Engineering and Safety Center Technical Report	Document #: NESC-RP-08- 00494	Version: 1.0
Title: Assessment of Orion Crew Module Ocean Wave Model			Page #: 97 of 158

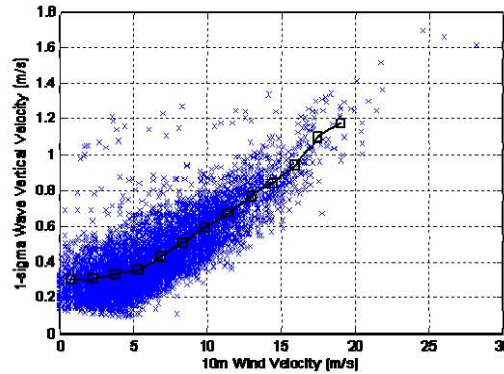


Figure 19. Wave Vertical Velocity Variance

2.5.1 Correlation to Wave Slope


A key consideration in the design of the Crew Module is the combination of wave slopes and vertical wave velocities that are possible. For a single wave, these two variables are perfectly correlated with a correlation coefficient equal to ± 1 depending on the direction of the wave. Consider a coordinate system with +x pointing in the direction of the wind, +z pointing upward and +y completing the right-handed system. If a wave is moving in the direction of the wind, then a positive slope corresponds to the back side (trailing) of the wave, wave vertical velocity is negative, and the correlation coefficient is -1. Conversely, when a wave is moving in a direction opposite to the wind, a positive slope corresponds to the front side (leading) of the wave, wave vertical velocity is positive, and the correlations coefficient is +1.

To understand the correlation between wave slope and wave vertical velocity, the covariance was computed using buoy data that includes directional spreading. Similar to the covariance of upwind-downwind and crosswind slope, the covariance of wave vertical velocity with both components of wave slope can be written as,

$$\sigma_{ud,wvv}^2 = \sum_{j=1}^m \left[\sum_{i=2}^n \left[- \left(\frac{\omega_i^3}{g} \right) D_i(\theta_j) S(f_i) df_i \cos(\theta_j - \theta_{wind}) \right] d\theta_j \right] \quad [25]$$

$$\sigma_{c,wvv}^2 = \sum_{j=1}^m \left[\sum_{i=2}^n \left[- \left(\frac{\omega_i^3}{g} \right) D_i(\theta_j) S(f_i) df_i \sin(\theta_j - \theta_{wind}) \right] d\theta_j \right] \quad [26]$$

Results of covariance calculations are presented in Figure 20 in terms of correlation coefficients based on the year-2007 records of the Nantucket buoy. An average curve, effective correlation, is also include to illustrate the trends. Correlation with upwind-downwind slope varies at low wind speed. As one would expect, correlation coefficient tends toward increasingly negative values as wind speed increases. Above roughly 10 m/s there are very few records with positive correlation coefficients. Correlation with crosswind slope is variable across all wind speeds.

	<p>NASA Engineering and Safety Center Technical Report</p>	<p>Document #: NESC-RP-08- 00494</p>	<p>Version: 1.0</p>
<p>Title: Assessment of Orion Crew Module Ocean Wave Model</p>			<p>Page #: 98 of 158</p>

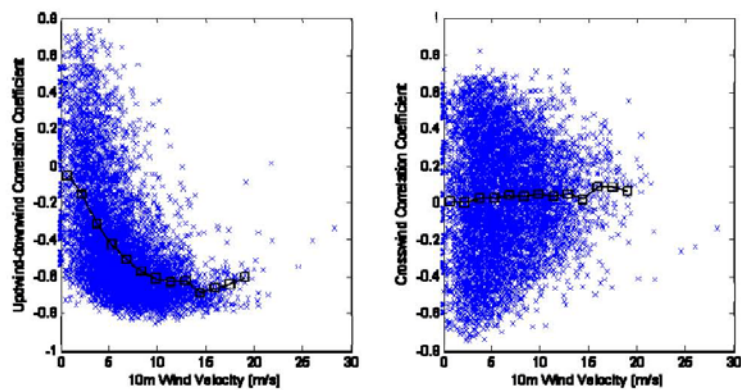


Figure 20. Correlation of Wave Vertical Velocity and Wave Slope Components

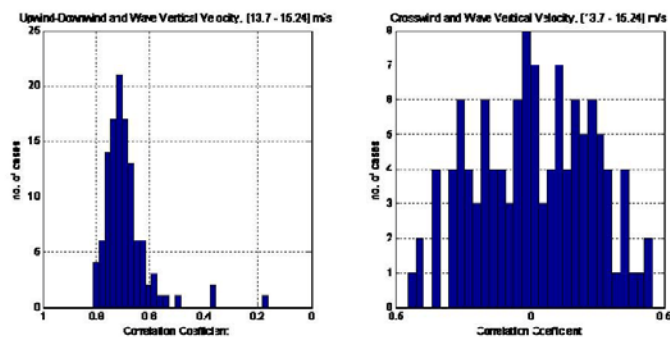


Figure 21. Distribution of Correlation Coefficients at High Wind Speeds [13.7 – 15.24] m/s



NASA Engineering and Safety Center Technical Report

Document #:
**NESC-RP-08-
00494**

Version:
1.0

Title:

Assessment of Orion Crew Module Ocean Wave Model

Page #:
99 of 158

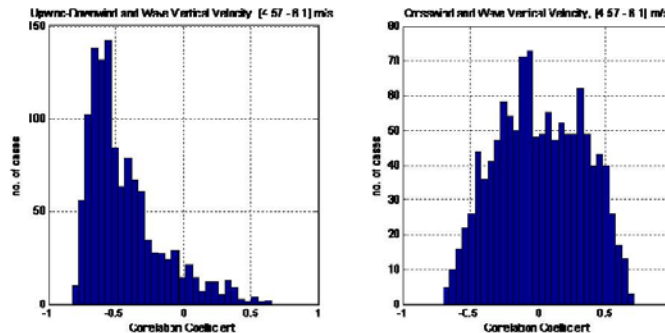


Figure 22. Distribution of Correlation Coefficients at Mild Wind Speeds [4.57 to 6.1] m/s

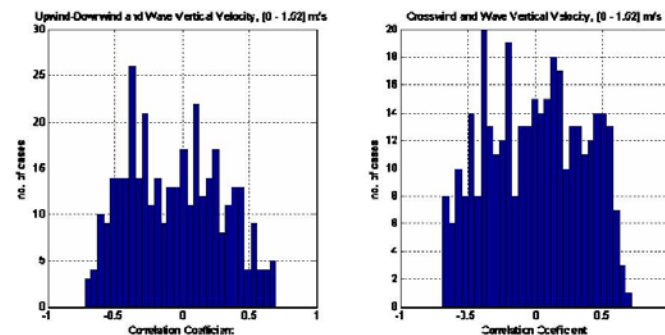



Figure 23. Distribution of Correlation Coefficients at Low Wind Speeds [0 to 1.52] m/s

Assuming an effective correlation coefficient to represent variation in the degree of correlation between two variables is not a good assumption in all cases. However, given that the spread in each frequency bin is unimodal (see Figure 21 through Figure 23), such an assumption may be reasonable. To investigate, we again turn to Monte Carlo simulations. In this case, trials were performed using 100 records in each wind speed bin with 5000 slopes and wave vertical velocities generated for each record. Records from 2007 were used, which were drawn from the Nantucket buoy. A total of 5 trials were completed for each wind speed bin with different random seeds used in each case. For comparison purposes, the truth model used the true covariance matrix (wave vertical velocity, upwind-downwind slope, crosswind slope) of each record. The test model assumed true variances but with covariances (off-diagonal terms in the covariance matrix) based on modeled correlation coefficients. The modeled correlation coefficients were as follows.

upwind-downwind slope to wave vertical velocity:	effective correlation from Figure 20.
crosswind slope to wave vertical velocity:	0.0
upwind-downwind slope to crosswind slope:	0.0

	NASA Engineering and Safety Center Technical Report	Document #: NESC-RP-08-00494	Version: 1.0
Title: Assessment of Orion Crew Module Ocean Wave Model			Page #: 100 of 158

Results for three wind speed bins are tabulated below. Since the concern for Crew Module design is two-dimensional (wave vertical velocity vs. wave slope), results were normalized by the standard deviations of the truth model then converted to spherical coordinates. Values in the table below represent the 99.7% magnitude considering all records.

10-m Wind Speed [m/s]	99.7% Magnitude Trial 1	99.7% Magnitude Trial 2	99.7% Magnitude Trial 3	99.7% Magnitude Trial 4	99.7% Magnitude Trial 5
13.72-15.24	5.8858	5.8115	5.7906	5.7785	5.7974
model	5.8457	5.7851	5.7538	5.7334	5.7539
error	0.0401	0.0264	0.0368	0.0451	0.0436
4.57-6.10	6.2064	6.1838	6.1645	6.1543	6.1923
model	6.1056	6.1195	6.0891	6.0703	6.1009
error	0.1008	0.0643	0.0754	0.0841	0.0914
0 – 1.52	6.7742	6.7057	6.7154	6.6979	6.7417
model	6.5807	6.6078	6.5745	6.5439	6.575
error	0.1936	0.0979	0.1409	0.154	0.1667

Table 3. Differences in the 99.7% Values for Magnitude for 5 Simulations Trials

Based on the results of the simulation trials, the reasonableness of these correlation assumptions is confirmed. Errors at high wind seed are very small. At lower wind speeds they grow to roughly 0.15 or 3%. For all records analyzed in this study the largest individual error was on the order or 0.7 or roughly 12%. Again, this was not a concern for this model but may warrant consideration when developing operational procedures.

2.5.2 Confidence Intervals

2.5.2.1 Confidence Interval about the Wave Vertical Velocity Variance of an Individual Record

Following the same process as outlined in Section 2.4.6 but with $S(f_i)$ in equation [22] replaced with $\omega_i^2 S(f_i)$, confidence intervals on wave vertical velocity variance can be computed. Figure 24 demonstrates 90% confidence interval factors (I_p , I_r) for wave vertical velocities for records with 10-m wind speeds in the [13.7 – 15.24] m/s range. The confidence bounds roughly correspond to -30% to +60%.

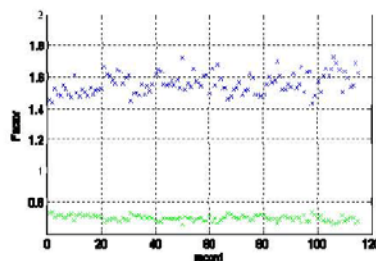



Figure 24. 90% Confidence Intervals for Wave Vertical Velocity for High Wind Speeds

2.5.2.2 Confidence Interval about Effective Wave Vertical Velocity Variance

	NASA Engineering and Safety Center Technical Report	Document #: NESC-RP-08- 00494	Version: 1.0
Title: Assessment of Orion Crew Module Ocean Wave Model			Page #: 101 of 158

Confidence intervals around the effective wave vertical velocity were computed in the same manner as described in Section 2.4.6.2. The results, tabulated in Table 4 show very similar trends as seen for effective nondirectional slope variance.

Wind Speed [m/s]	Lower Limit (95%) [%]	Upper Limit (95%) [%]
0.762	0.7345	1.1565
2.286	0.9158	1.072
3.81	0.8914	1.0669
5.334	0.9067	1.0651
6.858	0.9282	1.0576
8.382	0.9366	1.0617
9.906	0.9402	1.0526
11.43	0.9213	1.0642
12.954	0.9274	1.0679
14.478	0.9059	1.0868
16.002	0.8955	1.0921
17.526	0.8584	1.1346
19.05	0.0	1.2924

Table 4. Confidence Intervals relative to Effective Wave Vertical Velocity Variance

2.6 Wave Direction and Wave Azimuth


In early wave modeling efforts, wave direction was used to define the orientation of the wave slope relative to the Crew Module. More importantly, perhaps, wave direction dictated whether wave slope and wave vertical velocity had a positive or negative correlation.

The Apollo model assumed a \cos^2 distribution on the interval of ± 90 deg. for wave direction (defined as the difference between wave and wind directions). This was an admittedly simple assumption due to complexity of the problem and the scarceness of directional data at that time. Even with the buoy data available today, specifying wave direction is dependent on the application. The wave field is truly a 2-D spectrum and many different forms of wave direction can be defined. Wave direction as defined in buoy data refers to the mean wave direction associated with the frequency with the highest spectral density. One could refine this definition to use the principal wave direction associated with that same frequency. Or, since wave slope is important, the mean or principal wave direction associated with the frequency with the most slope energy may be a better measure. Unfortunately, none of these simple definitions significantly help refine the wave model.

However, since a suitable model was developed in the previous section to relate wind vertical velocity to wave slope, we can ignore wave direction and simply compute wave azimuth. The difference here is that wave azimuth indicates how the wave slope is oriented relative to the wind, providing no information about the direction it is moving.

Referring back to Figure 1, components of wave slope can be related to total wave slope and wave azimuth through,

$$\mu_{\text{rel}} = \cos^{-1} \left(\frac{i_{\text{rel}}}{\|i_{\text{rel}}\|} \cdot X_{\text{rel}} \right) = \cos^{-1} \left(\frac{1}{\sqrt{1 + \tan^2 \mu \cos^2 \psi}} \right) = \tan^{-1}(\tan \mu \cos \psi) \quad [27]$$

	NASA Engineering and Safety Center Technical Report	Document #: NESC-RP-08- 00494	Version: 1.0
Title: Assessment of Orion Crew Module Ocean Wave Model			Page #: 102 of 158

$$\mu_c = \cos^{-1} \left(\frac{i_c}{\|i_c\|} \cdot Y_H \right) = \cos^{-1} \left(\frac{1}{\sqrt{1 + \tan^2 \mu \sin^2 \psi}} \right) = \tan^{-1} (\tan \mu \sin \psi) \quad [28]$$

Which, after some manipulation yields,

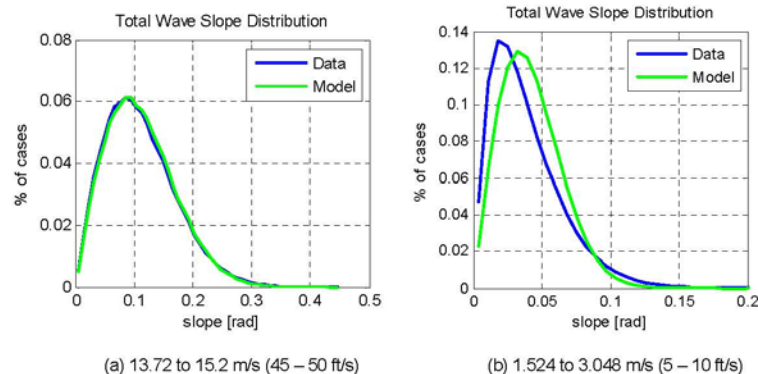
$$\psi = \tan^{-1} \left(\frac{\tan \mu_c}{\tan \mu_{ad}} \right) \quad [29]$$

where again, wave azimuth represents the deviation from wind direction.

2.7 3-Sigma Adjustments

A key simplifying assumption of the Monte Carlo wave model is to use the effective variance in nondirectional slope and wave vertical velocity to represent these parameters. As demonstrated in Figure 3 and Figure 19, there is considerable variation about the effective variance lines. Theoretically, however, the variance associated with the union of multiple zero mean random variables is equal to the average of their unique variances. Hence, we can accurately represent the variance at a given wind speed as the average of variances computed for records at or near that same wind speed.

Although the variance may be accurately represented in this manner, the distributions of wave vertical velocity as well as upwind-downwind and crosswind wave slopes are not necessarily Gaussian. This was even demonstrated for an individual record in Section 2.4.5. For simplicity, however, it is desirable to assume a Gaussian distribution for these model parameters. At high speeds, the Gaussian assumption fits the data well as evidenced in by comparison of total slope distribution in Figure 25(a). Here, the modeled slopes were derived assuming a single effective variance at the given wind speed. Conversely, the data represents the distribution built by combining slopes from multiple records randomly drawn from the data, each with their own unique variance value. Even though the comparison is quite good, the 3-sigma (99.8 percentile) slope value seen in the data is slightly higher than predicted by the model (roughly 5%). At low wind speeds, the Gaussian assumption does not capture the data as well, as seen in Figure 25(b). Although the model is conservative in terms of mean slope, the 3-sigma slope of the data is roughly 20 to 25% higher. The issue here has to do with the higher spread in variances at low wind speeds as demonstrated in Figure 26. At higher wind speeds the spread seen across records is tighter and more normally distributed. Similar findings and claims can be made when analyzing wave vertical velocity.





NASA Engineering and Safety Center Technical Report

Document #:
**NESC-RP-08-
00494**

Version:
1.0

Title:

Assessment of Orion Crew Module Ocean Wave Model

Page #:
103 of 158

Figure 25. Total Slope Distribution, Model vs. Data

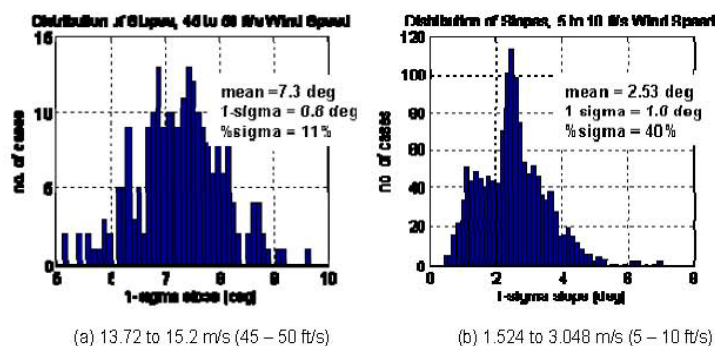


Figure 26. Variation in 1-Sigma Slope Over Multiple Buoy Records

Since important figures of merit to designers of the CM are the 3-sigma values of total slope and wave vertical velocity an adjustment to the modeled variances was derived to shift the modeled distributions further to the right. These were determined iteratively and are tabulated below. To see the impact of these adjustments on comparisons of the model to the data see the discussion on model verification in 3.1.3.


	Wind Speed [m/s]			
	0.0	2.286	14.478	19.05
3-sigma Scale Factor – Slope	1.25	1.25	1.08	1.045
3-sigma Scale Factor - Velocity	1.2	1.2	1.105	1.05

Table 5. 3-Sigma A adjustment Factors for Wave Slope and Wave vertical velocity

3.0 The Integrated Model

The following summarizes the integrated steps of the wave model discussed in the previous section. The model values documented here were derived using 1 year of Nantucket and Cape Cod buoy data (Nantucket: 3/27/07 – 3/31/08, Cape Cod: 5/31/07 – 5/08). These buoys were chosen since they provide the directional data necessary to ground assumptions on slope components and correlations with wave vertical velocity. Manual adjustments to the resulting model parameters are also noted below where appropriate.

1. Determine nondirectional slope variance based on the 10-meter wind speed using the effective variance curve.

	NASA Engineering and Safety Center Technical Report	Document #: NESC-RP-08- 00494	Version: 1.0
Title: Assessment of Orion Crew Module Ocean Wave Model			Page #: 104 of 158

```
v_brk = [0 0.7620 2.2860 3.8100 5.3340 6.8580 8.3820 9.9060 11.4300 12.9540 14.4780 16.0020
17.5260 19.0500] %m/s
```

```
mumodel = [0.0024 0.0024 0.0023 0.0027 0.0037 0.0054 0.0076 0.0101 0.0124 0.0143 0.0163 0.0184
0.0204 0.0218];
```

$$\sigma^2 = \text{interp1}(v_brk, mumodel, V_{wind})$$

2. Compute the 3-sigma slope adjustment factor to account for the non-normality of the effective variance calculated in step 1. Adjust the effective slope variance.

```
sig3break = [0.0 2.2860 9.9060 14.4780 19.05]; %m/s
sig3_mumodel = [1.25 1.25 1.07 1.05 1.05];
sig3_mu = interp1(sig3break, sig3_mumodel)
```

$$\sigma^2 = \sigma^2 * sig3_mu^2$$

3. Compute upwind-downwind (σ_{ud}^2) and crosswind (σ_c^2) slope variances based on the 10-meter wind speed using the effective breakdown curve. Here, we assume a breakdown of 0.50 (50/50) at zero wind speed.

```
Kud = [0.50 0.5066 0.5148 0.5376 0.5637 0.5920 0.6034 0.6071 0.6040 0.5978 0.6013 0.5907
0.5799 0.5617];
Kc = (1-Kud);
```

$$\sigma_{ud}^2 = K_{ud} \sigma^2$$

$$\sigma_c^2 = K_c \sigma^2$$

4. Cast upwind-downwind (μ_{ud}) and crosswind (μ_c) slopes as independent, normally distributed random variables with the variances determined in steps 1-3.

$$\mu_{ud} = \tan^{-1}(\sigma_{ud} \cdot r_{n1})$$

$$\mu_c = \tan^{-1}(\sigma_c \cdot r_{n2})$$


where r_{n1} and r_{n2} are zero-mean, unit-variance Gaussian random variables.

5. Compute the total slope as $\mu = \tan^{-1}(\sqrt{\tan^2 \mu_{ud} + \tan^2 \mu_c})$.
6. Compute the wave azimuth as $\theta = \tan^{-1}(\frac{\tan \mu_c}{\tan \mu_{ud}})$.
7. Determine the wave vertical velocity variance, σ_{wvy}^2 , based on the 10-meter wind speed using the effective wave vertical velocity variance curve.

```
vwmmodel = [0.0950 0.0950 0.0906 0.1008 0.1207 0.1668 0.2398 0.3427 0.4572 0.5720 0.6991 0.8791
1.1844 1.3046] %m/s
```

$$\sigma_{wvy}^2 = \text{interp1}(v_brk, vwmmodel, V_{wind})$$

8. Compute the 3-sigma slope adjustment factor to account for the non-normality of the effective variance calculated in step 7. Adjust the effective wave vertical velocity variance.

	NASA Engineering and Safety Center Technical Report	Document #: NESC-RP-08- 00494	Version: 1.0
Title: Assessment of Orion Crew Module Ocean Wave Model			Page #: 105 of 158

```
sig3_vwvmodel = [1.2 1.2 1.1187 1.07 1.07];
sig3_vwv = interp1(sig3break,sig3_vwvmodel)
```

$$\sigma_{vwv}^2 = \sigma_{vwv}^2 * sig3_{vwv}^2$$

9. Determine the correlation coefficient, $\rho_{ud,vwv}$, between upwind-downwind wave slope and wave vertical velocity using the effective correlation coefficient curve.

```
rhmodel = [0.0 -0.0395 -0.1399 -0.2944 -0.4149 -0.5048 -0.5716 -0.5816 -0.5999 -0.6124 -0.6494 -
0.6330 0.6112 -0.5871];
```

$$\rho_{ud,vwv} = \text{interp1}(v_brk, rhmodel, V_{wind})$$

10. Infer wave vertical velocity using the variance computed in step 8, σ_{vwv}^2 , the random number generated in step 4, r_{n1} , as well as the correlation coefficient, $\rho_{ud,vwv}$, calculated in step 9.

$$V_{w,v} = \sigma_{vwv} [\rho_{ud,vwv} r_{n1} + r_{n3} \sqrt{(1 - \rho_{ud,vwv}^2)}]$$

where r_{n3} is a zero-mean, unit-variance Gaussian random variable.

3.1 Model Verification

3.1.1 Wave Vertical Velocity Variance

Wave vertical velocity calculations were verified using wave tank measurements from Mase and Kirby [1992]. Here, a series of experiments were performed with wave gauge measurements including 3 located at water depths of 30, 35, and 47 cm (see Figure 27). The surface heights measured by the wave gauges were converted into energy spectra by Dr. Kaihatu et. al [2007]. Of these three gauges, the 47 cm gauge is considered to be in deep water relative to the wave lengths of the waves generated in the experiment. Those at 30 and 35 are considered to be in the transition region between deep and shallow water.

The scales involved are certainly smaller than those relevant to CEV (peak wave energy in this experiment occurs at roughly 1 Hz) but this data set does provide a direct check of the methodology used in estimating wave vertical velocity variance. Figure 28 illustrates the distribution of wave vertical velocities at the 47 cm depth computed from the wave gauge data through numerical differentiation. The adjacent table compares the variance (From Time Series) in this distribution against a variance computed directly from the energy spectrum (From Spectrum). Results are in excellent agreement. It is interesting that the variance decreases with water depth. This is typical behavior as wave heights tend to diminish in the transition region before growing in shallow water.

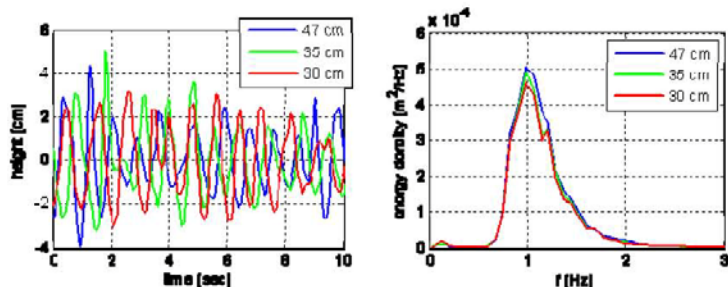


Figure 27. Wave Heights and Associated Spectral Densities, Mase and Kirby [1992, Run 2]

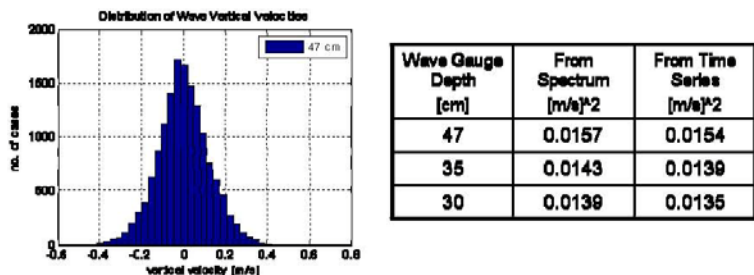


Figure 28. Wave Vertical Velocity Distribution and Comparison to Model Calculations


3.1.2 Slope Variance using Simulated Data

Unfortunately, no data set has been found that provides direct wave slope measurements. To provide some level of verification of the wave slope model comparisons of slope variance predictions were made relative to simulated slopes. The simulated slopes were based on a TBD second simulation over a 100 square meter wave field with uniform node spacing of 0.5 meters. Two simulations were run, one with wave frequencies limited to 0.555 Hz and one with a spectral densities extended out to 0.625 Hz. In these simulations, the wave field is generated by converting directional spectral densities to individual wave amplitudes and initializing each individual wave with a random phase angle. With directional spreading resolved every 5 degrees, the total number of waves in the wave field is 3816 for 0.555 Hz case and 4320 for the 0.625 Hz case.

Record Simulated: Nantucket buoy, November 3, 2007, 2300 hrs.

Note to Reviewers: simulations supporting this verification effort are still in progress. Updates shall be provided as soon as the come available.

	Upwind-Downwind Slope Variance	Crosswind Slope Variance
--	--------------------------------	--------------------------

	NASA Engineering and Safety Center Technical Report	Document #: NESC-RP-08- 00494	Version: 1.0
Title: Assessment of Orion Crew Module Ocean Wave Model			Page #: 107 of 158

	[rad ^2]	[rad ^2]
From Spectrum (freq. limit = 0.555)	0.135	0.112
From Simulated Wave Field (freq. limit = 0.555)	TBD	TBD
From Spectrum (freq. limit = 0.625)	0.143	0.120
From Simulated Wave Field (freq. limit = 0.625)	TBD	TBD

Table 6. Simulated Data Comparisons

3.1.3 Overall Model Assumptions


To test the sufficiency of the overall wave model assumptions outlined above a series of simulation cases were run against buoy records. For each wind speed investigated, 200 records were randomly selected from the 2007-2008 data of the Nantucket and Cape Cod buoys. Then, 2000 slopes, wave vertical velocities, and wave azimuths were generated for each record following the model steps outlined above. In turn, the statistics of these values were compared to those of a truth model. For completeness, this process was repeated with 5 different Monte Carlo seeds. The truth model is very similar in structure to the model but uses no simplifying assumptions. More specifically, for each record analyzed,

- upwind-downwind and crosswind variances are computed directly from the buoy record.
- wave vertical velocity variance is computed directly from the buoy record.
- covariances between all three key model components, upwind-downwind slope, crosswind slope, and wave vertical velocity, are all computed directly from the buoy record and utilized to generate properly correlated values.

Results for various wind speed ranges are included below

[1.524 to 3.048] m/s (5 to 10 ft/s)

At low wind speeds model distributions are noticeably different than truth data. As discussed in Section 2.7, these differences primarily have to do with the fact that a Gaussian distribution is not a great fit of variations seen at these wind speeds. The 3-sigma adjustments added to ensure the model captures 3-sigma statistics further degrades the qualitative comparison. That being said, the model distribution is similar in shape and is conservative. The correlation between wave vertical velocity and upwind-downwind slope is well captured (see Figure 31), wave azimuth distributions are in excellent agreement, and 3-sigma statistics are on target (see Table 7).

	NASA Engineering and Safety Center Technical Report	Document #: NESC-RP-08- 00494	Version: 1.0
Title: Assessment of Orion Crew Module Ocean Wave Model			Page #: 108 of 158

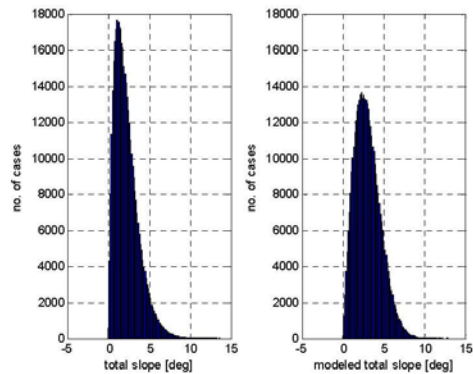


Figure 29. Total Slope Distributions

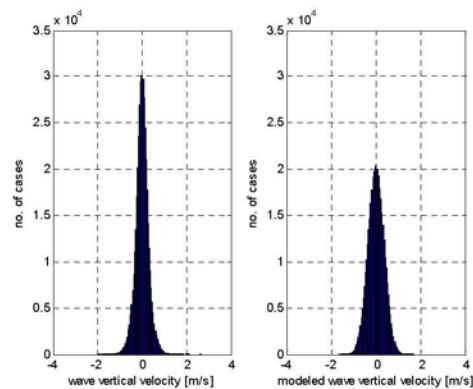


Figure 30. Wave Vertical Velocity Distributions



NASA Engineering and Safety Center Technical Report

Document #:
**NESC-RP-08-
00494**

Version:
1.0

Title:

Assessment of Orion Crew Module Ocean Wave Model

Page #:
109 of 158

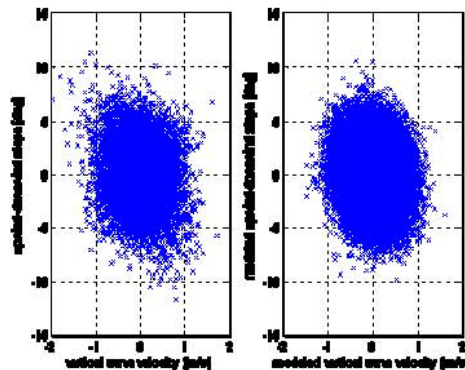


Figure 31. Upwind-Downwind and Wave Vertical Velocity Correlation

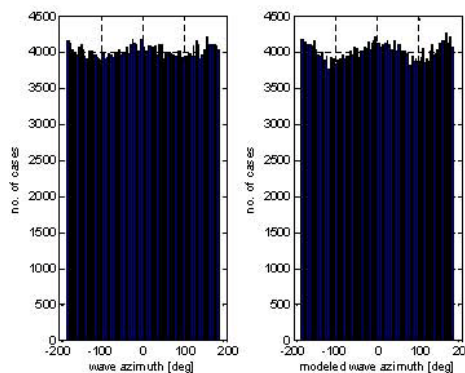


Figure 32. Wave Azimuth Distributions

3-sigma Total Slope	Trial 1	Trial 2	Trial 3	Trial 4	Trial 5
Truth [deg]	8.2629	8.2693	8.1974	8.2082	8.2529
Model [deg]	8.2279	8.2401	8.1898	8.2301	8.2015
Error [deg]	0.035	0.0292	0.0076	-0.0219	0.0513



NASA Engineering and Safety Center Technical Report

Document #:
**NESC-RP-08-
00494**

Version:
1.0

Title:

Assessment of Orion Crew Module Ocean Wave Model

Page #:
110 of 158

3-Sigma Vertical Velocity					
Truth [m/s]	0.9804	0.9908	0.9755	0.9743	0.9785
Model [m/s]	0.9945	0.9951	0.9927	0.9937	0.9923
Error [m/s]	-0.0141	-0.0043	-0.0171	-0.0195	-0.0138

Table 7. Errors in 99.7% Values for Total Slope, Wave Vertical Velocity

[9.1440 to 10.6680] m/s (30 to 35 ft/s)

At medium wind speeds model distributions are in better agreement than seen at low speeds. The model continues to predict fewer wave slopes and wave vertical velocities near the origin than the truth data. The correlation between wave vertical velocity and upwind-downwind slope is again well captured (see Figure 35). Wave azimuth distributions are in great agreement. As expected, these distributions are less uniform than seen at low wind speeds. 3-sigma statistics are also very consistent with the truth data. (see Table 8).

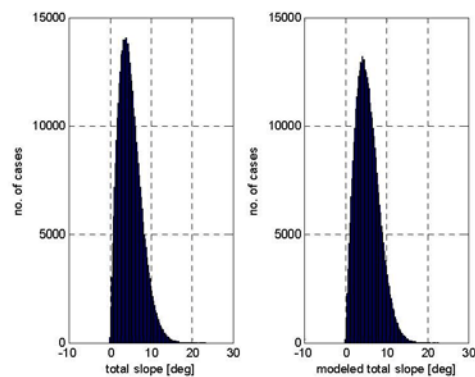



Figure 33. Total Slope Distributions

	NASA Engineering and Safety Center Technical Report	Document #: NESC-RP-08- 00494	Version: 1.0
Title: Assessment of Orion Crew Module Ocean Wave Model			Page #: 111 of 158

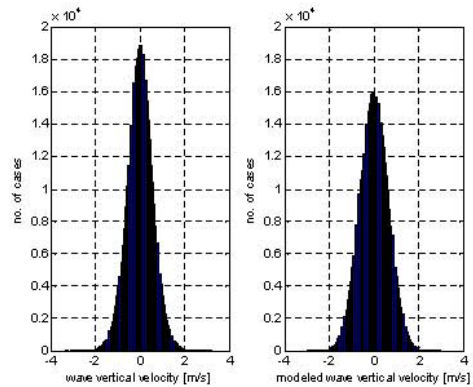


Figure 34. Wave Vertical Velocity Distributions

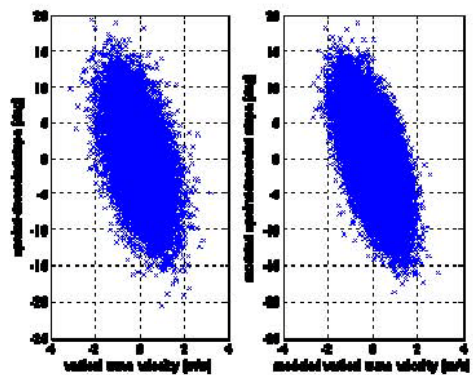



Figure 35. Upwind-Downwind and Wave Vertical Velocity Correlation

	NASA Engineering and Safety Center Technical Report	Document #: NESC-RP-08- 00494	Version: 1.0
Title: Assessment of Orion Crew Module Ocean Wave Model			Page #: 112 of 158

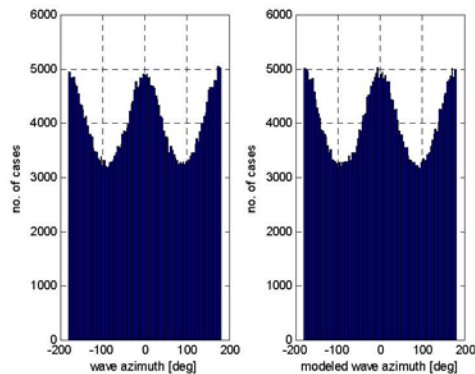



Figure 36. Wave Azimuth Distributions

3-sigma Total Slope	Trial 1	Trial 2	Trial 3	Trial 4	Trial 5
Truth [deg]	14.8588	14.8247	14.9313	14.8913	14.8599
Model [deg]	14.9761	14.9192	14.9374	14.9818	14.8721
Error [deg]	-0.1174	-0.0945	-0.0061	-0.0905	-0.0123
3-Sigma Vertical Velocity					
Truth [m/s]	1.7553	1.7556	1.7513	1.7512	1.7629
Model [m/s]	1.7813	1.7824	1.7781	1.7799	1.7773
Error [m/s]	-0.026	-0.0267	-0.0267	-0.0287	-0.0144

Table 8. Errors in 99.7% Values for Total Slope, Wave Vertical Velocity

[13.72 to 15.24] m/s (45 to 50 ft/s)

At high wind speeds, overall distributions of key model outputs are quite comparable to the truth results. The model returns fewer wave slopes and wave vertical velocities near the origin, which at this wind speed is mainly an artifact of the 3-sigma scaling factors. As demonstrated in Table 9, these scaling factors are providing their intended purpose as 3-sigma wave slopes and wave vertical velocities are on

	NASA Engineering and Safety Center Technical Report	Document #: NESC-RP-08- 00494	Version: 1.0
Title: Assessment of Orion Crew Module Ocean Wave Model			Page #: 113 of 158

target. As seen at the lower wind speeds, wave azimuth distribution and correlation between upwind-downwind wave slope and wave vertical velocity are in excellent agreement with the truth data.

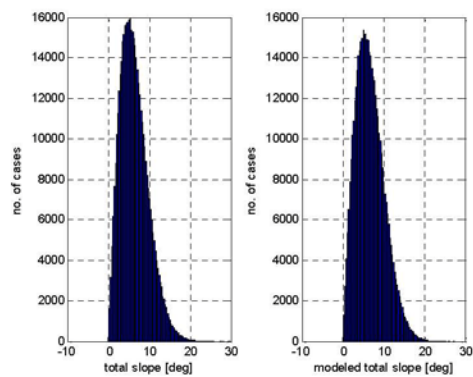


Figure 37. Total Slope Distributions

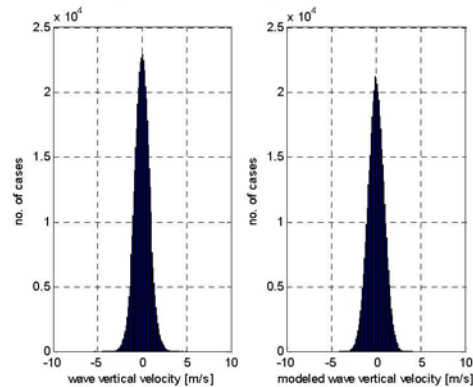


Figure 38. Wave Vertical Velocity Distributions



NASA Engineering and Safety Center Technical Report

Document #:
**NESC-RP-08-
00494**

Version:
1.0

Title:

Assessment of Orion Crew Module Ocean Wave Model

Page #:
114 of 158

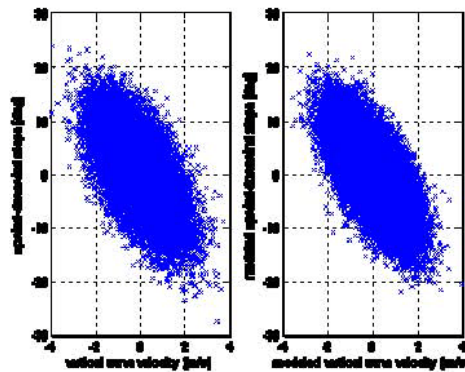


Figure 39. Upwind-Downwind and Wave Vertical Velocity Correlation

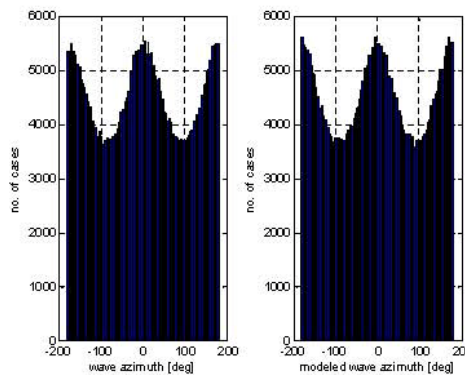



Figure 40. Wave Azimuth Distributions

3-sigma Total Slope	Trial 1	Trial 2	Trial 3	Trial 4	Trial 5
Truth [deg]	18.0455	18.1556	18.1149	18.0883	18.1483
Model [deg]	18.1142	18.0584	18.1463	18.1782	18.1162
Error [deg]	-0.0687	0.0972	-0.0314	-0.0899	0.032

	NASA Engineering and Safety Center Technical Report	Document #: NESC-RP-08-00494	Version: 1.0
Title: Assessment of Orion Crew Module Ocean Wave Model			Page #: 115 of 158

3-Sigma Vertical Velocity					
Truth [m/s]	2.4182	2.4223	2.4194	2.4168	2.4219
Model [m/s]	2.4159	2.4257	2.4113	2.4141	2.4139
Error [m/s]	0.0023	-0.0034	0.0081	0.0027	0.0081

Table 9. Errors in 99.7% Values for Total Slope, Wave Vertical Velocity

4.0 Summary and Conclusions

The modeling techniques and well documented overview of the Apollo model by Cummings et al. [1972] provided a solid foundation for the present effort. Opportunities for improvement of the Apollo model were recognized with the help of oceanographic experts and pursued using buoy data.


A detailed approach for computing the probabilistic distributions of wave slope, wave vertical velocity, and wave azimuth was developed leveraging NOAA's NDBC and Scripps' CDIP buoys. Simplifying assumptions were made to facilitate the application of the model, which were shown to be reasonable for the present application.

A series of simulation cases were performed to test performance of the model against available test data and buoy records. Errors calculated from these trials confirm the reasonableness of the model for capturing sea characteristics across a long period of record. The magnitude of errors seen in individual records may be a concern within the context of operational, e.g. day-of-flight, procedures. In such cases, it is recommended the full fidelity of the summarized methods be leveraged.

5.0 Acknowledgements


The author wishes to acknowledge [Jim Corliss](#) of the NASA Langley Research Center for providing both his technical and programmatic guidance to this effort. In addition, the following acknowledgements are warranted:

- [Dr. James Kaihatu](#) of Texas A&M University for his review of the Apollo model and his consulting in all areas of the effort.
- [Dr. William Perrie](#) of the Bedford Institute of Oceanography for his review of the Apollo model and his consulting, and [Bechara Toulany](#) particularly in computing confidence intervals.
- [Matt Toniolo](#) and [Scott Kowalchuck](#), also of Analytical Mechanics Associates, for their reviews and assistance in validating application of this model to landing Monte Carlo analysis.
- Members of the Ocean Landing working group particularly representatives of NASA MSFC's E&C SIG., which include [Vernon Keller](#) (NASA Marshall Space Flight Center), [B.J. Barbre](#) (Jacobs Sverdrup), and [Kristin Cummings](#) (JTI), for their reviews.

	NASA Engineering and Safety Center Technical Report	Document #: NESC-RP-08- 00494	Version: 1.0
Title: Assessment of Orion Crew Module Ocean Wave Model			Page #: 116 of 158

6.0 References

- [1] The Coastal Data Information Program, <http://cdip.ucsd.edu/>, Scripps Institute of Oceanography, University of California, San Diego.
- [2] Cote, L.J., J.O., Davis, W. Markes, R.J. McGough, E. Mehr, W.J. Pierson, Jr., J.F. Ropek, G. Stephenson, and R.C. Vetter, 1960, "The directional spectrum of a wind generated sea as determined from data obtained by the Stereo Wave Observation Project". Meteorological Papers, New York University College of Engineering, 2(6), 88 pgs.
- [3] Cummings, A.D., A.M. Whitnah, D.B. Howes, and B.J. Wells, 1972, "Concepts and Procedures Used to Determine Certain Sea Wave Parameters", NASA Technical Note TN D-6961, National Aeronautics and Space Administration.
- [4] Marshall D. Earle, 1996, "Nondirectional and Directional Wave Data Analysis Procedures, NDBC Technical Document 96-01, Stennis Space Center, January.
- [5] M.D. Earle, K.E. Steele, D.W.C. Wange, 1999, "Use of advanced directional wave spectra analysis methods", Ocean Engineering, Vol. 26, pp. 1421-1434.
- [6] K. Hasselmann, T.P. Barnett, E. Bouws, H. Carlsen, D.E. Carwright, K. Enkee, J.A. Ewing, H. Gienapp, E.E. Hasselmann, P. Kruseman, A. Meerburg, P. Muller, D.J. Olbers, K. Richter, W. Sell, and H. Walden, 1973, "Measurements of wind-wave growth and swell decay during the joint North Sea wave project (JONSWAP)", *Deutsches Hydrographisches Zeitschrift*, 8(12), 95.
- [7] G. M. Jenkins, and D. G. Watts, 1968, *Spectral Analysis and its Application*. Holden-Day, 525 pp.
- [8] Long, C.E. and D.T. Resio, 2007: Wind wave spectral observations in Currituck Sound, North Carolina. *J. Geophys. Res.*, **112**, doi:10.29/2006JC003835.
- [9] Walter H. Michel, 1999, "Sea Spectra Revisited", *Marine Technology*, Vol. 36, No. 4., pp. 211-227.
- [10] NDBC, "Frequently Asked Questions", <http://www.ndbc.noaa.gov/faq.shtml>, September 19, 2007.
- [11] M.K. Ochi and E.N. Hubble, 1976, "On six-parameter wave spectra," *Proc. 15th Int. Conf. Coastal Engineering*, 1, pp 301-328.
- [12] W.J. Pierson, and L. Moskowitz, 1964, "A proposed spectral form for fully developed wind seas based on the similarity theory of S.A. Kitaigorodskii," *J. Geophys. Res.*, 69, 5181-5190.
- [13] Dominic Reeve, Andrew Chadwick, and Christopher Fleming, 2004, *Coastal Engineering: Processes, Theory and Design Practice*, Spon Press, New York, NY, pp. 69-85.
- [14] Don Resio and W. Perrie. 2008, "A two-scale approximation for efficient representation of nonlinear energy transfers in a wind wave spectrum. Part 1: Theoretical Development". In press in *J. Phys. Oceanogr.*
- [15] Knut Torsethagen and Sverre Haver, 2004, "Simplified Double Peak Spectral Model for Ocean Waves", *Proc. ISOPE Conf.*, vol. 3, pp. 76-84.
- [16] Bootstrapping (Statistics), [http://en.wikipedia.org/wiki/Bootstrapping_\(statistics\)](http://en.wikipedia.org/wiki/Bootstrapping_(statistics))
- [17] Mase, H. and Kirby, J. T., "Modified frequency domain KdV equation for random wave shoaling", *Proc. 23d Intl. Conf. Coastal Engineering*, Venice, 474-487, October 1992.
- [18] Kaihatu, J.M., Veeramony, J., Edwards, K.L., and Kirby, J.T. (2007). "Asymptotic behavior of frequency and wavenumber spectra of nearshore shoaling and breaking waves." *Journal of Geophysical Research*, 112, doi: 10.1020/2006JC003817.

	NASA Engineering and Safety Center Technical Report	Document #: NESC-RP-08- 00494	Version: 1.0
Title: Assessment of Orion Crew Module Ocean Wave Model			Page #: 117 of 158

Appendix C. Wave Simulations (AMA, Inc. Report, Section 3.1.2)

To provide some level of verification of wave slope model calculations, comparisons of slope variance predictions were made relative to simulated slopes. Simulated wave fields were conducted by superimposing waves based on pre-defined or buoy-measured spectral energy levels. Phase angles required to initialize the waves were specified at random assuming a uniform probability distribution on the interval 0 to 2 pi. The amplitude of each wave was computed from the wave energy as:

$$A_{i,j} = \sqrt{2E_{i,j}} \quad [1]$$

where A and E refer to the amplitude and energy of each wave in the field and the i and j represent the wave's direction and frequency indices. The wave direction interval was divided into 5 deg increments resulting in a total of 76 directional dimensions. Wave energy was extrapolated from 0.485 Hz to frequencies of 0.625 Hz in 0.01 Hz increments, which, considering the frequencies bins reported by NDBC, resulted in a total of 60 frequency bins. The total number of waves in the field is then $76 \times 60 = 4560$ waves, assuming each wave has a nonzero energy.


In theory, the wave slope variance computed from the energy spectrum should be possible to replicate by either:

1. Simulating a single point over a sufficient range of time and time resolution.
2. Simulating multiple points over a sufficient spatial range and spatial resolution.

In cases comprised of only a few waves of similar frequencies it is possible to estimate the periodicity of the wave field and limit the simulation time or range accordingly. In general, however, this is not straightforward. The approach taken here was to simulate over a long duration and/or spatial range and monitor the convergence of the calculated variances in comparison to those predicted from the spectra.

Simulation Test Case 1: Two Waves, 1 Location vs. Time

The first case simulates two waves moving in the same direction but with different frequencies (0.33 and 0.20 Hz) and measured at a single location. Both waves were configured at a wave direction of 30 deg. relative to the wind. The energy of each wave was set to 0.5 m² such that the amplitude of each was 1 meter. Figure 1 illustrates the surface height and upwind-downwind wave slope over time. The calculated slope variance (MUUD Variance Calculated) was computed from the simulated data and compared to the expected variance, which was derived from the energy spectrum. The two are in excellent agreement (0.081740 vs. 0.081982 rad²).

	NASA Engineering and Safety Center Technical Report	Document #: NESC-RP-08-00494	Version: 1.0
Title: Assessment of Orion Crew Module Ocean Wave Model			Page #: 118 of 158

Similar agreement can be seen in Figure 2 , which illustrates results for crosswind slope (0.027247 vs. 0.027327 rad²).

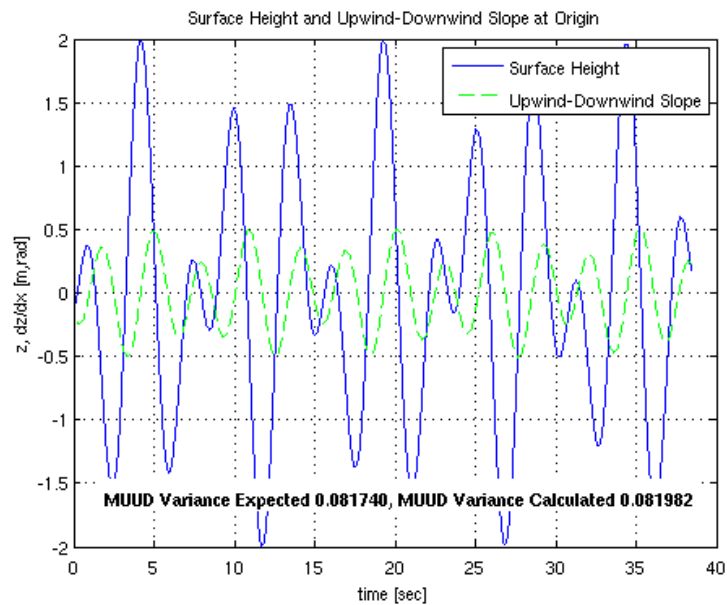


Figure 1. Surface Height and Upwind-Downwind Wave Slope vs. Time, Test 1

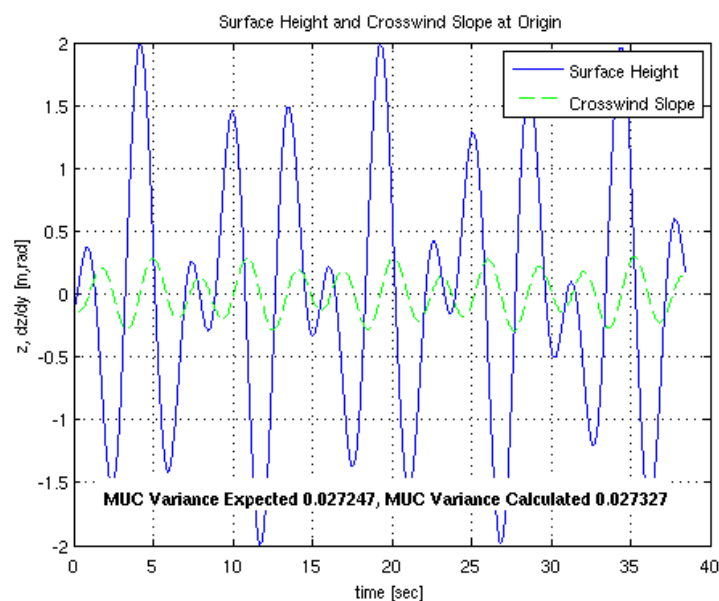



Figure 2. Surface Height and Crosswind Wave Slope vs. Time, Test 1

	NASA Engineering and Safety Center Technical Report	Document #: NESC-RP-08- 00494	Version: 1.0
Title: Assessment of Orion Crew Module Ocean Wave Model			Page #: 119 of 158

Simulation Test Case 2: 2 Waves, Multiple Locations at One Time

The second case simulates the same two waves from the first case (0.33 and 0.20 Hz, 1 m amplitude). However, here the waves are both coming from a direction of 180 deg. and measurements are made at multiple locations at a single instance in time. Figure 3 illustrates the surface height and upwind-downwind wave slope vs. downrange distance (x). The calculated slope variance is based on spatial range of 400 meters with measurements spaced every 0.5m. The convergence of the calculated variance is illustrated in Figure 4. Here the calculated variance is plotted against the range included in the variance calculation. As the range increases, the calculated variance converges on the expected value.

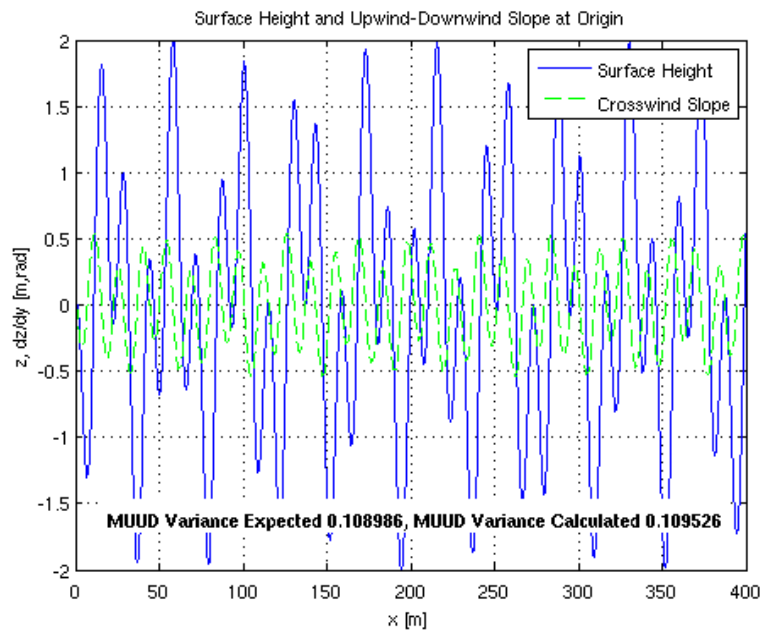



Figure 3. Surface Height and Upwind-Downwind Wave Slope vs. Location, Test 2

	NASA Engineering and Safety Center Technical Report	Document #: NESC-RP-08- 00494	Version: 1.0
Title: Assessment of Orion Crew Module Ocean Wave Model			Page #: 120 of 158

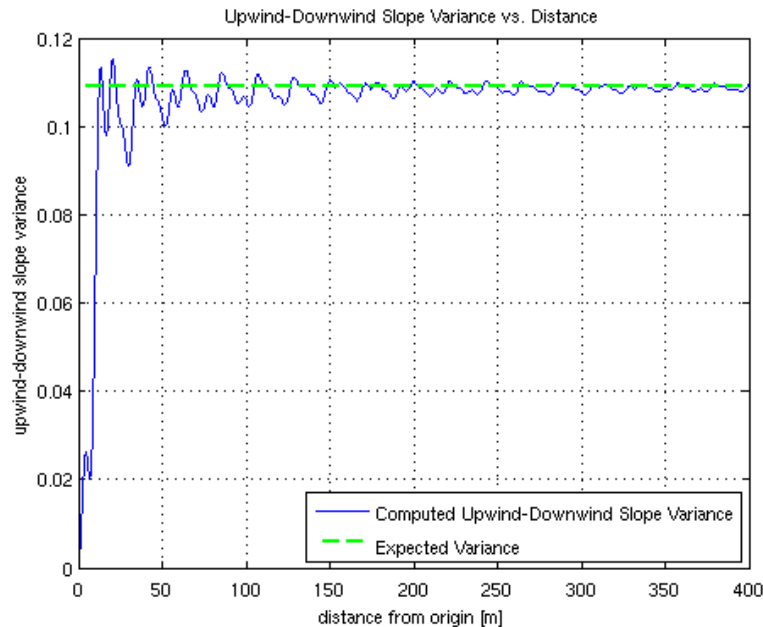



Figure 4. Upwind-Downwind Wave Slope Variance vs. Range of Measurements, Test 2

Simulation Test Case 3: Nondirectional Spectrum, Multiple Locations at One Time

The third case is the same as the second only the energy spectrum as been replaced with the nondirectional spectrum of a buoy record (Nantucket buoy, November 3, 2007, 2300 hrs). All the energy is assumed to be coming from the direction of 180 degrees. Figure 5 provides the surface height and upwind-downwind wave slope histories vs. downrange distance. With waves superimposing to amplitudes above 6 meters it is difficult to include both height and slope on the same plot. Nonetheless, the calculated and expected variances are in excellent agreement. The calculated variance was based on a range of 3500 meters with a resolution of 0.5m. Convergence of the calculated variance is illustrated in Figure 6, which shows that the calculated variance, in this case) falls within 5% of the expected value after about 600 meters. Note that this result may be sensitive to the simulated spectrum as well as the phase angles randomly selected for each wave.

	NASA Engineering and Safety Center Technical Report	Document #: NESC-RP-08-00494	Version: 1.0
Title: Assessment of Orion Crew Module Ocean Wave Model			Page #: 121 of 158

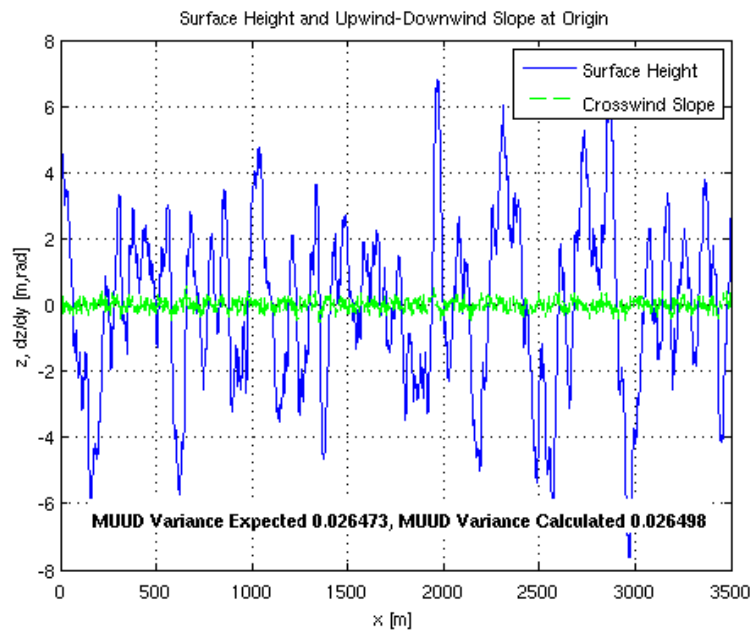


Figure 5. Surface Height and Upwind-Downwind Wave Slope vs. Location, Test 3

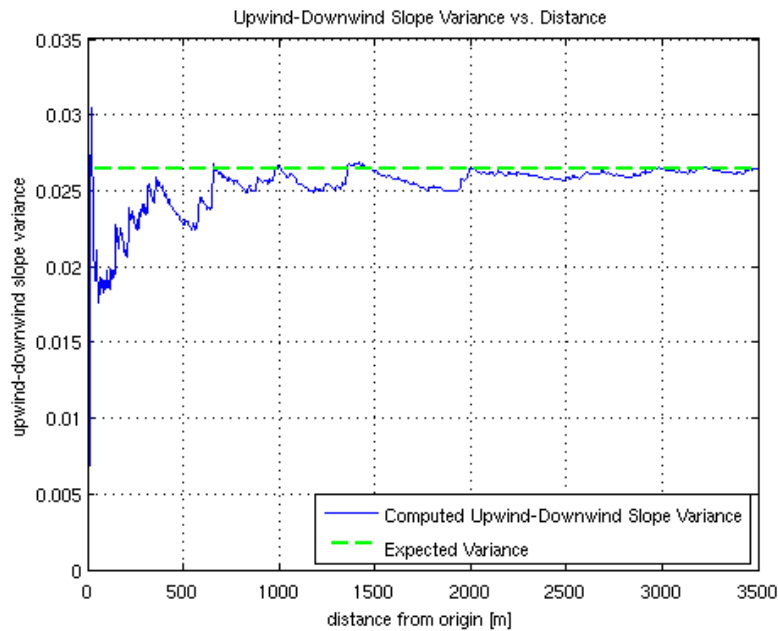



Figure 6. Upwind-Downwind Wave Slope Variance vs. Range of Measurements, Test 3

	NASA Engineering and Safety Center Technical Report	Document #: NESC-RP-08- 00494	Version: 1.0
Title: Assessment of Orion Crew Module Ocean Wave Model			Page #: 122 of 158

Simulation Test Case 4: Directional Spectrum, Multiple Locations at One Time

The fourth case utilizes the same nondirectional spectrum employed in case three but also applies the directional spreading indicated in the buoy record. Convergence of the calculated variance, as seen in Figure 7 and Figure 8, takes longer in this case with a 5% accuracy achieved after a downrange distance of approximately 3000 meters. In this case, measurements were taken along a line aligned with the wind (x-axis) as well as a line perpendicular to the wind direction (y-axis) with a spatial resolution of 0.5 meters. Distance from the origin seen in the figures below refers to the distance along the x-axis for the upwind-downwind variance calculation and the y-axis for the crosswind variance calculation.

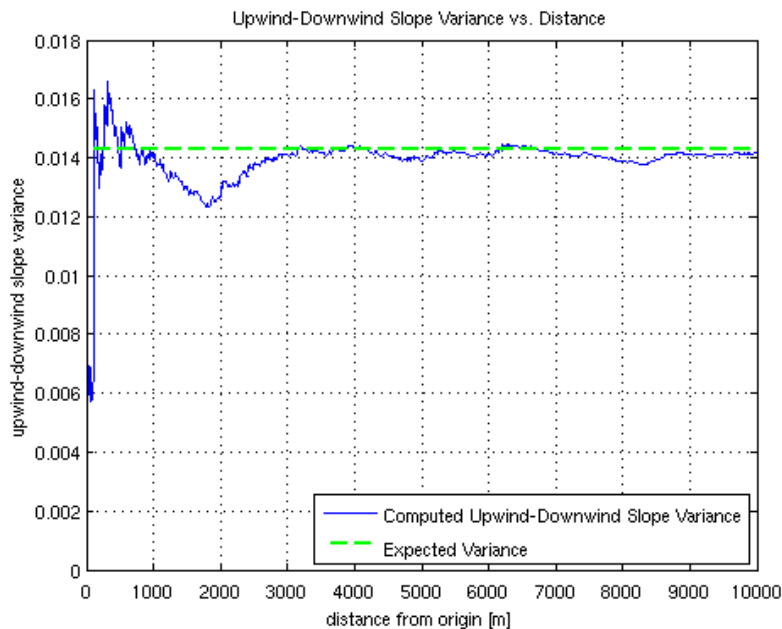



Figure 7. Upwind-Downwind Wave Slope Variance vs. Range of Measurements, Test 4

	NASA Engineering and Safety Center Technical Report	Document #: NESC-RP-08- 00494	Version: 1.0
Title: Assessment of Orion Crew Module Ocean Wave Model			Page #: 123 of 158

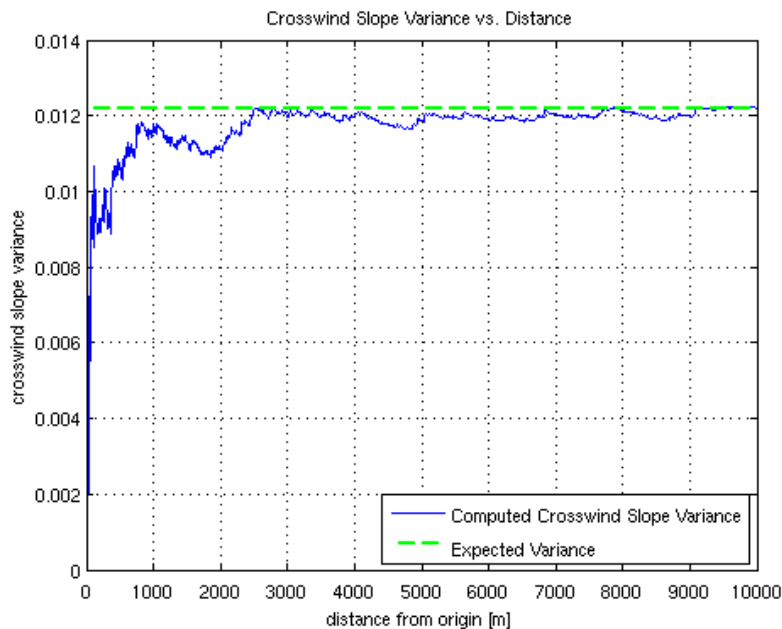



Figure 8. Crosswind Wave Slope Variance vs. Range of Measurements, Test 4

Simulation Test Case 5: Directional Spectrum, One Location vs. Time

The final test case was similar to case 4 with one key difference. Instead of simulating slopes over multiple locations, a single measurement location was simulated for a long period of time. More sensitivity to the Monte Carlo seed was seen in these simulations with many cases not converging to the expected values after 20 minutes of simulation (see Figure 9 and Figure 10).

	NASA Engineering and Safety Center Technical Report	Document #: NESC-RP-08- 00494	Version: 1.0
Title: Assessment of Orion Crew Module Ocean Wave Model			Page #: 124 of 158

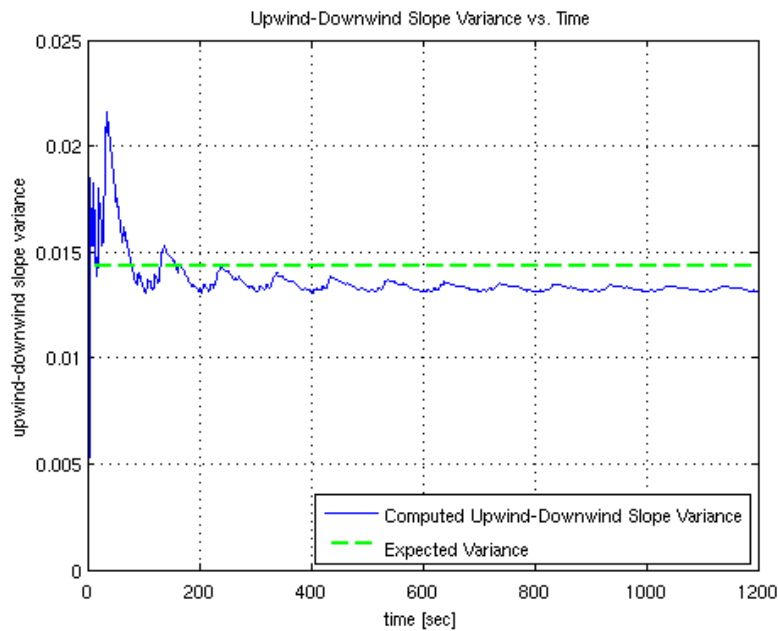


Figure 9. Upwind-Downwind Wave Slope Variance vs. Range of Measurements, Test 5

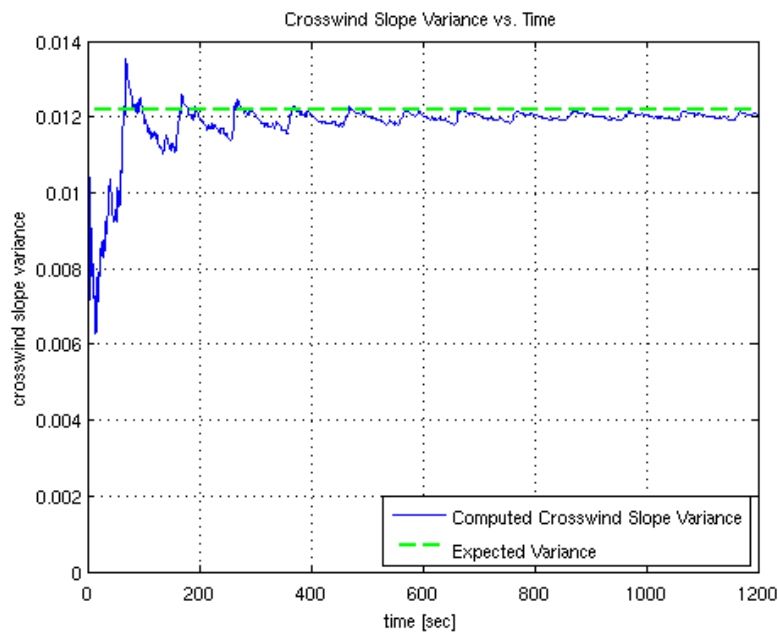



Figure 10. Crosswind Wave Slope Variance vs. Range of Measurements, Test 5

	NASA Engineering and Safety Center Technical Report	Document #: NESC-RP-08- 00494	Version: 1.0
Title: Assessment of Orion Crew Module Ocean Wave Model			Page #: 125 of 158

Appendix D. Spatial-Temporal Variabilities

[Time periods selected were based on that data availability and consistency in the buoy location, measurement device, and analysis packages.]

The following series of graphics are derived from an analysis of five NDBC buoys (44018, 44004, 44014, 41012), four located along the off-nominal path in the Atlantic Ocean; the last set of figures are data obtained at NDBC buoy 46047. For each buoy location, the following graphics are produced:

1. Four panel plot of the
 - a. Mean monthly significant wave height the record period.
 - b. Variance of the mean monthly significant wave height
 - c. Maximum monthly significant wave height
 - d. Number of records for the given month.
2. Three panel plot of the
 - a. Mean significant wave height averaged over all years for the month
 - b. Variance in the mean significant wave height
 - c. Maximum significant wave height
3. Four panel plot of the
 - a. Probability of significant wave heights $< 1\text{-m}$ in the given month
 - b. Probability of significant wave heights $\leq 1\text{-m}$ and $< 2\text{-m}$ in a given month
 - c. Probability of significant wave heights $\leq 2\text{-m}$ and $< 3\text{-m}$ in a given month
 - d. Probability of significant wave heights $\leq 3\text{-m}$ and $< 4\text{-m}$ in a given month
4. Three panel plot of the monthly mean probabilities over the record length for
 - a. Probability of significant wave heights $< 1\text{-m}$
 - b. Probability of significant wave heights $\leq 1\text{-m}$ and $< 2\text{-m}$
 - c. Probability of significant wave heights $\leq 2\text{-m}$ and $< 3\text{-m}$
 - d. Probability of significant wave heights $\leq 3\text{-m}$ and $< 4\text{-m}$
5. The mean probabilities of the four classes over each month and the cumulative of significant wave heights $< 4\text{-m}$



NASA Engineering and Safety Center Technical Report

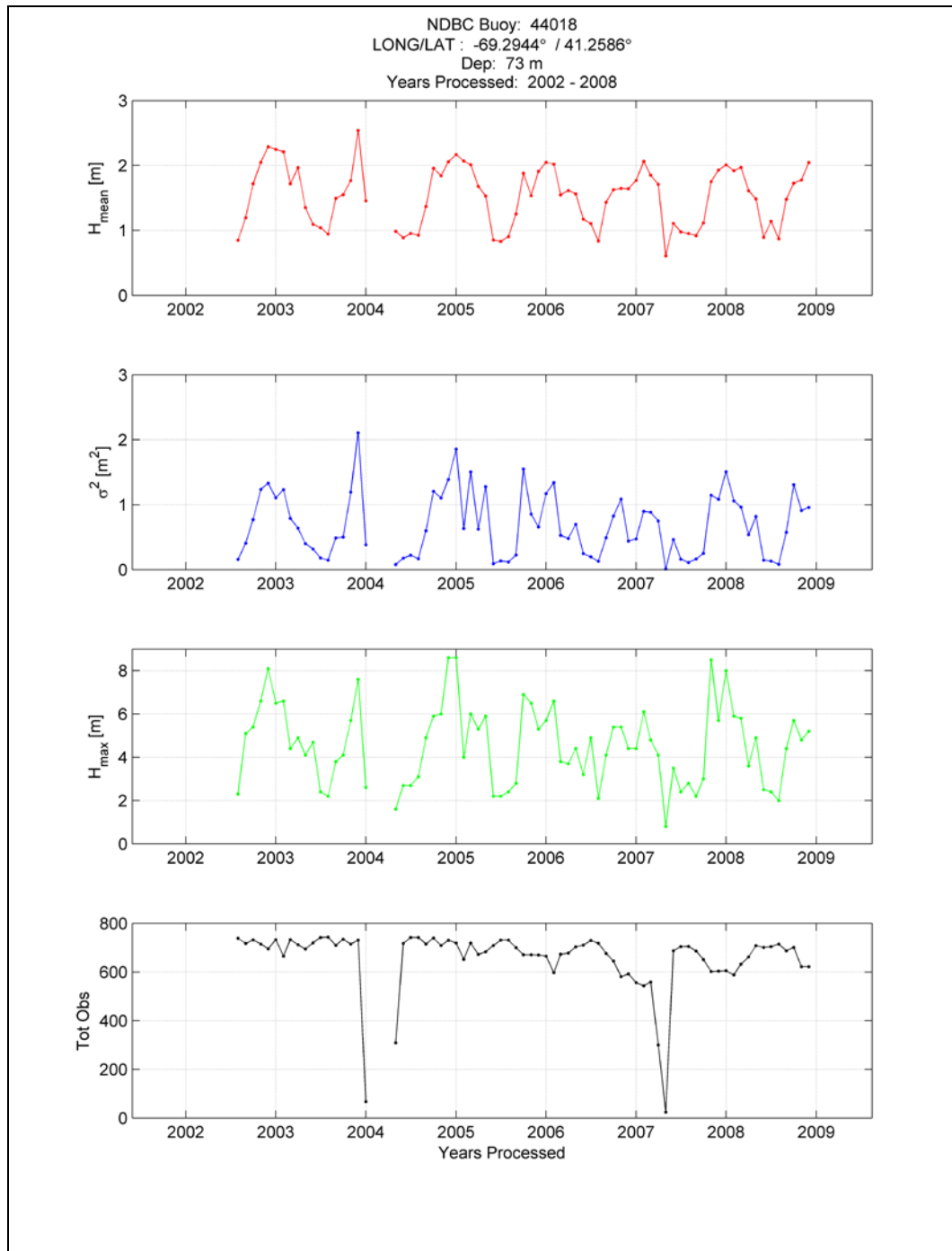
Document #:
**NESC-RP-08-
00494**

Version:
1.0

Title:

Assessment of Orion Crew Module Ocean Wave Model

Page #:
126 of 158





NASA Engineering and Safety Center Technical Report

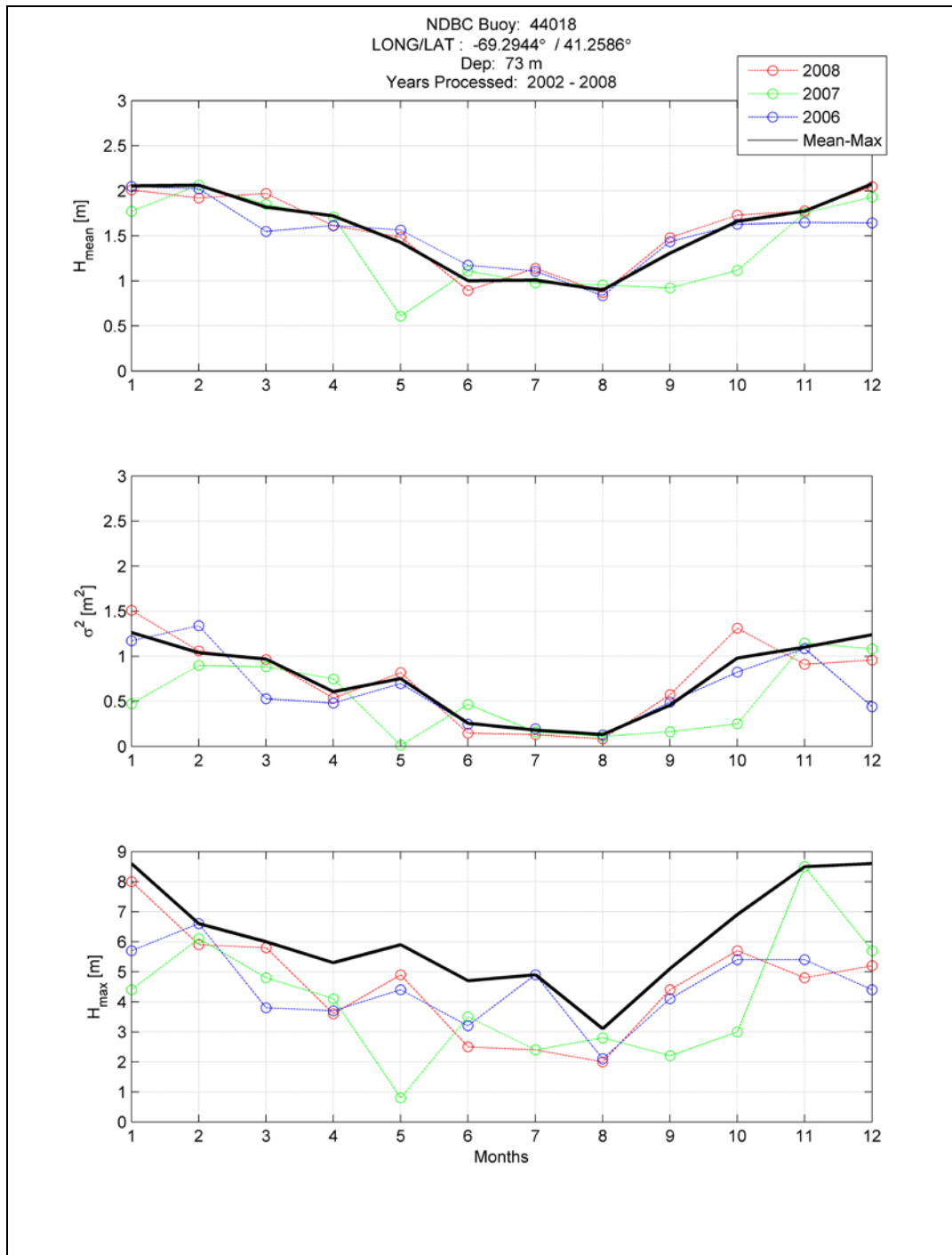
Document #:
**NESC-RP-08-
00494**

Version:
1.0

Title:

Assessment of Orion Crew Module Ocean Wave Model

Page #:
127 of 158





NASA Engineering and Safety Center Technical Report

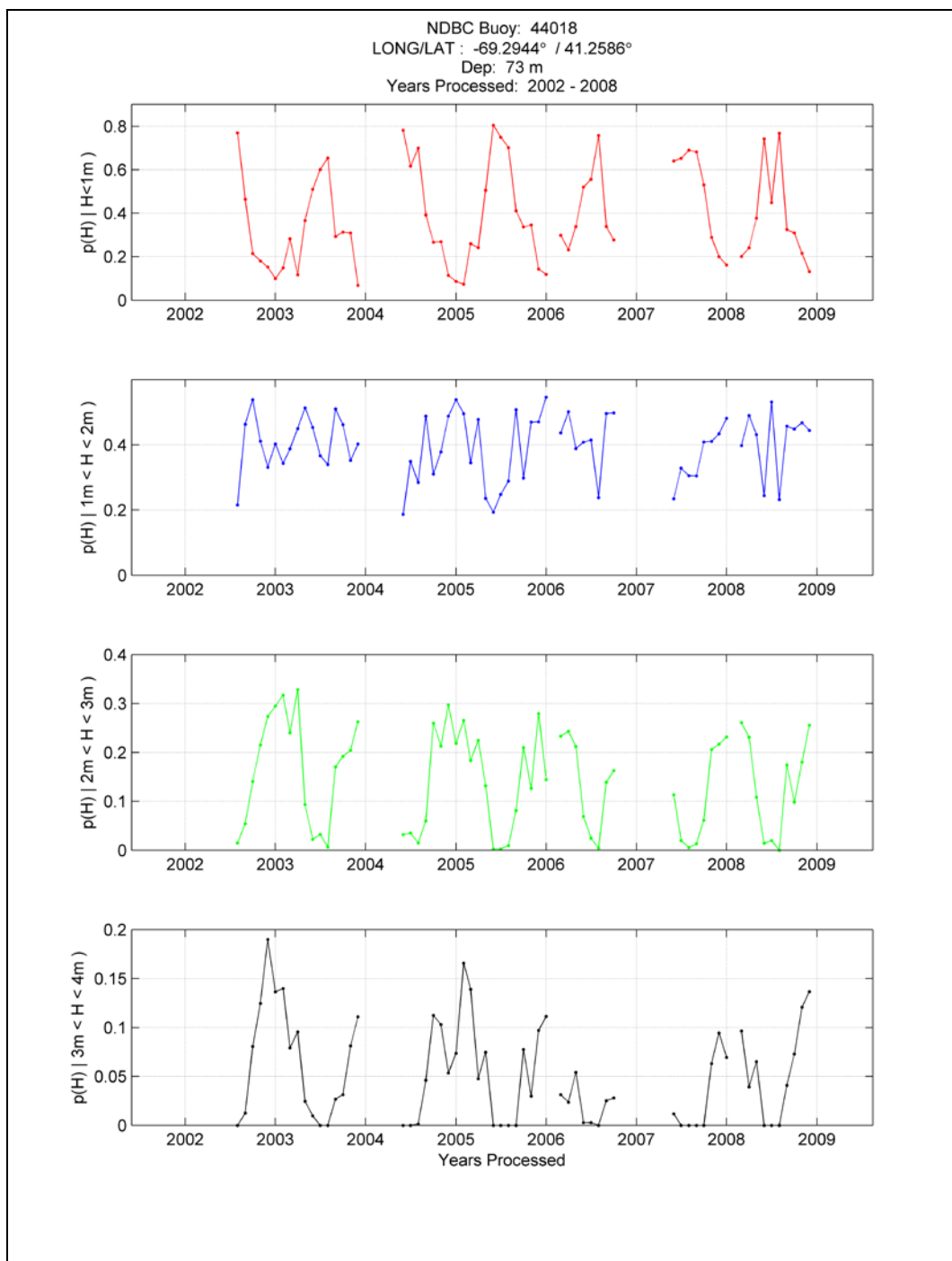
Document #:
**NESC-RP-08-
00494**

Version:
1.0

Title:

Assessment of Orion Crew Module Ocean Wave Model

Page #:
128 of 158





NASA Engineering and Safety Center Technical Report

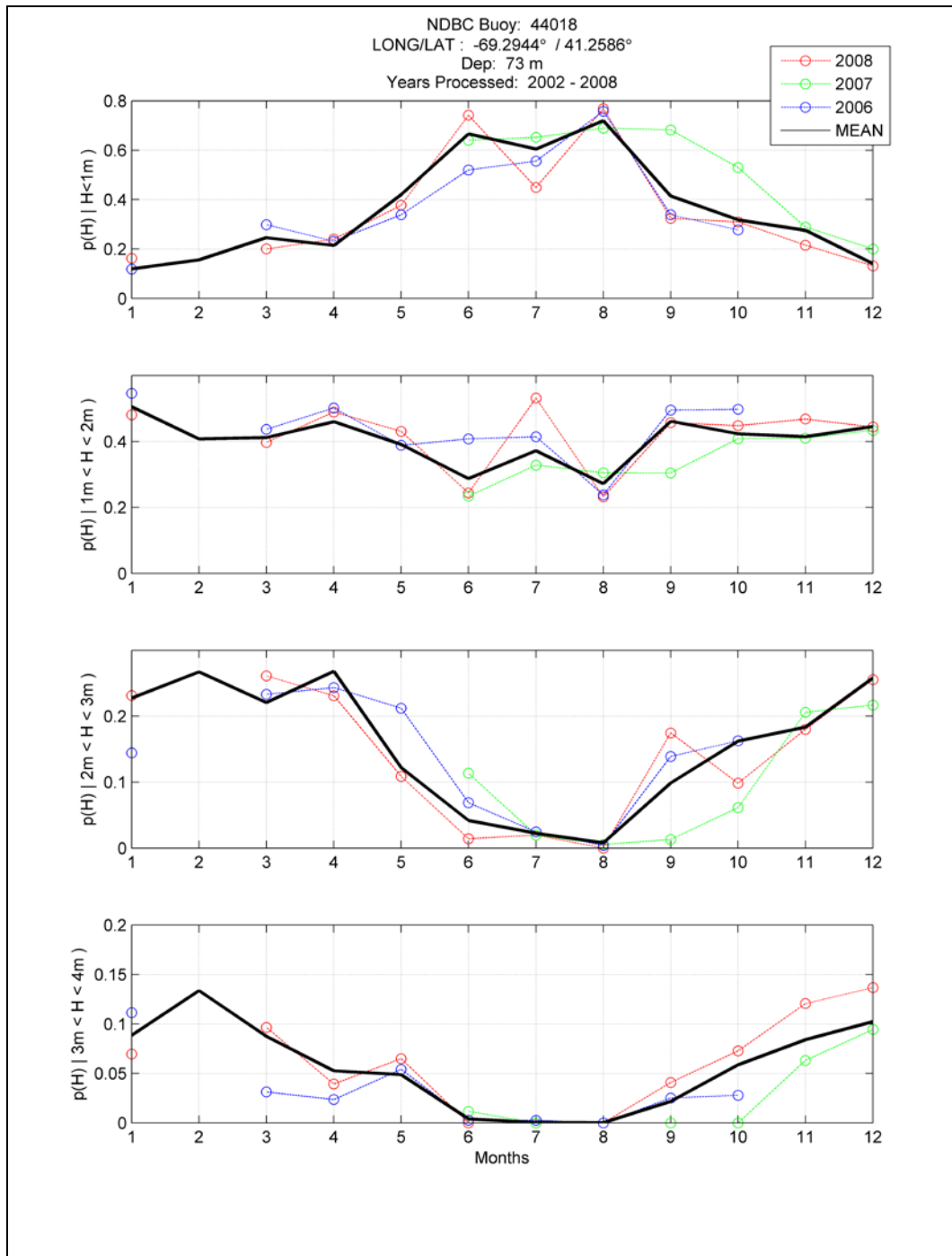
Document #:
**NESC-RP-08-
00494**

Version:
1.0

Title:

Assessment of Orion Crew Module Ocean Wave Model

Page #:
129 of 158





NASA Engineering and Safety Center Technical Report

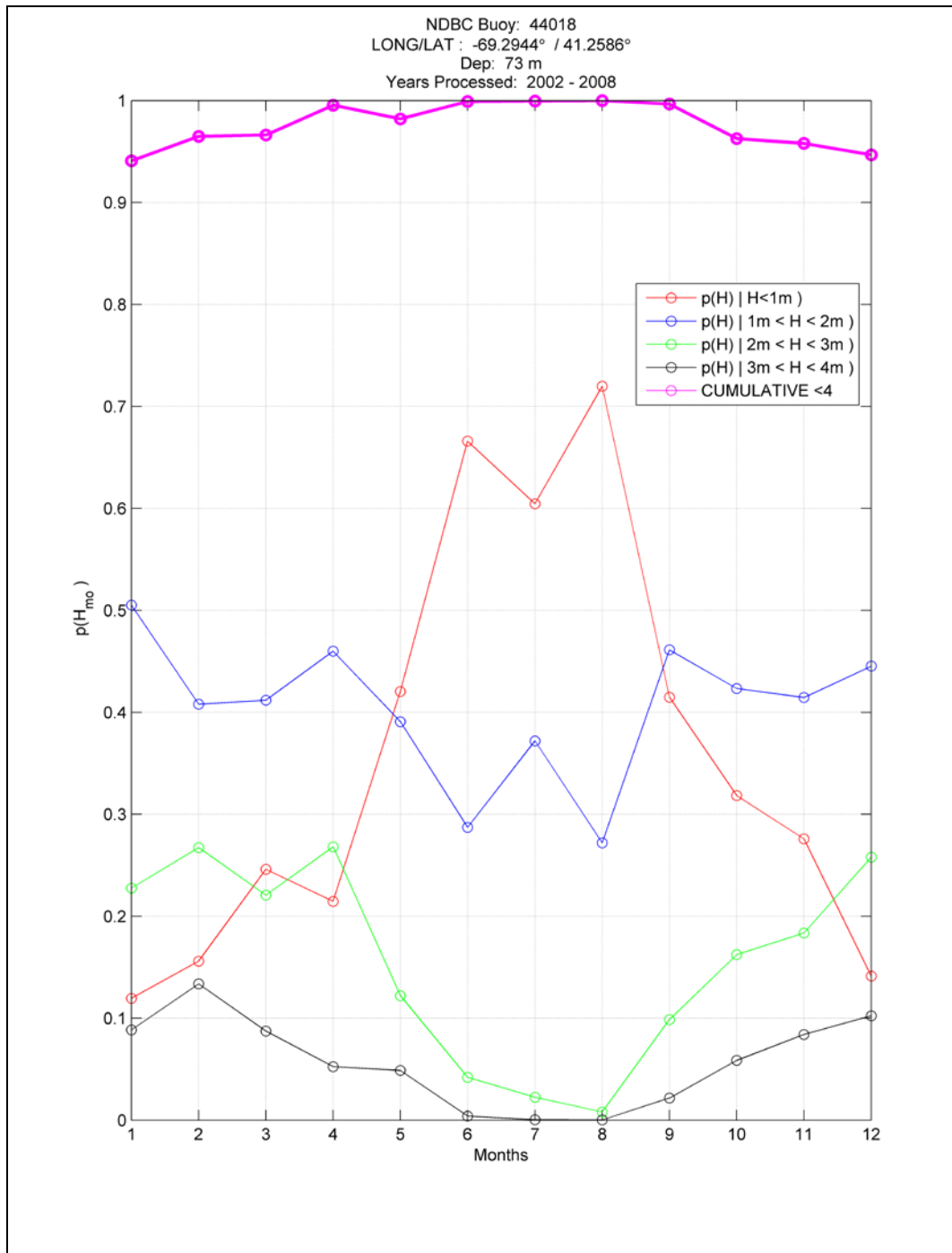
Document #:
**NESC-RP-08-
00494**

Version:
1.0

Title:

Assessment of Orion Crew Module Ocean Wave Model

Page #:
130 of 158





NASA Engineering and Safety Center Technical Report

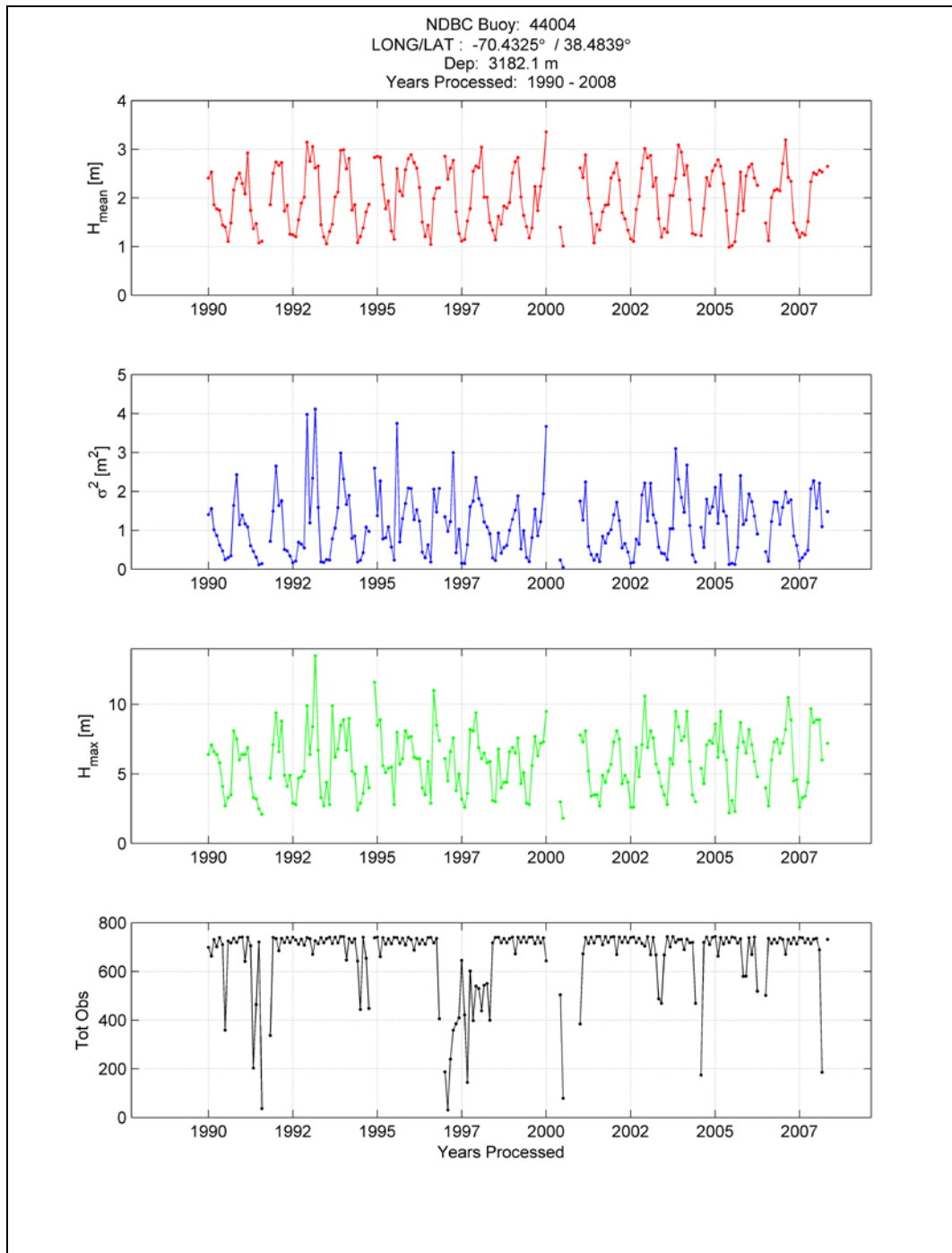
Document #:
**NESC-RP-08-
00494**

Version:
1.0

Title:

Assessment of Orion Crew Module Ocean Wave Model

Page #:
131 of 158





NASA Engineering and Safety Center Technical Report

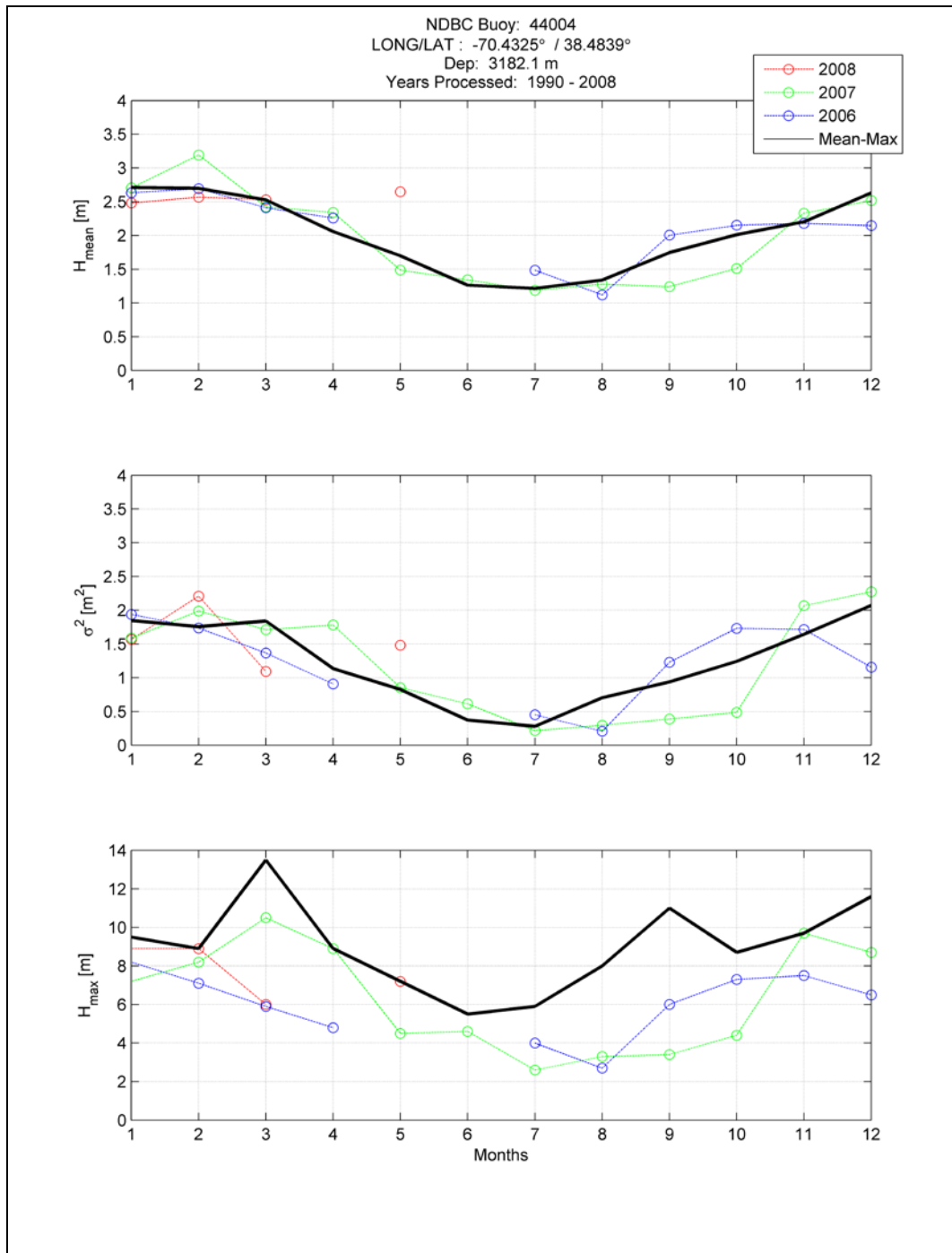
Document #:
**NESC-RP-08-
00494**

Version:
1.0

Title:

Assessment of Orion Crew Module Ocean Wave Model

Page #:
132 of 158





NASA Engineering and Safety Center Technical Report

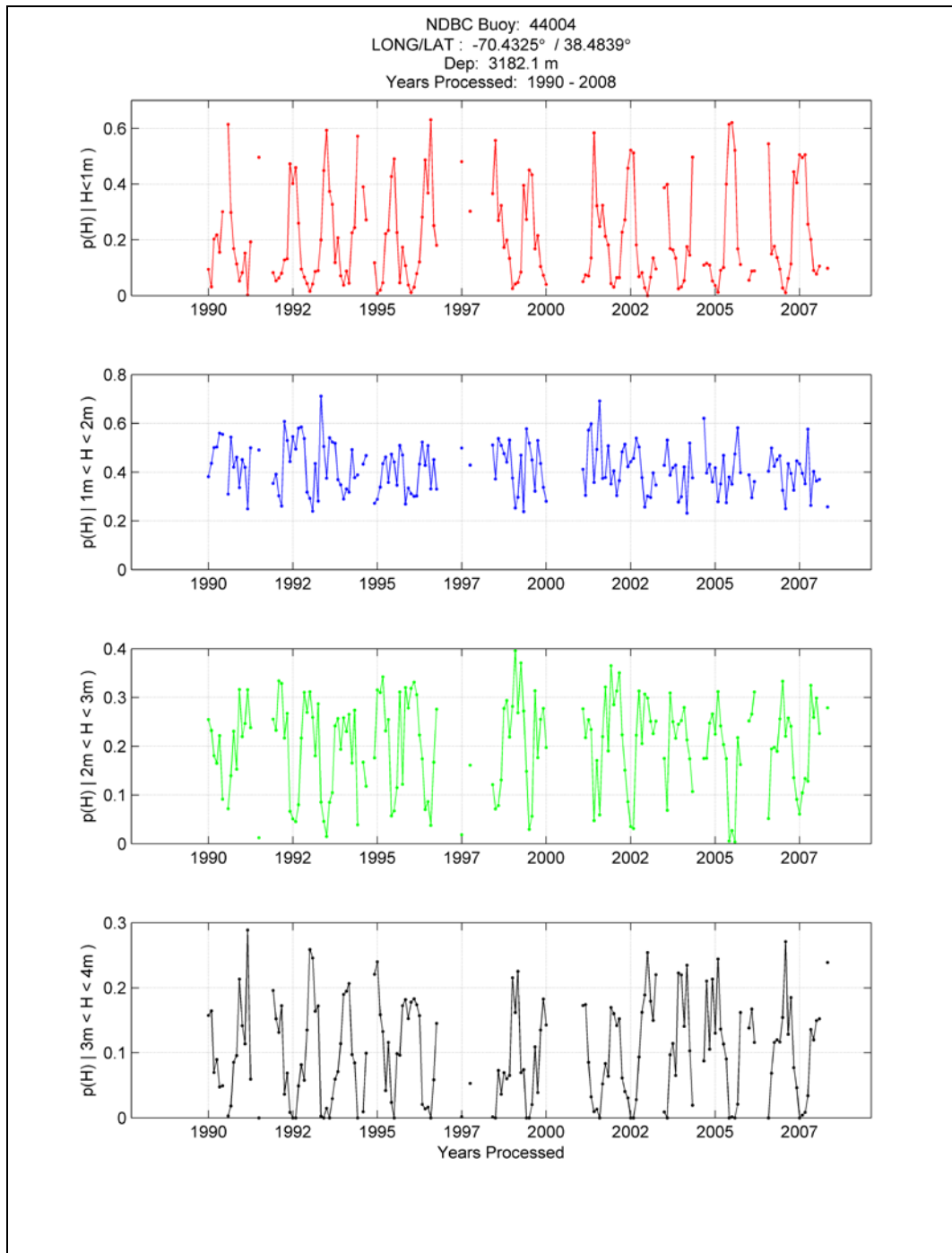
Document #:
**NESC-RP-08-
00494**

Version:
1.0

Title:

Assessment of Orion Crew Module Ocean Wave Model

Page #:
133 of 158





NASA Engineering and Safety Center Technical Report

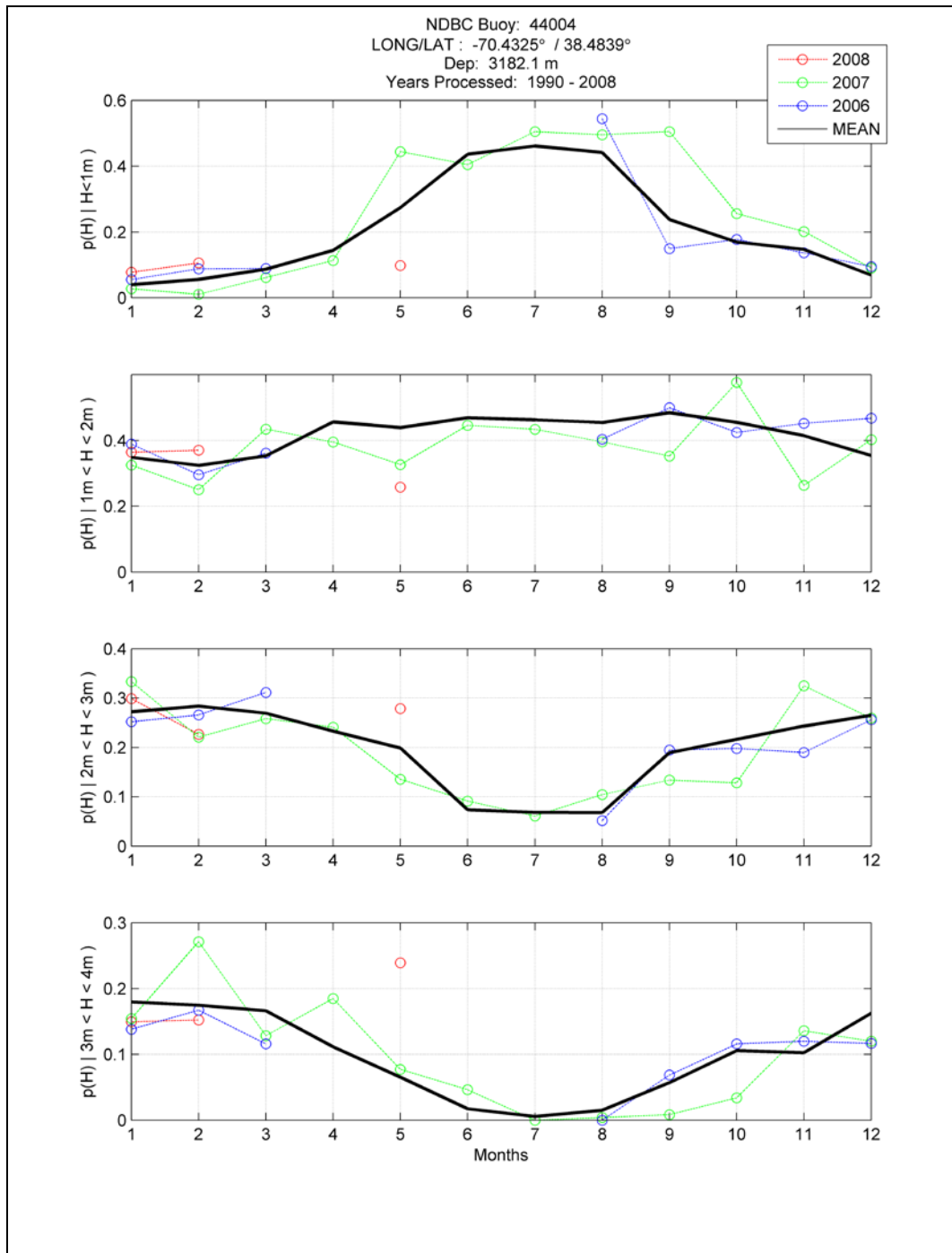
Document #:
**NESC-RP-08-
00494**

Version:
1.0

Title:

Assessment of Orion Crew Module Ocean Wave Model

Page #:
134 of 158





NASA Engineering and Safety Center Technical Report

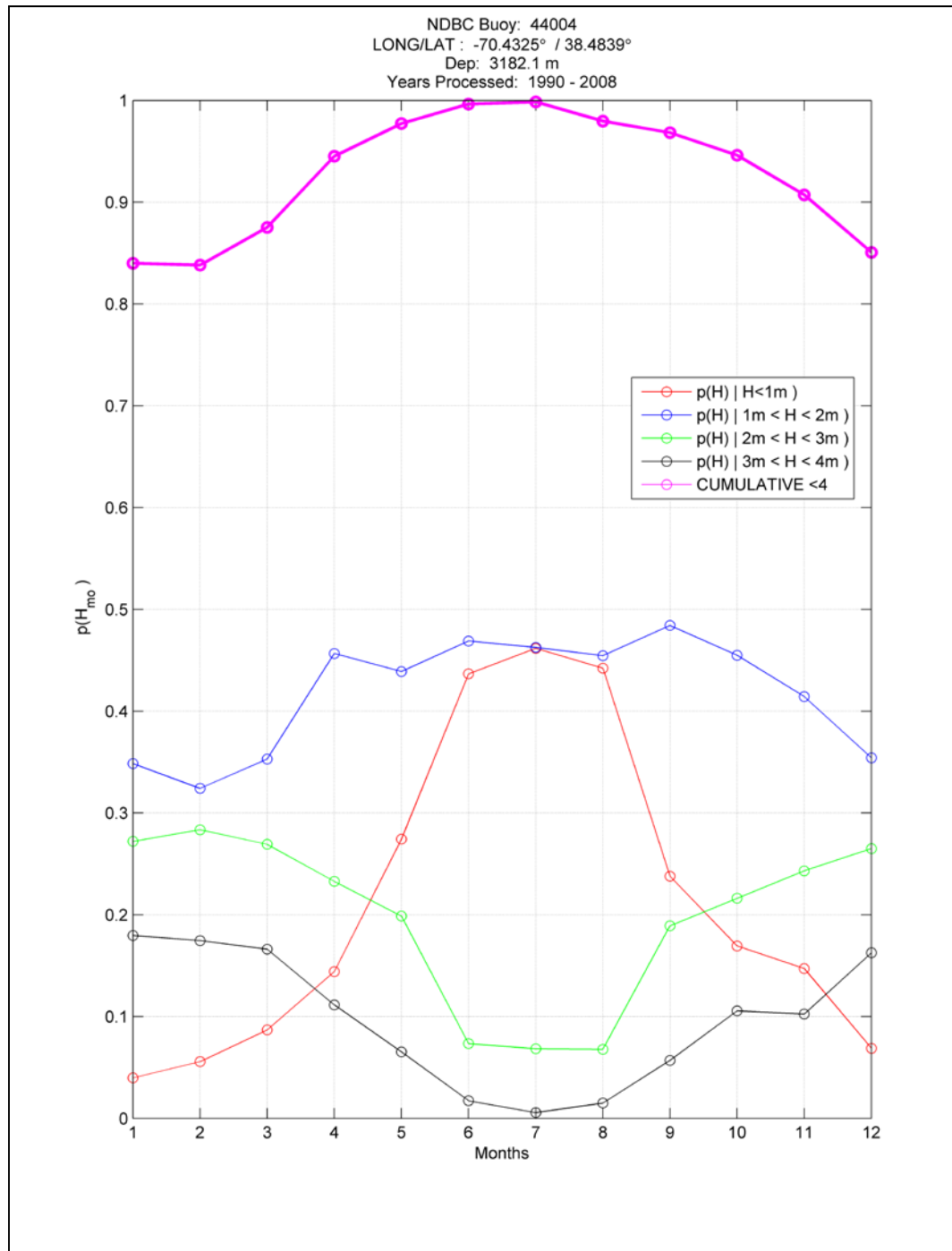
Document #:
**NESC-RP-08-
00494**

Version:
1.0

Title:

Assessment of Orion Crew Module Ocean Wave Model

Page #:
135 of 158





NASA Engineering and Safety Center Technical Report

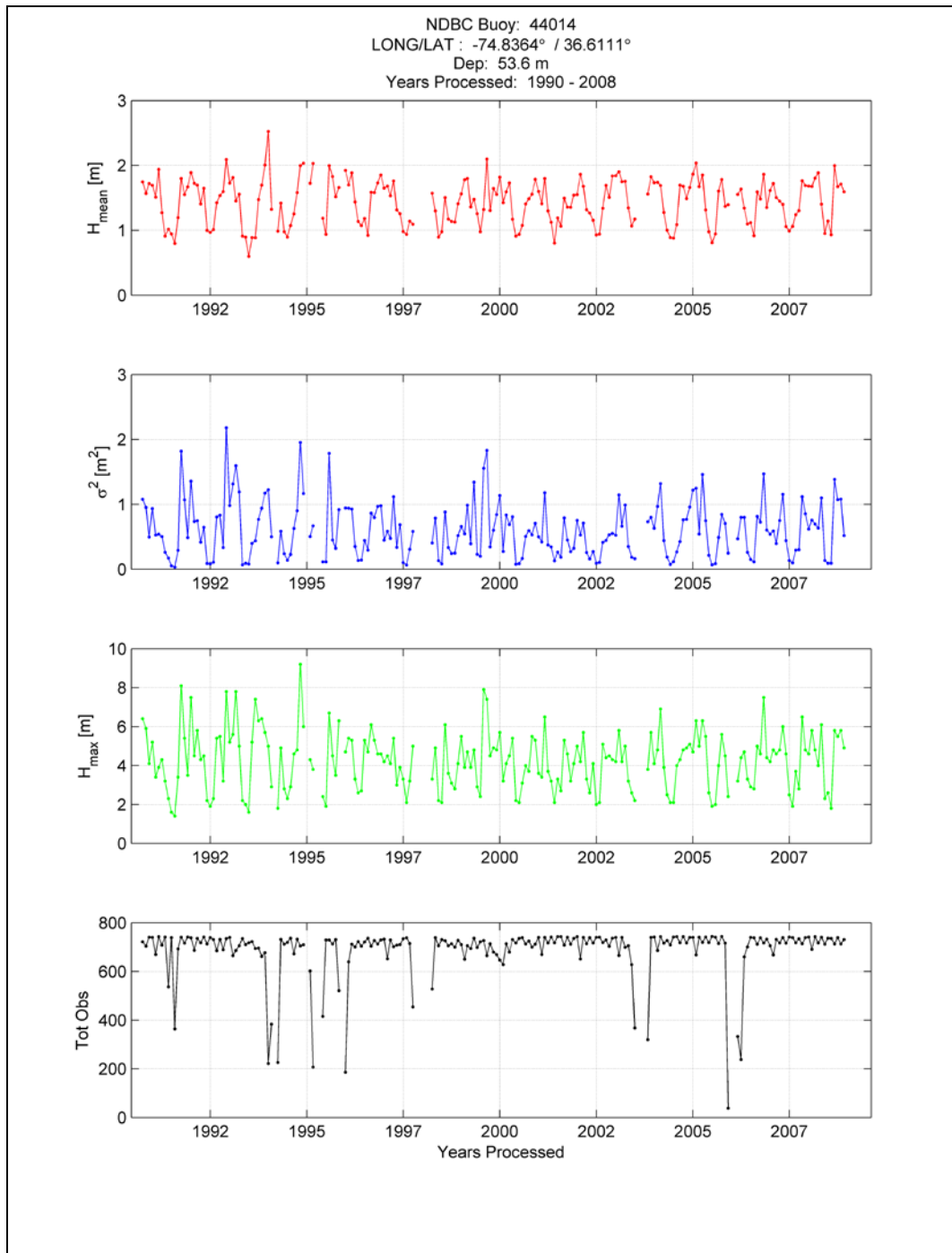
Document #:
**NESC-RP-08-
00494**

Version:
1.0

Title:

Assessment of Orion Crew Module Ocean Wave Model

Page #:
136 of 158





NASA Engineering and Safety Center Technical Report

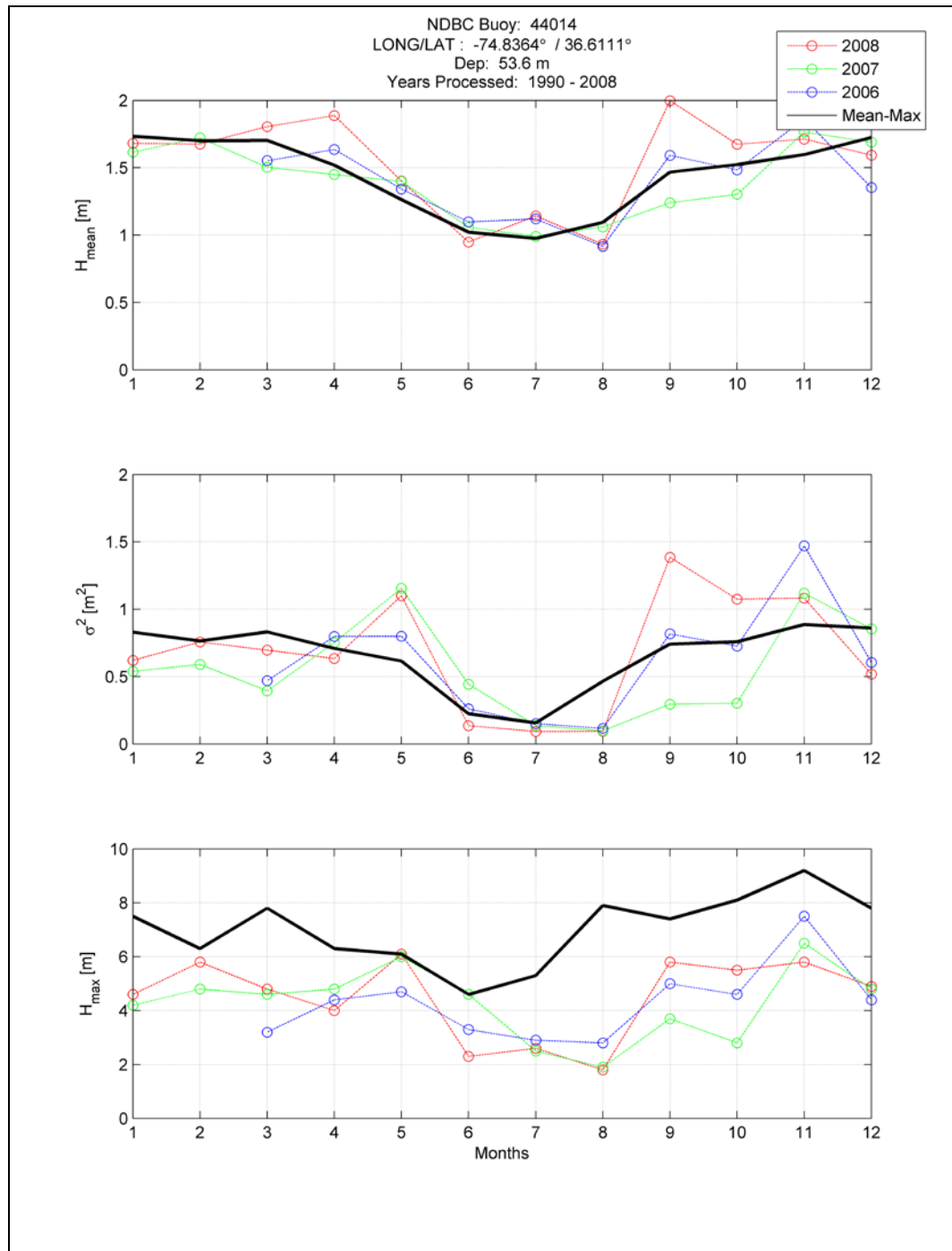
Document #:
**NESC-RP-08-
00494**

Version:
1.0

Title:

Assessment of Orion Crew Module Ocean Wave Model

Page #:
137 of 158





NASA Engineering and Safety Center Technical Report

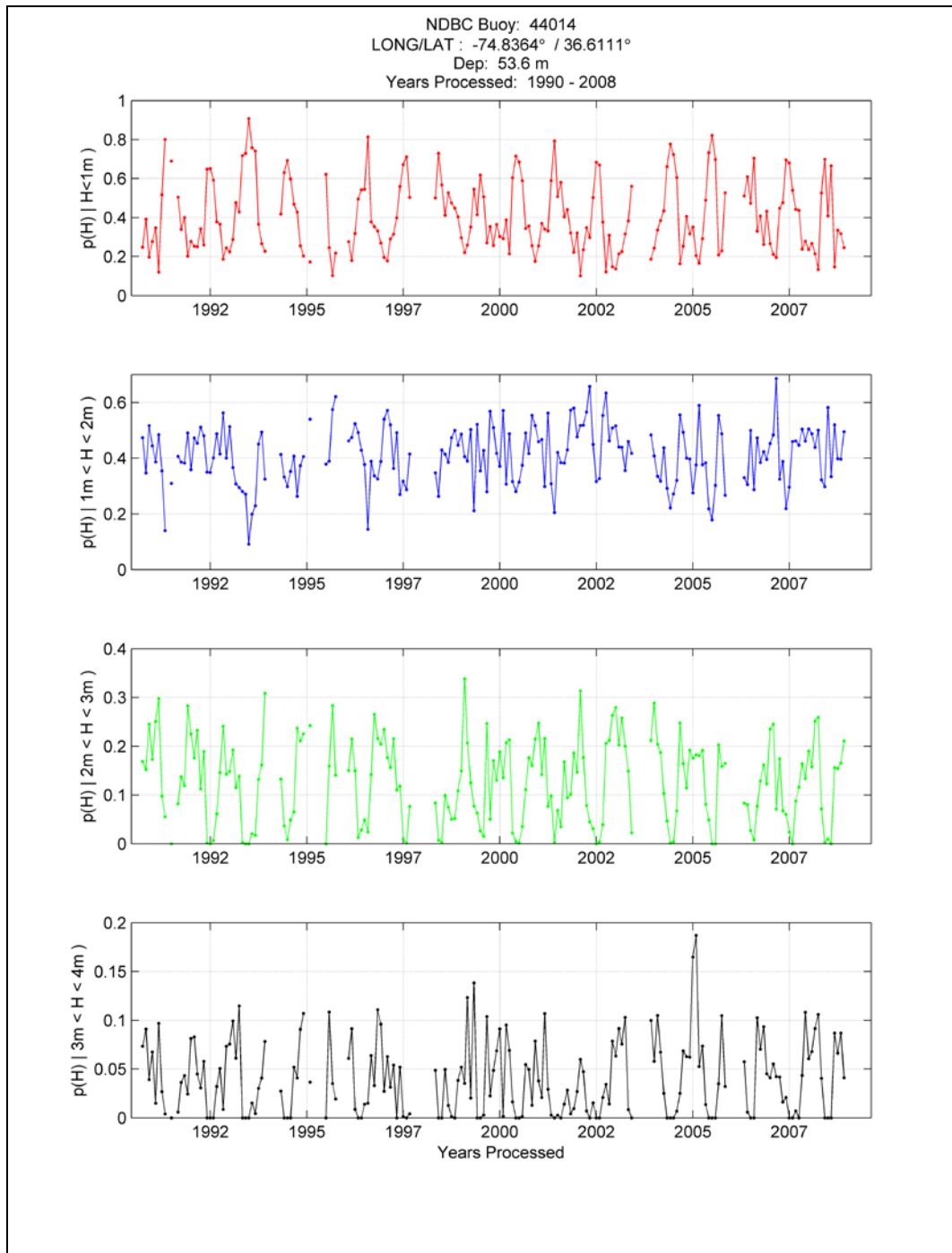
Document #:
**NESC-RP-08-
00494**

Version:
1.0

Title:

Assessment of Orion Crew Module Ocean Wave Model

Page #:
138 of 158





NASA Engineering and Safety Center Technical Report

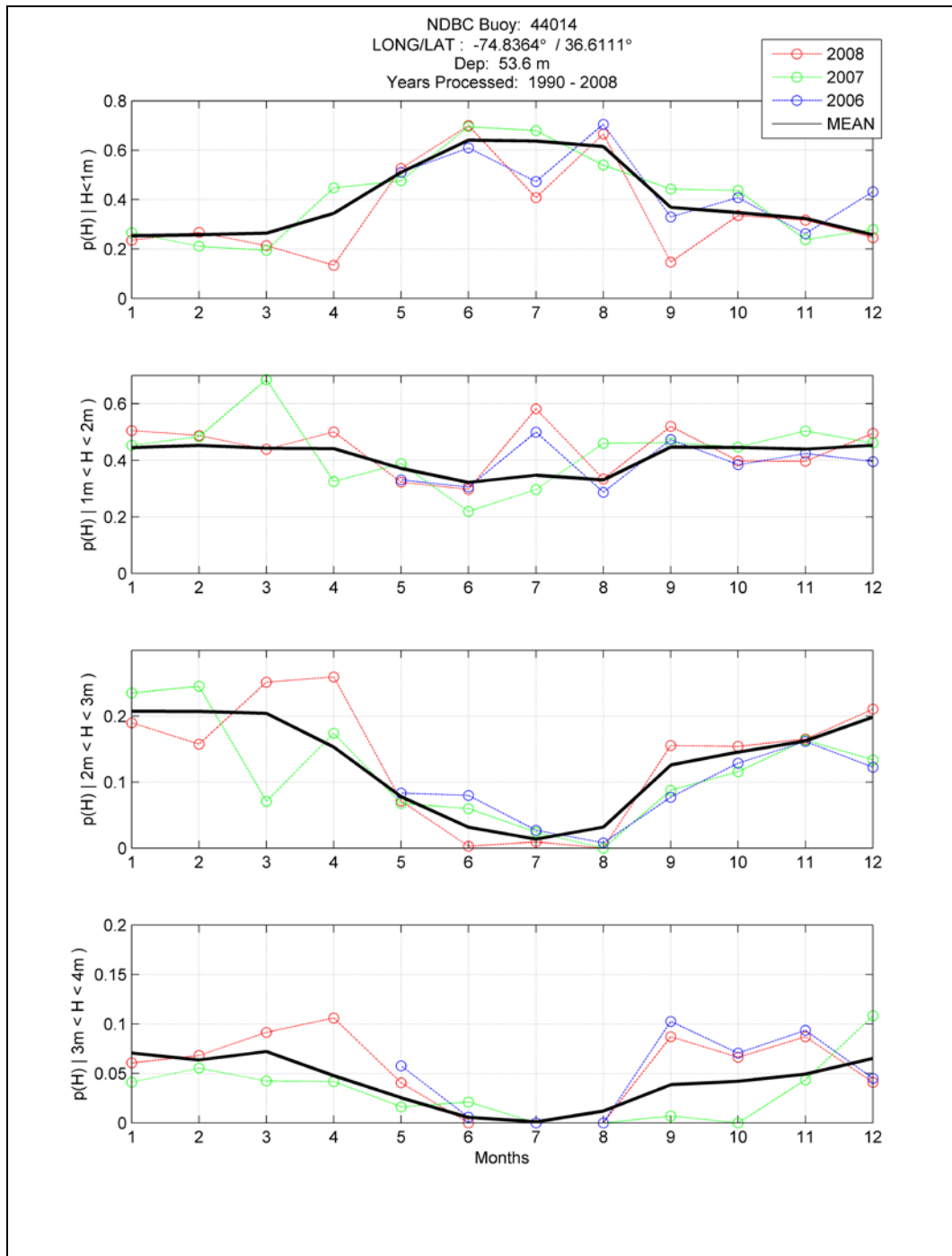
Document #:
**NESC-RP-08-
00494**

Version:
1.0

Title:

Assessment of Orion Crew Module Ocean Wave Model

Page #:
139 of 158





NASA Engineering and Safety Center Technical Report

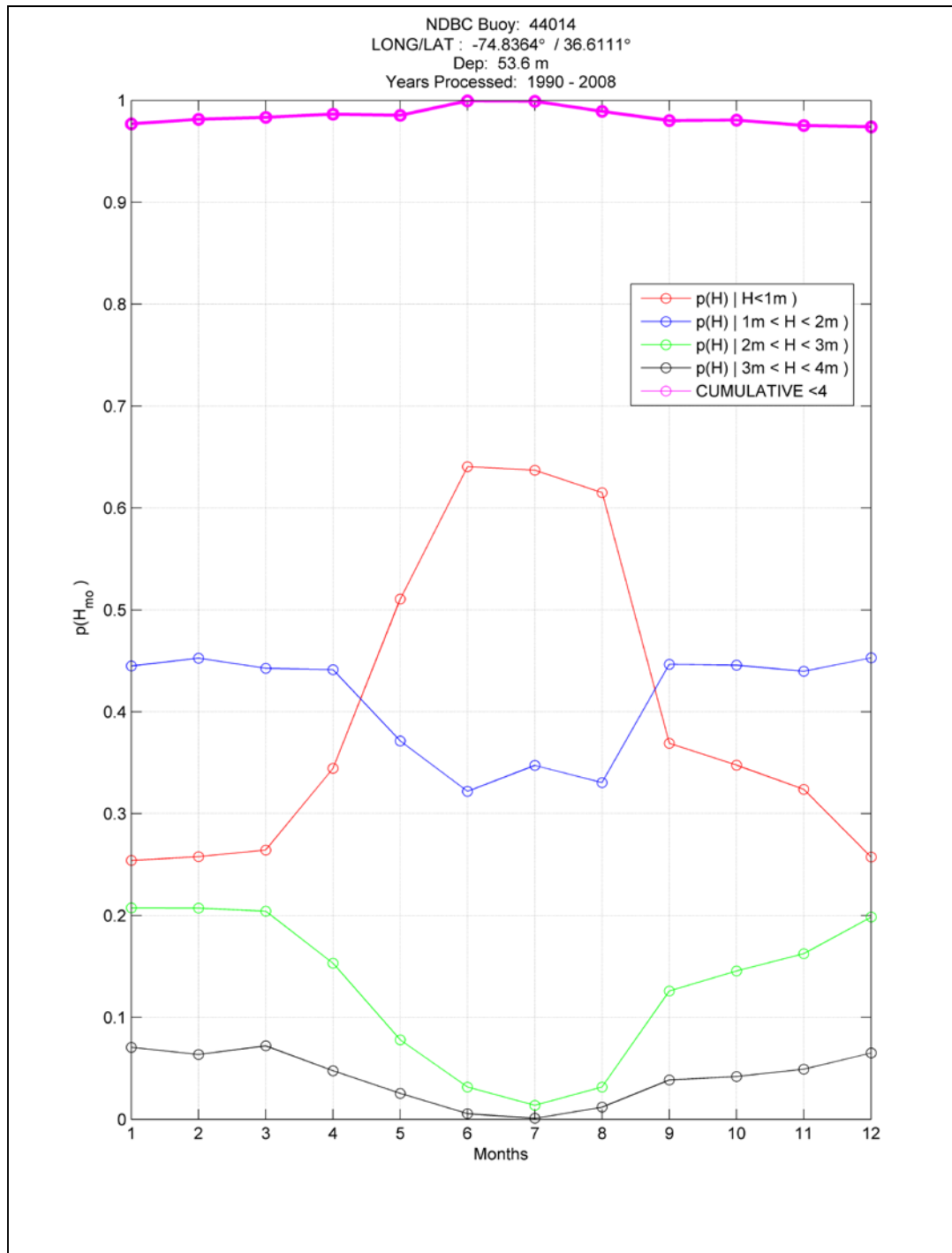
Document #:
**NESC-RP-08-
00494**

Version:
1.0

Title:

Assessment of Orion Crew Module Ocean Wave Model

Page #:
140 of 158





NASA Engineering and Safety Center Technical Report

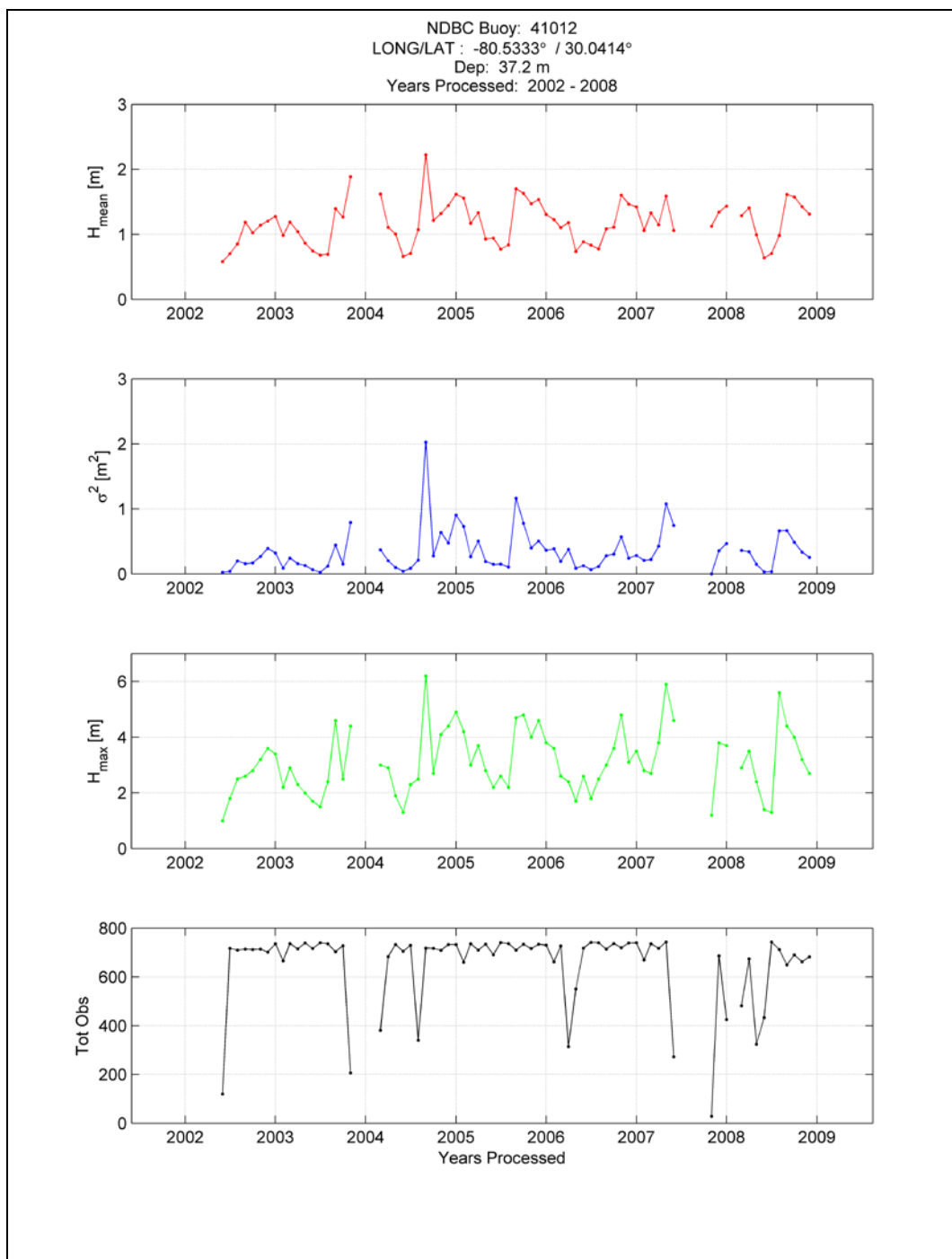
Document #:
**NESC-RP-08-
00494**

Version:
1.0

Title:

Assessment of Orion Crew Module Ocean Wave Model

Page #:
141 of 158





NASA Engineering and Safety Center Technical Report

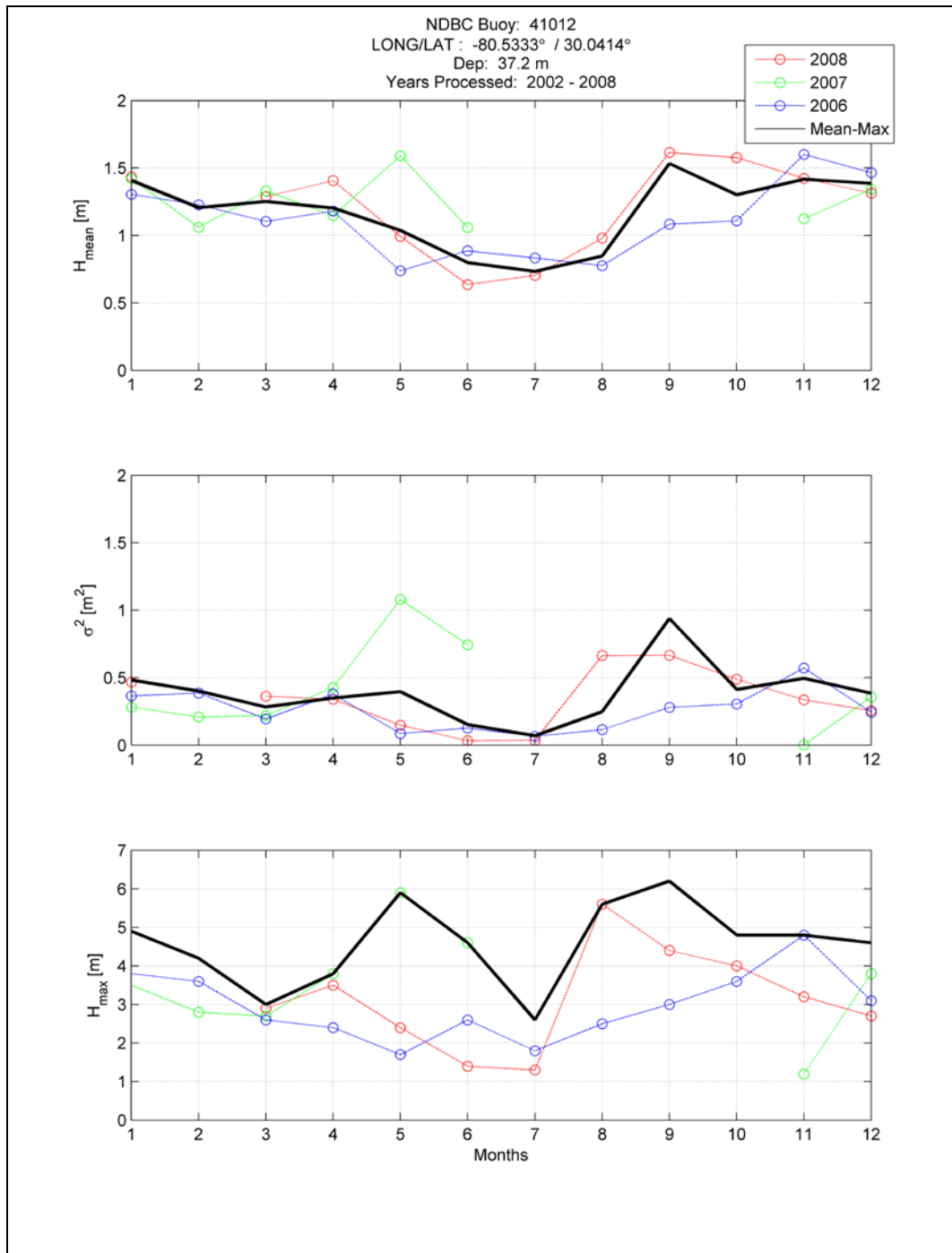
Document #:
**NESC-RP-08-
00494**

Version:
1.0

Title:

Assessment of Orion Crew Module Ocean Wave Model

Page #:
142 of 158





NASA Engineering and Safety Center Technical Report

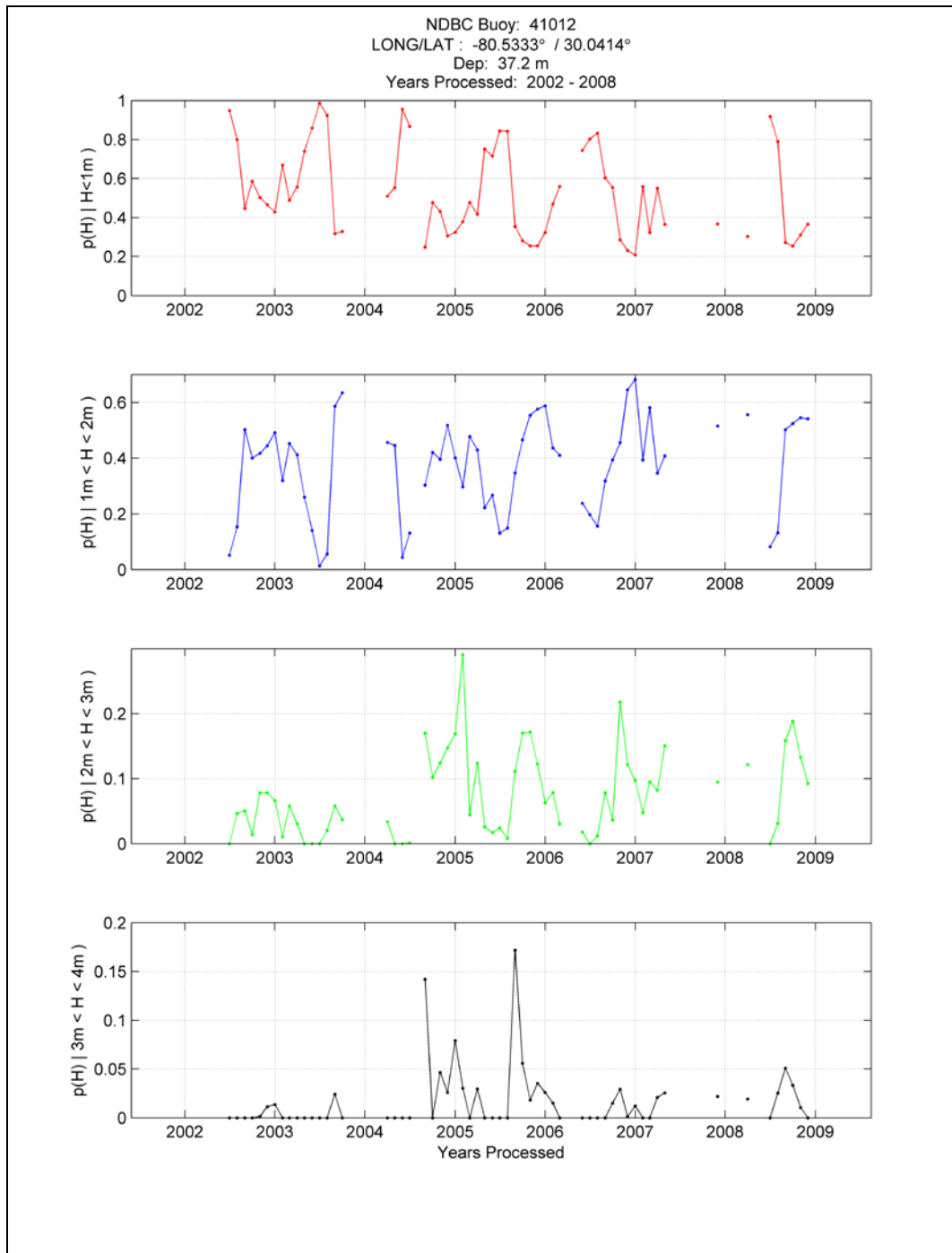
Document #:
**NESC-RP-08-
00494**

Version:
1.0

Title:

Assessment of Orion Crew Module Ocean Wave Model

Page #:
143 of 158





NASA Engineering and Safety Center Technical Report

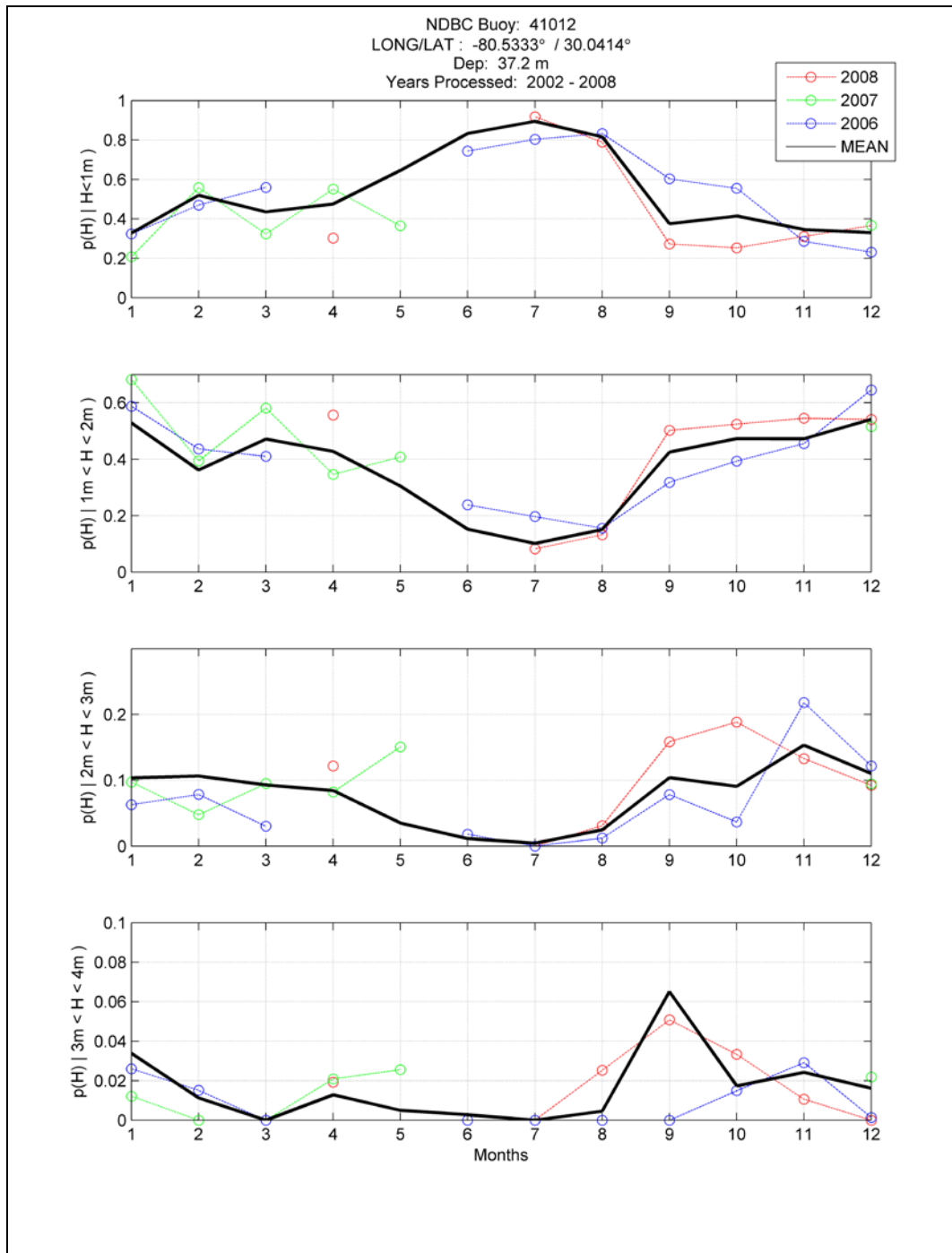
Document #:
**NESC-RP-08-
00494**

Version:
1.0

Title:

Assessment of Orion Crew Module Ocean Wave Model

Page #:
144 of 158





NASA Engineering and Safety Center Technical Report

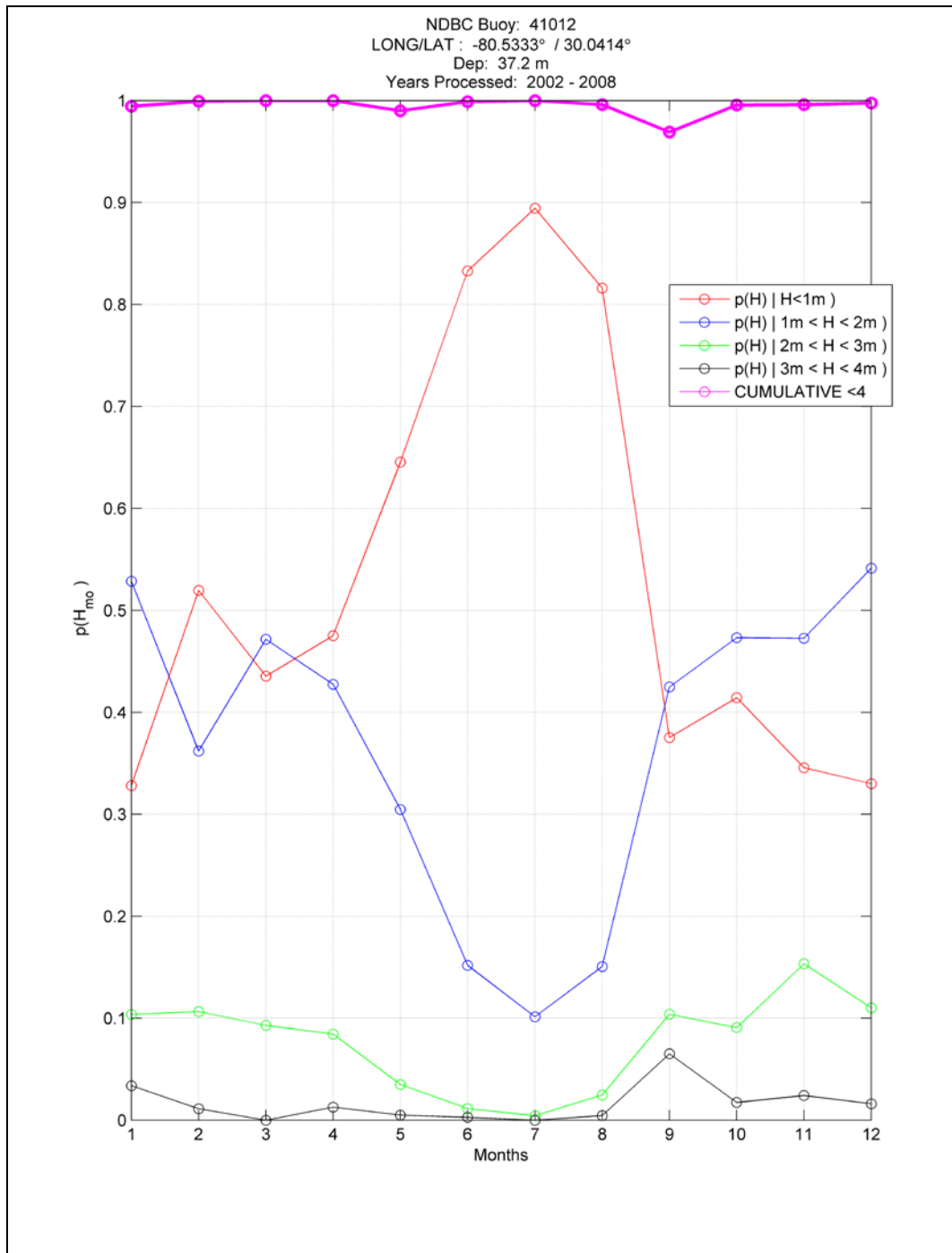
Document #:
**NESC-RP-08-
00494**

Version:
1.0

Title:

Assessment of Orion Crew Module Ocean Wave Model

Page #:
145 of 158





NASA Engineering and Safety Center Technical Report

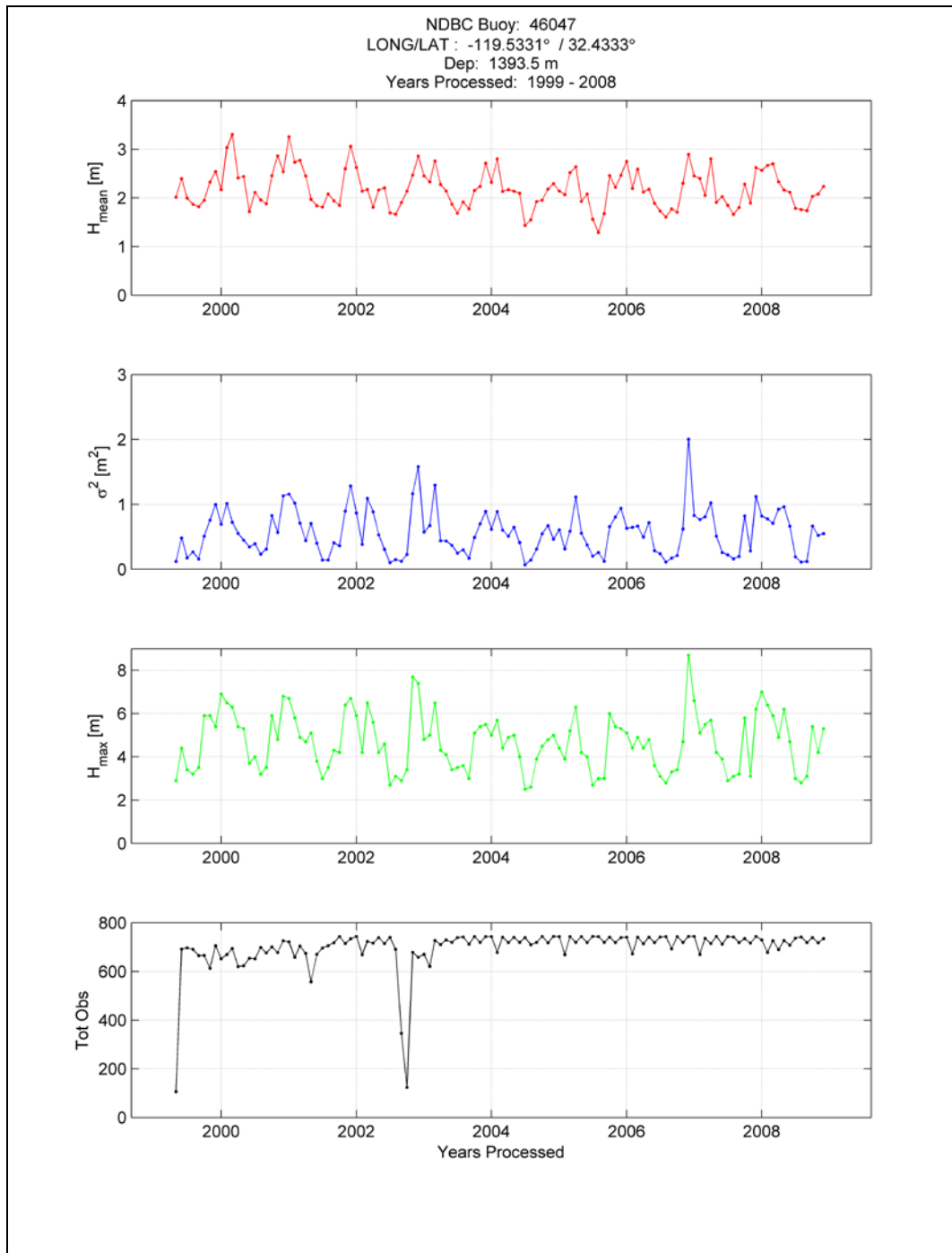
Document #:
**NESC-RP-08-
00494**

Version:
1.0

Title:

Assessment of Orion Crew Module Ocean Wave Model

Page #:
146 of 158





NASA Engineering and Safety Center Technical Report

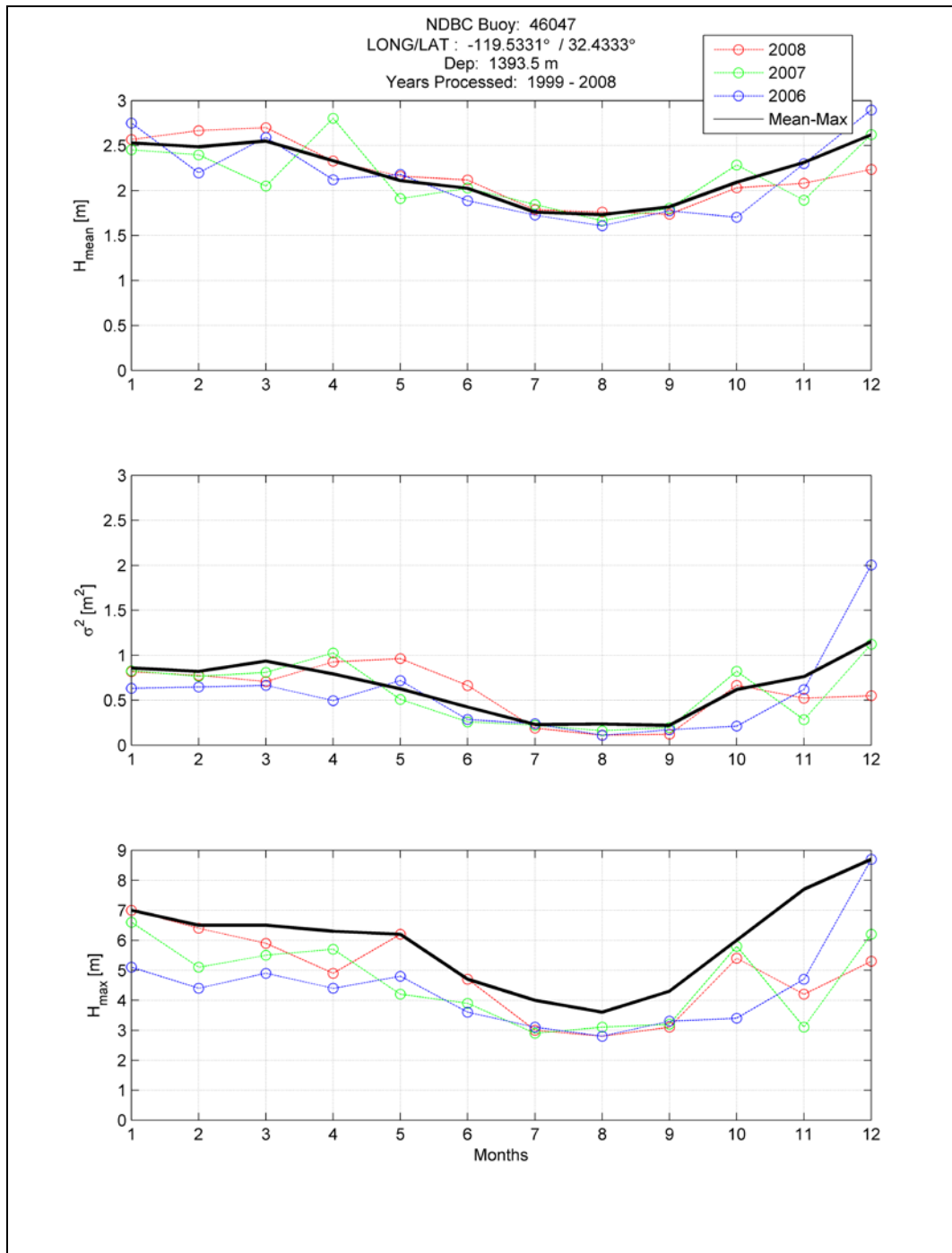
Document #:
**NESC-RP-08-
00494**

Version:
1.0

Title:

Assessment of Orion Crew Module Ocean Wave Model

Page #:
147 of 158





NASA Engineering and Safety Center Technical Report

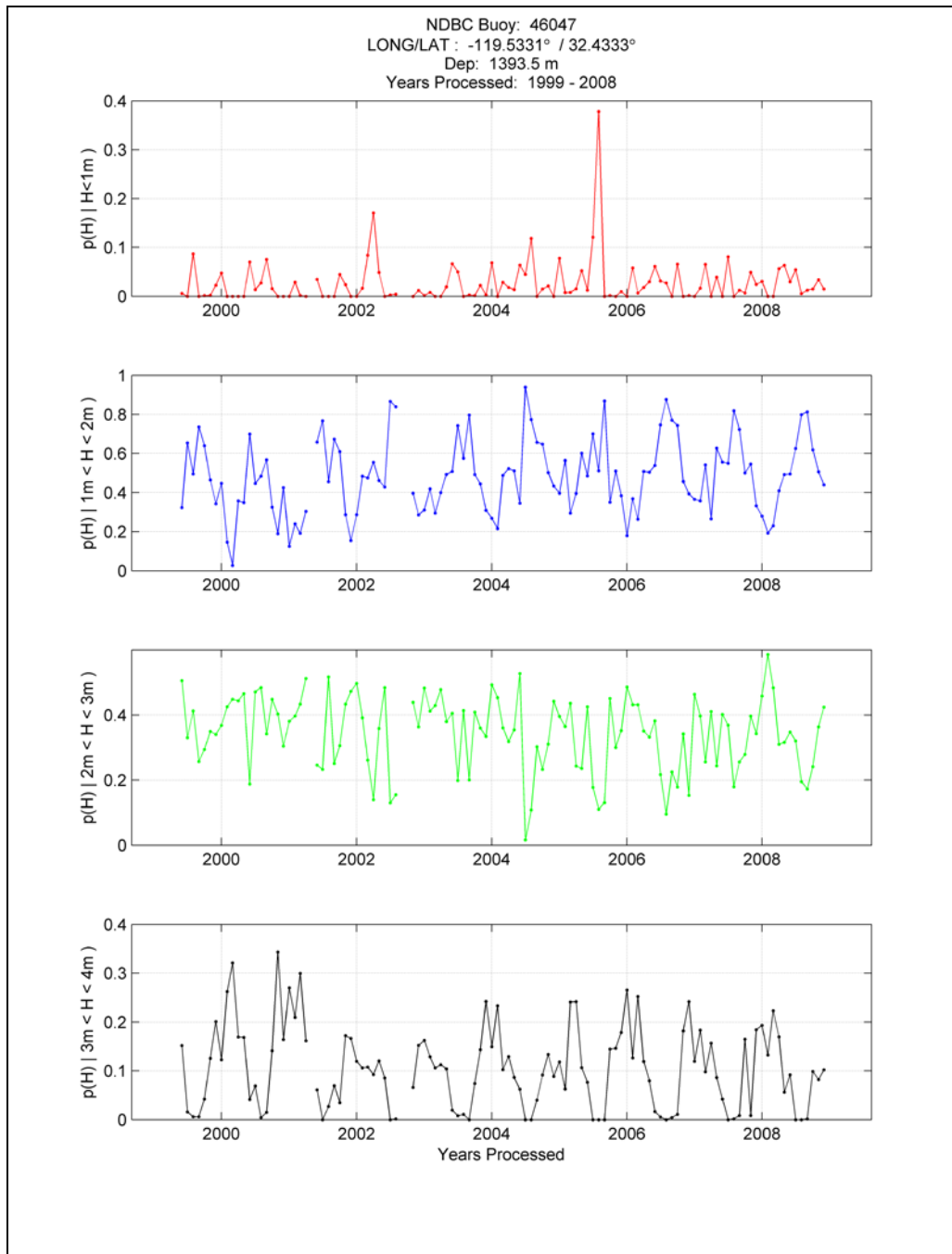
Document #:
**NESC-RP-08-
00494**

Version:
1.0

Title:

Assessment of Orion Crew Module Ocean Wave Model

Page #:
148 of 158





NASA Engineering and Safety Center Technical Report

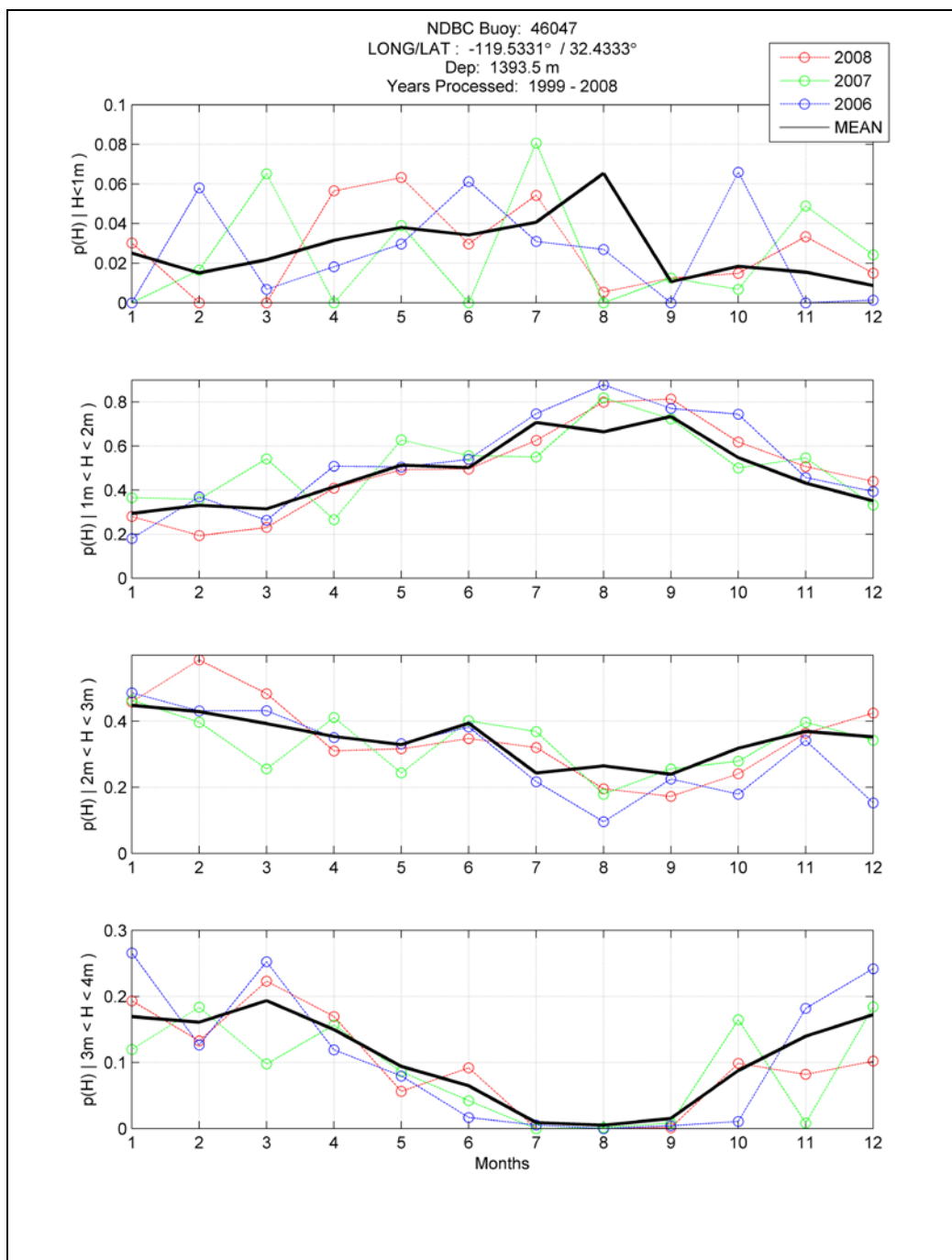
Document #:
**NESC-RP-08-
00494**

Version:
1.0

Title:

Assessment of Orion Crew Module Ocean Wave Model

Page #:
149 of 158





NASA Engineering and Safety Center Technical Report

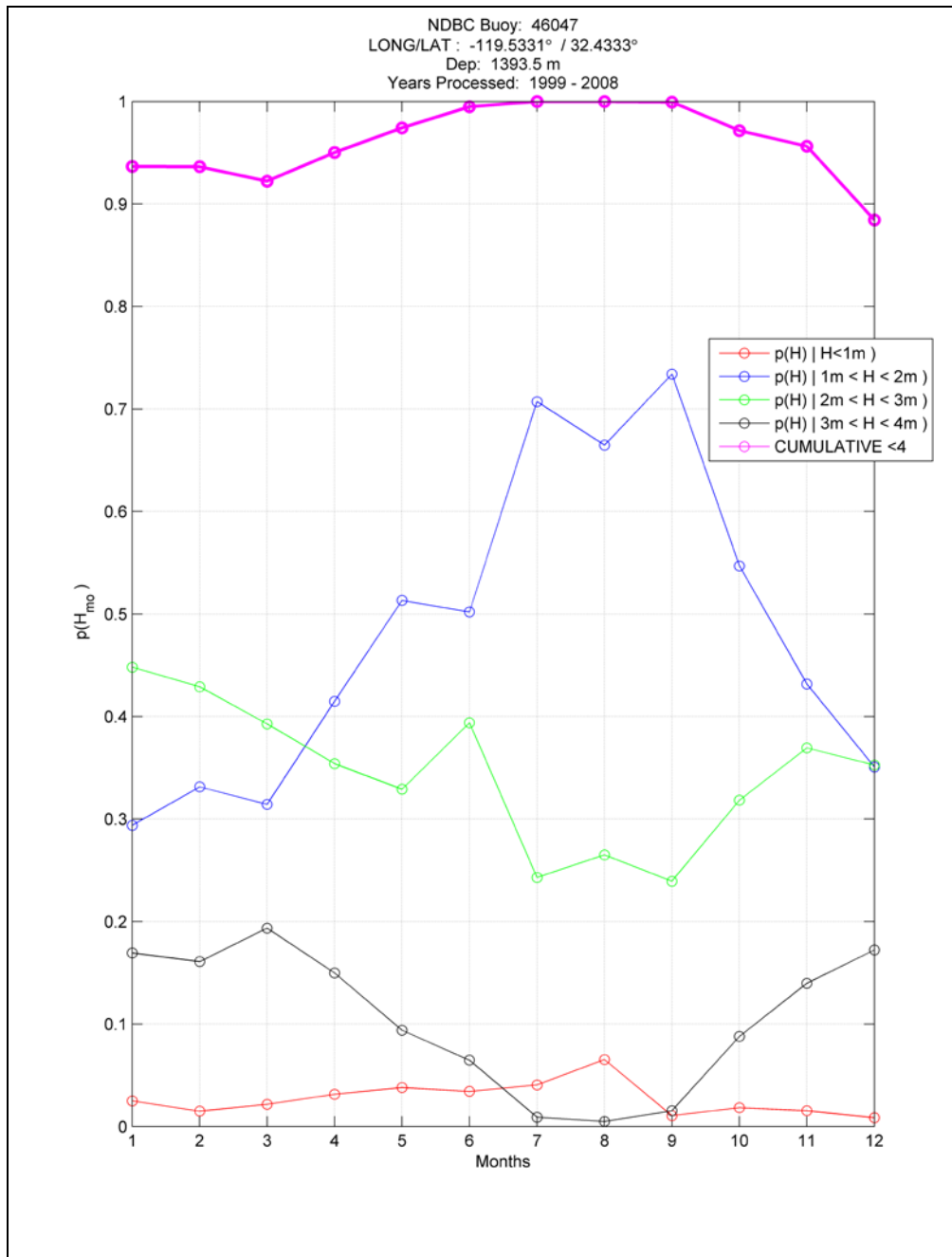
Document #:
**NESC-RP-08-
00494**


Version:
1.0

Title:

Assessment of Orion Crew Module Ocean Wave Model

Page #:
150 of 158



	NASA Engineering and Safety Center Technical Report	Document #: NESC-RP-08- 00494	Version: 1.0
Title: Assessment of Orion Crew Module Ocean Wave Model			Page #: 151 of 158

Appendix E. NDBC Wave Measurements (Data Format)


Data Availability and Formats:

Wave data are available from the NDBC website for each station's Historical Data Page. The URL for each page is of the form: http://www.ndbc.noaa.gov/station_history.php?station=SSSSS

where SSSSS represents the 5-digit station identifier (e.g., 44014)

The files are compressed using the gzip utility, but when uncompressed are in a columnar text format. Before 2007, the first four columns of each record represent the Year, Month, Day, and Hour of the observation. From 2007 onward, a fifth column containing the Minute of the observation was added. Data are organized by parameter and year (or month for the present year), as follows:

- Wave parameters (significant wave height, dominant wave period, and average wave period) in the “real time standard meteorological data”. The data are located in the <http://www.ndbc.noaa.gov/data/historical/stdmet/> directory and their filenames are of the form: SSSSShYYYY.txt.gz where SSSSS represents the station identifier and YYYY the year (this convention is used for the remainder of the file descriptions). Missing data are indicated by the use of 99.9 or 999.9 depending on the precision of the parameter. From 2007 on, the files contain two column header rows – the top indicates the parameter (see <http://www.ndbc.noaa.gov/measdes.shtml#stdmet>) and the second row the unit of measure. Before 2007, only the parameter column header row is present.
- Wave spectral density versus wave frequency in the <http://www.ndbc.noaa.gov/data/historical/swden/> directory and their filenames are of the form SSSSSwYYYY.txt.gz. If the number of frequencies changed during the year, a second file of the form SSSSSwbYYYY.txt.gz is made. The frequencies in Hz form the column header row. The value of 999.00 represents missing data.
- Mean wave direction (α_1) versus wave frequency in the <http://www.ndbc.noaa.gov/data/historical/swdir/> directory. Filenames are of the form SSSSSdYYYY.txt.gz with a change in frequency bands indicated as SSSSSdbYYYY.txt.gz. Missing data are indicated by the value of 999.
- Principal wave direction (α_2) versus wave frequency in <http://www.ndbc.noaa.gov/data/historical/swdir2/> directory. Filenames are of the

	NASA Engineering and Safety Center Technical Report	Document #: NESC-RP-08- 00494	Version: 1.0
Title: Assessment of Orion Crew Module Ocean Wave Model			Page #: 152 of 158

form SSSSSiYYYY.txt.gz with a change in frequency bands indicated as SSSSSibYYYY.txt.gz. Missing data are indicated by the value of 999.

- First normalized polar coordinates from the Fourier coefficients (r_1) versus wave frequency in the <http://www.ndbc.noaa.gov/data/historical/swr1/> directory. Filenames are of the form SSSSSjYYYY.txt.gz with a change in frequency bands indicated as SSSSSjbYYYY.txt.gz.
- Second normalized polar coordinate from Fourier coefficients (r_2) versus wave frequency in the <http://www.ndbc.noaa.gov/data/historical/swr2/> directory. Filenames are of the form SSSSSkYYYY.txt.gz with a change in frequency bands indicated as SSSSSkbYYYY.txt.gz.


Notes:

- (1) r_1 and r_2 are scaled by a factor of 100 in the data files and must be divided by 100 before use in any application.*
- (2) Valid values for α_1 and α_2 are 1 to 360 degrees where 360 represent True North. Values outside that range should be ignored.*

In addition to the data above, NDBC collects other wave parameters not made public, but which are available since 1999 in the NDBC database. Among the parameters are:

- The Check Ratio or Check Factor for each frequency. NDBC wave measurements assume a linear system (see Barrick *et al.*, 1989 which discusses and identifies nonlinear effects) and the deviation of the check ratio from 1.0 at frequencies with significant spectral densities can be indicative on non-linearity.
- The directional statistics of the Maximum, Mean, Minimum and Standard Deviation of the Pitch, Roll, Tilt (combined pitch and roll), slope with respect to the buoy's bow and slope with respect to the buoy's beam of the sampled time series.
- Buoy's average forward direction (true) that can be used to re-orient the directional statistics to True Direction.

The NDBC web pages have spectral wave data going back to 1995. Data before that and since 1996 are available from the National Oceanographic Data Center in F291 format in the Coastal Buoy Data Archive (also known as the NOAA Environmental Buoy Database, <http://www.nodc.noaa.gov/BUOY/buoy.html>). Data are organized by station identifier and collected in monthly files. The F291 format is explained at: <http://www.nodc.noaa.gov/General/NODC-Archive/f291.html>.


	NASA Engineering and Safety Center Technical Report	Document #: NESC-RP-08- 00494	Version: 1.0
Title: Assessment of Orion Crew Module Ocean Wave Model			Page #: 153 of 158

The F291 records contain positions and wave acquisition times through the years, and also have spectral density data at higher resolutions than the NDBC webpage files. The F291 files also contain wind speed and direction at the hourly intervals and *Continuous Winds*.

NDBC provides climatological plots and tables for each station for data through 2001. A description of the tables and plots can be found at <http://www.ndbc.noaa.gov/climatedesc.shtml>.

The tables and plots are PDF files available from each station's historical page, which is of the form: http://www.ndbc.noaa.gov/station_history.php?station=SSSSS

where SSSSS represents the 5-digit station identifier (e.g., 44018).

	NASA Engineering and Safety Center Technical Report	Document #: NESC-RP-08- 00494	Version: 1.0
Title: Assessment of Orion Crew Module Ocean Wave Model			Page #: 154 of 158

Appendix F. CDIP Wave Measurements (Data Format)

CDIP Spectral File Format

Each spectral file is composed of two parts, a header and the spectrum.

- **header** - the first 10 lines of the file, which contain information about the station and data sample
- **wave spectrum** - wave spectral information, generally split into 64 or 128 bands.


Sample header

File Name: sp07601199801091641 Analyzed(UTC): 1998 09/23 0103 hrs
Station Name: DIABLO CANYON BUOY
Location: 35 12.50 N 120 51.60 W Sensor Type: Spherical Drctnl Buoy
Water Depth(m): 23 MLLW Sensor Depth(m): N/A Sensor Elev(m): 23.0
Shore Normal(deg): N/A Source File: df07600199801091708
Sample Length(s): 1600 Sample Rate(Hz): 1.282
Hs(m): 1.27 Tp(s): 15.38 Dp(deg): 246 Ta(s): 5.56

<u>freq</u>	<u>Band</u>	<u>energy</u>	<u>Dmean</u>	<u>a1</u>	<u>b1</u>	<u>a2</u>	<u>b2</u>	<u>Check</u>
Hz	width	m*m/Hz	deg					factor

Header field descriptions

- **File Name** - sp03601199812122400
 - length=19 characters, arranged as follows: file type (2 char); station (3); data set (2); year (4); month (2); day (2); hour (2); minute (2)
 - The date/time is the UTC time at the start of the first observation in the file
- **Analyzed** - The UTC time the spectral file was produced.
- **Station Name** - The geographical or other commonly used name for a station.
- **Location** - The latitude and longitude of the station specified in degrees and decimal minutes.
- **Sensor Type** - The type of instrument used to measure the waves, or the type of model used to generate predictions. A list of types follows.
 - pressure sensor
 - spherical non-drctnl buoy
 - spherical drctnl buoy
- **Water Depth** - Water Depth, the measured water depth at the station location. If measured (or corrected) with respect to a datum such as MLLW, the datum is placed after the depth as in the example above.

	NASA Engineering and Safety Center Technical Report	Document #: NESC-RP-08- 00494	Version: 1.0
Title: Assessment of Orion Crew Module Ocean Wave Model			Page #: 155 of 158


- **MLLW** - Mean Lower Low Water, a tidal datum. The average of the lower low water heights of each tidal day observed over the National Tidal Datum Epoch, a specific 19-year Metonic cycle. Only the lower low water of each pair of low waters, or the only low water of a tidal day is included in the mean. For more information visit NOAA's [Oceanographic Products and Services Division](#).
- **Sensor Depth** - Mean value, in meters, of the time series of samples used to produce the spectral wave energy. For a pressure sensor, this is the mean depth measured above the sensor during the sample.
- **Sensor Elev** - The height of the primary wave sensor above the bottom in meters. For a floating (buoy), or surface piercing (wave staff) gage, this would be the same as the nominal depth.
- **Shore Normal** - The direction of a vector normal to, and pointing away from, the shoreline in degrees clockwise from true North. Should only be provided/utilized when depth contours at the gauge, and between gauge and shore, are straight and parallel.
- **Source File** - The file name of the time series, (or other input file type) used to produce the spectrum.
- **Sample Length** - The length, in seconds, of the sample time series used to measure the waves.
- **Sample Rate** - The sampling rate, in hertz, of the sample time series used to measure the waves.
- **Hs (Hm0)** - Significant wave height in meters; derived from the zeroth moment of the reported energy spectrum. $Hm0 = 4(m0)^{.5}$
- **Tp*** - Peak period, in seconds; inverse of the frequency with the highest energy density in the reported spectrum.
- **Dp*** - Mean direction from which energy is coming at the peak period, in degrees clockwise from true North.
- **Ta** - Average period, in seconds; $Ta = m0/m1$, where m0 and m1 are the zero'th and first moments of the reported energy spectrum.

CDIP XY File Format

CDIP's xy files contain the displacement time series for directional buoys. These data are not corrected for magnetic declination.

The files include x (magnetic North-South, N positive), y (West-East, W positive), and z (vertical) displacement values. These files are formatted as follows:

```
Name: POINT LA JOLLA BUOY                                (start of header)
Station: 09501
Deployment latitude: 32 51.10' N
```


	NASA Engineering and Safety Center Technical Report	Document #: NESC-RP-08- 00494	Version: 1.0
Title: Assessment of Orion Crew Module Ocean Wave Model			Page #: 156 of 158

Deployment longitude: 117 21.00' W
Water depth(m): 179.83
Local magnetic variation(deg): 13 E
Data type: Datawell vectors
Gauge type: Datawell Mark 2 directional buoy
Sample rate(Hz): 1.280
Field software version: datawell_acq v2
Field station type: sun
Method of analysis: Datawell
GPS: yes

Start time: 20001224185950 UTC
End time: 20001224192949 UTC
Sample length(hh:mm:ss): 00:30:00
Total number of vectors: 2304
Error-free vectors: 100.0%


```

----- (end of header)
20001224185950      3      31      49      (start of data)
20001224185951      6       2      55
20001224185952      9     -26      63
20001224185952     16     -39      44
20001224185953     17     -30      12
20001224185954     33      -8      13
20001224185955     52      -7      16
20001224185955     54     -25      20
20001224185956     51    -44       7
20001224185957     42    -49     -21
20001224185958     21    -31     -63
20001224185959    -13     13    -77
20001224185959    -27     45    -68
20001224190000    -29     46    -37
20001224190001    -16     33     -6
. . . .

```

THE HEADER:

The header of the xy file is copied directly from the corresponding Datawell vector (df) file. It contains two sections. The first gives basic information about the sensor: the position, the sample rate, the buoy type, etc. The second section contains the start time, end time, and sample length of the data. It also contains diagnostic information that depends on the sensor type. For directional buoys, this is the total number of vectors received and the percentage of these vectors that are considered to be error-free. (Note that only the start time is set in the field and returned with the data; all other entries in this section are calculated and added by CDIP's processing programs.)

	NASA Engineering and Safety Center Technical Report	Document #: NESC-RP-08- 00494	Version: 1.0
Title: Assessment of Orion Crew Module Ocean Wave Model			Page #: 157 of 158

Comments may have been added at the bottom of the third section. A dashed line (-----) separates the header from the data; all comments are placed above this line.

It is possible that the start and end times in the header will not correspond to the actual start and end times of the displacement data in the file. This is because any displacement values which are not clearly received at the shore station are omitted from the xy file. Only vectors that are marked 'Error-free' by the Datawell receiver (i.e., vectors with error codes of one or zero) are included in the xy file. Thus whenever the header value 'Error-free vectors' is less than 100%, there will be time gaps within the displacement data; when a gap falls at the beginning or end of the data, the start or end time will not match its header value. (For a more detailed discussion of the error codes and their interpretation, see the Datawell vector description, .docs/processing/directional_buoys/df_format.txt).

THE DATA:


Each line of data in the xy file consists of four columns. The first column gives the UTC time of the sample to the nearest second; the format of this number is YYYYMMDDhhmmss. The second column is the x (North-South, N positive) displacement in centimeters, the third column is the y (West-East, W positive) displacement in cm, and the fourth and final column is the z (vertical) displacement in cm.

Time: YYYYMMDDhhmmss	X disp (cm)	Y disp (cm)	Z disp (cm)
. . . .			
20001224185953	17	-30	12
20001224185954	33	-8	13
20001224185955	52	-7	16
20001224185955	54	-25	20
20001224185956	51	-44	7
20001224185957	42	-49	-21
20001224185958	21	-31	-63
. . . .			

Since the sample period is less than a second - 0.78125 secs - many of the lines are marked with the same time, e.g., there are two at 20001224185955 in the example above. These two samples were taken 0.78125 seconds apart, not at the same time; to the nearest second, however, they are both from 2000/12/24 18:59:55 UTC.

where data is not clearly received and is marked with an error code greater than 1 in the diskfarm file, there will be a gap in the displacements in the xy file. For example, below there is a two-minute gap in the data (where the time skips from 19:02:57 to 19:04:58):

. . . .			
20001224190250	10	33	-39

	NASA Engineering and Safety Center Technical Report	Document #: NESC-RP-08- 00494	Version: 1.0
Title: Assessment of Orion Crew Module Ocean Wave Model			Page #: 158 of 158

```

20001224190251      0      56      -20
20001224190252     -13      61       29
20001224190253     -11      35       63
20001224190254       1      -4       65
20001224190254      11     -37       54
20001224190255      16     -57       29
20001224190256      13     -72       23
20001224190257       8     -82       18
20001224190458      -4     -21        0
20001224190459      -1     -22     -19
20001224190459       0     -12     -51
20001224190500     -17       9     -58
20001224190501     -31      34     -60
20001224190502     -42      63     -53
20001224190503     -48      97     -12
. . . .

```

To look at the error codes and the (likely erroneous) displacements from this gap, refer to the corresponding diskfarm (df) file. Note that not all problematic vectors are flagged bad by the receiver, and that spikes will sometimes be present in the xy files' displacements. These spikes are not edited out, but written to the xy files without modification. In general, however, it can be assumed that these spikes are transmission related, and are not present in the buoys' internal time series that are used for spectral and parameter processing.

REPORT DOCUMENTATION PAGE					Form Approved OMB No. 0704-0188	
<p>The public reporting burden for this collection of information is estimated to average 1 hour per response, including the time for reviewing instructions, searching existing data sources, gathering and maintaining the data needed, and completing and reviewing the collection of information. Send comments regarding this burden estimate or any other aspect of this collection of information, including suggestions for reducing this burden, to Department of Defense, Washington Headquarters Services, Directorate for Information Operations and Reports (0704-0188), 1215 Jefferson Davis Highway, Suite 1204, Arlington, VA 22202-4302. Respondents should be aware that notwithstanding any other provision of law, no person shall be subject to any penalty for failing to comply with a collection of information if it does not display a currently valid OMB control number.</p> <p>PLEASE DO NOT RETURN YOUR FORM TO THE ABOVE ADDRESS.</p>						
1. REPORT DATE (DD-MM-YYYY) 01-05-2009		2. REPORT TYPE Technical Memorandum		3. DATES COVERED (From - To) November 2008-March 2009		
4. TITLE AND SUBTITLE Assessment of Ocean Wave Model used to Analyze the Constellation Program (CxP) Orion Project Crew Module Water Landing Conditions				5a. CONTRACT NUMBER		
				5b. GRANT NUMBER		
				5c. PROGRAM ELEMENT NUMBER		
6. AUTHOR(S) Smith, Bryan K.; Bouchard, Richard; Teng, Chung-Chu; Dyson, Rodger; Jensen, Robert; O'Reilly, William; Rogers, Erick; Wang, David; Volovoi, Vitali				5d. PROJECT NUMBER		
				5e. TASK NUMBER		
				5f. WORK UNIT NUMBER 869021.05.07.07.19		
7. PERFORMING ORGANIZATION NAME(S) AND ADDRESS(ES) NASA Langley Research Center Hampton, VA 23681-2199				8. PERFORMING ORGANIZATION REPORT NUMBER L-19687 NESC-RP-08-00494		
9. SPONSORING/MONITORING AGENCY NAME(S) AND ADDRESS(ES) National Aeronautics and Space Administration Washington, DC 20546-0001				10. SPONSOR/MONITOR'S ACRONYM(S) NASA		
				11. SPONSOR/MONITOR'S REPORT NUMBER(S) NASA/TM-2009-215752		
12. DISTRIBUTION/AVAILABILITY STATEMENT Unclassified - Unlimited Subject Category 16-Space Transportation and Safety Availability: NASA CASI (443) 757-5802						
13. SUPPLEMENTARY NOTES						
14. ABSTRACT Mr. Christopher Johnson, NASA's Systems Manager for the Orion Project Crew Module (CM) Landing and Recovery at the Johnson Space Center (JSC), and Mr. James Corliss, Project Engineer for the Orion CM Landing System Advanced Development Project at the Langley Research Center (LaRC) requested an independent assessment of the wave model that was developed to analyze the CM water landing conditions. A NASA Engineering and Safety Center (NESC) initial evaluation was approved November 20, 2008. Mr. Bryan Smith, NESC Chief Engineer at the NASA Glenn Research Center (GRC), was selected to lead this assessment. The Assessment Plan was presented and approved by the NESC Review Board (NRB) on December 18, 2008. The Assessment Report was presented to the NRB on March 12, 2009. This document is the final Assessment Report.						
15. SUBJECT TERMS CM; NESC; Orion Project; Wave model						
16. SECURITY CLASSIFICATION OF:			17. LIMITATION OF ABSTRACT	18. NUMBER OF PAGES	19a. NAME OF RESPONSIBLE PERSON	
a. REPORT	b. ABSTRACT	c. THIS PAGE			STI Help Desk (email: help@sti.nasa.gov)	
U	U	U	UU	163	19b. TELEPHONE NUMBER (Include area code) (443) 757-5802	